Geostatistical Modeling for Grade Control and Long Range Models

by

Norris Amihere

A thesis submitted in partial fulfillment of the requirements for the degree of

Master of Science

in

Mining Engineering

Department of Civil and Environmental Engineering
University of Alberta

Abstract

In general, less than one billionth of the volume of a deposit is sampled before production decisions. The grades and other rock properties are estimated in the unsampled volume. The success of a mine is dependent on accurate grade control. The grade control process establishes the final planned destination of mined material, directly influencing the operation's profitability. Mistakes at this stage are costly and irreversible. Resource models are considered long-term when used for long-term mine planning; an example is a Life of Mine (LOM) plan. Long-term models are based on widely-spaced drilling, which is gradually filled in as the project advances. Long-term models provide estimates of tonnage and grade for each period involved through to the end of the life of the mine. Long-term models are designed to estimate what will be achieved during grade control with acceptable accuracy.

Geostatistical modeling is challenging because of the geological variability/uncertainty in the grades. For example, when material needs to be directed to various stockpiles or treatment facilities, the procedure is frequently complicated by the need for numerous classifications. Grade control programs aim to minimize the misclassification of material, while the primary focus of long-term models is on the accuracy of estimated recoverable resources awaiting more data at the time of grade control. The prediction goals differ for grade control and long-term modeling; therefore, the appropriate geostatistical techniques and parameter setups differ. For this research, geostatistical models are generated through the following techniques: (1) Ordinary Kriging, (2) Expected sequential Gaussian Simulation, (3) Localized Uniform Conditioning, and (4) Localized Sequential Gaussian Simulation. The expected profits from realizations are demonstrated with a series of examples. The appropriate modeling techniques and parameter setups for grade control and long-term models in the presence of geological uncertainty are demonstrated and evaluated.

Dedication

"The more I learn, the more I realize how much I don't know."

- Albert Einstein

This thesis is dedicated to all those driven by a desire to enhance the human experience.

Acknowledgments

I am deeply thankful to Dr.Clayton Deutsch, my research supervisor and guiding mentor. His exceptional intellect, innovative insights, and unwavering patience have been instrumental in shaping this research work. I hold great admiration for his distinctive talent to inspire and streamline complex processes effortlessly.

I extend my gratitude to the Centre for Computational Geostatistics for the generous financial support provided throughout my academic journey, as well as for fostering an outstanding research atmosphere. I am grateful to all my CCG colleagues, Harold Velasquez and Karim Mokdad, for their consistent provision of valuable guidance and encouragement that fueled my enthusiasm.

I also would like to thank my family for their consistent support and encouragement throughout my graduate studies.

Table of Contents

List of Tables

List of Figures

List of Abbreviations

Abbreviation	Description
BH	Blasthole
CCG	Centre for Computational Geostatistics
CDF	Cumulative Distribution Function
DGM	Discrete Gaussian Model
DH	Drillhole
ExpSGS	Expected Sequential Gaussian Simulation
EV	Expected Value
FN	False Negatives
FP	False Positives
GC	Grade control
GSLIB	Geostatistical Software Library
IDW	Inverse Distance Weighting
IK	Indicator Kriging
LOM	Life of Mine
LUC	Localized Uniform Conditioning
LocSGS	Localized Sequential Gaussian Simulation
LTM	Long Term Model
LSP	Large Search Plan
M	Meters
MSE	Mean Square Error
MIK	Multiple Indicator Kriging
MGK	MultiGaussian Kriging
OK	Ordinary Kriging
PDF	Probability Density Function
PME	Percentage of Misclassified Errors
SGS	Sequential Gaussian Simulation
SK	Simple Kriging
SMU	Selective Mining Unit
SSP	Small Search Plan
STM	Short Term Model

Abbreviation	**Description**
3-D	Three-Dimensional
2-D	Two-Dimensional
UC	Uniform Conditioning
NPV	Net Present Value
RV	Random Variable

Chapter 1

Introduction

Many of the resources we depend on for various purposes, especially those that cannot be naturally replenished, require extraction from the Earth or other methods of procurement when they cannot be cultivated or grown. Mining is the extraction of valuable minerals and commodities from the Earth (Salomons, 1999). Nearly everything we rely upon is either made from metals and minerals or necessitates them for manufacturing, thereby presenting an opportunity to extract essential resources upon which the world relies to improve life. An adequate justification is needed before a mining activity can commence; this is determined by conducting a thorough study of the locality, including obtaining borehole samples to gain an insight into the geological resource. A geological model is built on this information. This model is a representation of the subsurface formation and its associated properties and can be used to determine the extent of any profitable resources in the geologic formation. The complex distribution of subsurface properties, coupled with limited data, poses challenges to the estimation of mineral resources. Geostatistical modeling is carried out at an appropriate Selective Mining Unit (SMU) scale to ensure the block model is appropriate for technical and economic assessment. This approach avoids the necessity of predicting small-scale variability within each block. Given that less than one billionth of the deposit volume is typically sampled, estimation of grades and other attributes is required for the unsampled region (Rossi & Deutsch, 2014). Modeling techniques can be considered in two categories: a group of estimation techniques that provide a single deterministic model with a single value estimated for each unsampled location and a second group of probabilistic techniques that generate quantified uncertainty in the form of a probability distribution of grades for each unsampled location.

Different estimation schemes are designed with different characteristics, including simplicity, reproducibility, and integration of large-scale geologic trends. Kriging is an extensively used technique for the estimation of grades. Inverse Distance Weighting (IDW) is common as well. Kriging is a linear unbiased estimator that minimizes the estimation variance using a domain-specific variogram model of spatial variability accounting for anisotropy and other spatial features (A. Journel & Huijbregts, 1978). The number of data and locations of data used to inform the estimate is often called the Kriging search plan (J. L. Deutsch & Deutsch, 2015). The Kriging search plan directly influences the computational time, stationarity, conditional bias, and histogram reproduction. These restrictions and concerns will be discussed in Chapter Two. The block estimates made by conventional IDW estimation or Kriging techniques, Simple Kriging (SK) and Ordinary Kriging (OK), have no reliable measure of uncertainty attached to them. In contrast, quantifying uncertainty and providing a range of possible values for each SMU allows for an unbiased model that reproduces

the appropriate histogram. This thesis will present and discuss two methods to generate a local distribution for the SMU being considered. There are pros and cons to each method regarding the complexity of the method, accounting for the support effect, and the assumptions that are required. When implemented carefully, each method is capable of reproducing the SMU distribution expected in the future. Sequential Gaussian Simulation (SGS), Uniform Conditioning (UC), MultiGaussian Kriging (MGK), and Indicator Kriging (IK) are common probabilistic estimators that directly predict variability/uncertainty in the mining block grades based on a probability distribution model. UC and SGS are demonstrated in this thesis.

For this thesis, the purpose of estimates is classified into two categories; the first is an interim estimation, where data is widely spaced, and additional information will be available before the final decision is made. This is particularly relevant for long-term predictions in an open-pit context before grade-control samples are available. The second situation is final estimation, which is conducted for selecting ore and waste. For example, this could occur during grade control in an open pit or when estimating stope grades in an underground mine where there is limited future flexibility. In the first case, local accuracy and precision is not the top priority; the primary focus is on the accuracy of the estimated global recoverable reserves. In the second case, local precision and accuracy are more important than global results. Grade control models are based on a large number of samples. In an open pit environment, Blasthole (BH) samples are obtained on closely spaced grids according to blasting requirements. Less frequently, grade control drilling is performed separately from blast hole drilling, for example, using dedicated Reverse Circulation (RC). In some geologic settings, surface trenches and channel samples are also used. The most closely spaced source of information for daily grade control tasks is BH samples, but often BH samples are less reliable than samples obtained from exploration or RC drill holes (Rossi & Deutsch, 2014). After obtaining samples, a grid is chosen, the grades are estimated for grid blocks, and the destination of mined material is determined. Blasting causes the movement of rocks. Thus, the pre-blast positions of grades should be adjusted according to the post-blast muck pile geometry. At the time of grade control in an open pit or when estimating stope grades in an underground mine with limited future flexibility, the emphasis is on local precision and exactitude of the estimates. Estimators for grade control are for the purposes of selecting ore and waste. These final estimates aim to calculate estimates that are correct in expected value based on a cutoff grade; that is, the actual value recovered will be equal to the estimates in expected value. There may be additional goals, such as correct classification to manage several stockpiles with different ore types and grades. Grade control should be a flexible procedure accounting for the uncertainty of the prediction and site-specific characteristics of the mining operation. This chapter introduces the challenges in grade control and long-term predictions that motivate the research of this thesis, as well as a description of the contributions and thesis outline. Section 1.1 discusses the limitations of current estimators for grade control and long-term models, which provides the background for the problem setting of this research. The outline of the thesis and a brief summary

of each chapter are presented in Section 1.2

1.1 Motivation and Goals

For a mining operation, it is crucial to minimize the misclassification of ore and waste during grade control and to accurately anticipate the future grade and tonnage of the material that can be extracted from interim models. The complex geological distribution of subsurface material properties cannot be fully understood from limited data. This results in an inevitable uncertainty. Conventional resource and reserve calculations are typically based on a single model, which has long been the standard practice in the mining industry. In common grade control practices, there are several potential reasons for misclassification errors.

i) Grade control typically relies on estimation methods. These methods provide deterministic estimates and do not account for non-linear recovery and uncertainty in profit. Therefore, they may need to be more suitable for multiple variables and complex profit calculations. They may not provide optimal decisions when the penalties for different misclassification errors are complex.

ii) In some cases, conventional grade control does not account for blast movement. Most mines use drilling and blasting to break rocks before excavation and hauling. Due to the energy of the explosion, the rock moves with blasting. Depending on the type of rocks, the displacement of grades can be up to 10-15 meters (Thornton et al., 2005). This means the pre-blast estimates are not final. The post-blast mapping of grades is of great importance for grade control.

iii) Grade estimates are typically used to develop boundaries (dig limits) for delimiting ore and waste or different destinations, including leach pads and stockpiles (Verly, 2005). It is difficult to delimit ore and waste zones precisely accounting for the mining practice; this can lead to increased dilution and ore loss. The use of dig limits is improved using expected profit maps, optimization, and accounting for mine-specific selectivity constraints (Isaaks, 1991; Norrena, 2007).

iv) Sampling errors are inevitable. They reduce the quality of the estimates for grade control. The influence of sampling errors on simulation and truck-based selection of rocks should be understood. The possibility of incurring sampling error should be considered.

Although estimation methods like Kriging or inverse distance weighting are very convenient and provide robust estimates, they might not be optimal for grade control because they do not account for uncertainty, possible non-linearity of recovery, and asymmetry in the profit function (e.g., more profit assigned to a correct ore or waste decision). This is achievable by assessing the uncertainty in profit through a proper profit function. If the best Kriging estimates are converted to profit, they may need to show correct profit values. Using many realizations and the expected profit at each unsampled location is necessary instead of a single estimate. In recent years, the use of conditional simulation for improved grade control has been proposed and adopted in mines (Collet & Corley, 2000). This thesis presents several examples illustrating the geostatistical modeling steps required

to quantify the spatial distribution of grades and the transfer of uncertainty in grades to expected profit to select optimal dig limits.

For all methods of quantifying local uncertainty, the long-standing argument against a model of this type has been the increase in computational expense and complexity in the calculations (Daniels & Deutsch, 2014). When a series of equiprobable values for each SMU must be generated and considered, the computational expense can be higher; however, computer processing speeds and parallelization make these calculations possible. The process for computing resources, reserves, or any other important transfer function, including mine planning, must be performed simultaneously on each model or all models. Using multiple realizations appears challenging due to the ambiguity introduced by multiple realizations, but the grade control decisions could be optimized over all realizations simultaneously. Various strategies for summarizing or localizing a model of uncertainty have been developed as a potential middle ground to avoid working with the entire model of uncertainty. Localization of uncertainty has gained significant attention of late and warrants some careful evaluation as a possible alternative to Kriging. The lure of generating a single model at the SMU scale without excessive histogram smoothing is appealing, but this process can yield unsightly artifacts and questionable local precision(Daniels, Deutsch, & Boisvert, 2014). The goal of this thesis is to compare estimators for grade control and long-term models and develop an improved understanding of techniques available for resource modeling.

1.2 Thesis Outline

This thesis addresses the problems outlined above. It serves as a guide for the implementation of Kriging with different search plans, simulation, localization and other aspects for improved geostatistical modeling for grade control and long term models.

Chapter 2 contains a review of implementation aspects for Kriging, simulation, uniform conditioning and localization. The purpose of selective mining units in regards to resource and reserves evaluation, mine planning, and long term models are also considered. Also, the decision of appropriate Kriging search plan and SMU block size is assessed, guiding principles for this decision will be discussed. Literature references addressing dig limit issues and the maximum profit/minimum loss grade control paradigm are provided in this chapter.

In Chapter 3, appropriate estimation and probabilistic techniques in the context of geostatistical modeling for grade control will be presented and evaluated. This includes techniques such as ordinary Kriging with different search plans, conditional simulation, and uniform conditioning. It covers the transfer of uncertainty in grade to uncertainty in profit and the expected profit estimate. The advantages and disadvantages of each method will be discussed, and a comparison of their performance will be presented based on case studies and examples from literature. The use of localization techniques for summarizing quantified SMU uncertainty into a single block model will also

be addressed in this chapter.

Chapter 4 focuses on geostatistical modeling for long term models. It covers the transfer of uncertainty in grade for long term models. The use of geostatistical models for long term mine planning is essential to ensure that mining operations are profitable in the long run. In this chapter, various methods for long-term modeling will be discussed, including ordinary Kriging with different search plans, conditional simulation, and localized uniform conditioning. The chapter will also consider the implications of long-term modeling on mine design and development, and will evaluate the advantages and disadvantages of each approach.

Chapter 5 discusses the limitations of the research presented in this thesis. It considers the assumptions made in the development of the various geostatistical models, and the limitations of the available data and technology used in the research. The chapter also provides conclusions and recommendations on improving grade control and long-range models. These recommendations are based on the findings presented in the previous chapters and highlight areas for future research and development.

Chapter 2

LITERATURE REVIEW

There are various methods for constructing geological models of deposits. These methods range from simple deterministic estimations to complex multivariate simulation techniques. Estimation is challenging due to geological variability. Different estimating methods serve different purposes. For instance, if the objective is simplicity and repeatability, methods such as polygonal areas of influence or inverse distance could be suitable. Alternatively, if the goal is to reveal large-scale geologic trends, then kriging or inverse distance could be appropriate. The traditional block modeling approach is estimating a single value in each block, obtaining the best possible prediction statistically. However, the block estimates made by conventional inverse distance or kriging techniques lack reliable measures of uncertainty. Probabilistic techniques, such as MultiGaussian Kriging (MGK), Sequential Gaussian Simulation (SGS), Uniform Conditioning (UC), and Indicator Kriging (IK) offers a way to quantify uncertainty with distributions of possible outcomes. These methods generate a distribution of possible grades at the unsampled locations. The goal of final estimation is to compute correct estimates in expected value, i.e., the true value recovered will equal the estimates in expected value. Correct classification may also be an additional goal. This chapter covers the theory behind some techniques for geostatistical modeling. The relevant literature is reviewed in the following sections.

2.1 Paradigms in Geological Modeling

Geostatistical theories were established before digital computers were widely available, which limited their use in earth sciences (Gelfand, 1955; A. Journel & Huijbregts, 1978; Wiener, 1966). Geological modeling was primarily done by hand, which was time-consuming and prone to errors. One of the earliest examples of a topographic map is the Turin Papyrus Map, which dates back to the 12th century BC. It was created for Ramesses IV's quarrying expedition and is one of the oldest known maps with accurate geographic content (Millard, 1987). This map was drawn on papyrus and provided valuable insights into the ancient Egyptian's understanding of topography and natural resources. However, geological modeling has expanded to include computer mapping, quantification of uncertainty, and active uncertainty management. Kriging algorithms are commonly used in modern geological modeling to improve the accuracy of initial hand mappings. Kriging is a geostatistical technique that uses statistical methods to interpolate values of unknown locations based on the spatial correlation of neighbouring data points (Srivastava, 1987). Probabilistic modeling techniques have also been developed to quantify uncertainties in geological estimations. These models use probability theory

to estimate the likelihood of various outcomes given a set of input parameters. The output of these models is a range of possible outcomes or realizations. Active uncertainty management involves using, for example, the efficient frontier proposed by Markowitz in 1952 to make informed decisions about resource allocation in the face of uncertainty. This technique involves identifying a set of efficient portfolios that maximize expected return for a given level of risk, allowing practitioners to choose a portfolio that best meets their specific objectives (Markowitz, 1952). In summary, using digital computers has revolutionized geological modeling, enabling the quantification of uncertainties and active management of risks. These paradigm expansions are not mutually exclusive but rather serve as supplements to one another. Figure 2.1 summarizes these paradigm expansions.

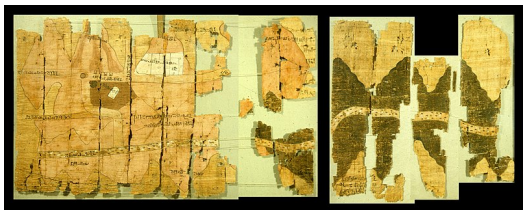

(a) Fragments of Turin papyrus - an ancient Egyptian mining map for Ramesses IV's quarrying expedition.(Photograph at the Turin Museum courtesy of J. Harrell).

$$z*(\mathbf{u}_0) - m(\mathbf{u}_0) = \sum_{i=1}^{n} \lambda_i \cdot (z(\mathbf{u}_i) - m(\mathbf{u}_i))$$

$$\sum_{j=1}^{n} \lambda_j \cdot C_{ij} = C_{i0}, \quad i = 1, \ldots, n$$

(b) Basic formulation for kriging.

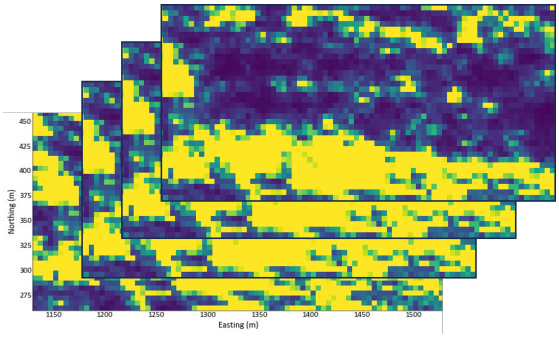

(c) Geological uncertainty represented by multiple realizations.

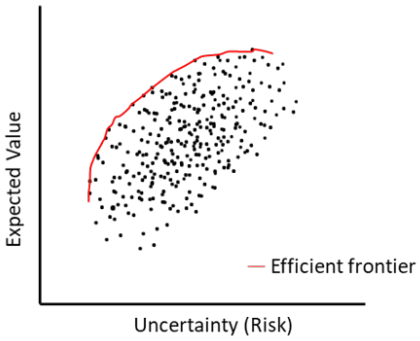

(d) Schematic of the efficient frontier proposed originally by Markowitz (1952)

Figure 2.1: Expansion of geological modeling paradigms from hand mapping (top left) to include computer mappings, quantification of uncertainty and active management of uncertainty(bottom right).

2.2 Scales of Relevance

Collecting, gathering, and initial data analysis are the first steps in mineral resource modeling. Regardless of the geostatistical method, four scales are often important to geological modeling. The domain (A), the data scale, the selective mining unit (SMU) scale, and the panel scale are represented in Figure 2.2. These scales are more relevant for surface mining, where there is significantly more data and greater flexibility during mining.

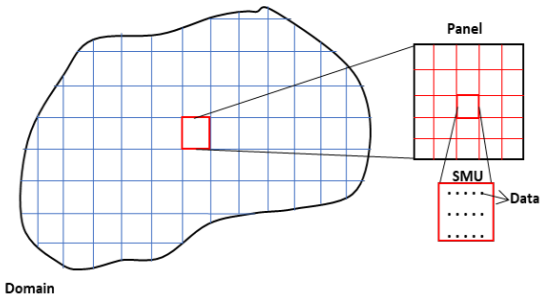

Figure 2.2: Schematic of scales of relevance to most geostatistical modeling techniques.

2.2.1 Estimation Domain

Estimation domains are the geological equivalent of geostatistical stationary zones. They are defined as a volume of rock with mineralization controls that result in approximately statistically homogeneous distributions of mineralization (Rossi & Deutsch, 2014). The spatial distributions of grades exhibit consistent statistical properties; however, this does not mean that the grades are constant within the domains. The concept of statistically homogeneous populations is termed stationarity. Stationarity is not an inherent attribute of the variable; instead, it is an attribute of the random function model (Chambers & Yarus, 2007). The available data are grouped into subsets based on different geological characteristics, such as structure, mineralogy, alteration, and lithology. Categorical variable models are used further to divide the data into different subsurface regions for analysis. These geological domains are assigned to a gridded block model, which should have sufficient resolution to represent the geological variations and provide the necessary resolution for engineering design. Having adequate data to infer the statistical parameters within each domain appropriately is crucial for defining the geological domains. It is important to note that geologic domains differ from estimation domains, as a single geologic variable defines the former. In contrast, a set of mineralization controls defines the latter and may contain multiple geological domains.

For the examples demonstrated in this thesis, regular grids of data points or block values are often considered as input or output. The conventions used throughout GSLIB are:

- The X axis is associated to the east direction. Grid node indices increase from 1 to nx in the positive x direction, where nx is the maximum number of grids/block nodes in the x direction.
- The Y axis is associated to the north direction. Grid node indices increase from 1 to ny in the positive y direction, where ny is the maximum number of grids/block nodes in the y direction.
- The Z axis is associated to the elevation. Grid node indices increase from 1 to nz in the positive z direction, where nz is the maximum number of grids/block nodes in the z direction.

The user can associate these three axes to any coordinates system that is appropriate for the problem at hand.

2.2.2 Selective Mining Unit

Calculating mineral resources and ore reserves from a block model requires choosing a selective mining unit (SMU) block size. Each block is assigned a grade or a distribution of grades. The resources or reserves are calculated from these block values. An SMU should represent the smallest volume of rock that can be selectively mined to separate ore and waste based on the available information, thus making the SMU block size representative of future mining practices. It considers the equipment, available data, geological controls, and mining operations, such as blasting (Rossi & Deutsch, 2014). In practice, many factors dictate the final tonnage and grade at the time of mining and additional information that will be gained prior to final selection. For this reason, two separate models are necessary. For long-term planning, a model is constructed at the SMU scale. When mining, a higher resolution, and better-informed grade control model will be used to determine final ore and waste selection.

To generate an estimate of ore tons and grade similar to what will be found at the time of mining, the SMU volume must be determined with regard to the mining process that will take place. Additional grade information paired with geochemical and geometallurgical measures will impact these results during mining. The SMU size is the block size that would lead to the same reserves as mined with the anticipated equipment, operational considerations, and availability of grade control information. The optimal SMU size can be determined in various ways, including the data spacing, mining method, practical experience, and reconciliation with historical production. A. Journel and Huijbregts (1978) suggest one-half to one-third of the data spacing as a general guideline for each SMU's size. The SMU size must be larger than the equipment bucket width and large relative to blast movement to allow adequate estimation and quantification of uncertainty at a scale relevant to future mining. In an open pit setting, SMUs with a height equal to that of the bench are practical for mine planning, while in an underground mine, a height equivalent to the size of anticipated lifts may be appropriate (Rossi & Deutsch, 2014).

2.2.3 Panel Scale

A panel can be defined as a group of SMUs. The SMUs need not be contiguous within the panels; however, that is the common choice. In this thesis, panels will be required for Uniform Conditioning as well as Localization. For Localization, panels are often regularly shaped, but some flexibility is permitted. The number of SMUs within each panel should be carefully determined in both cases. When regularly shaped panels are being considered, the SMU grid should nest neatly within the panel scale grid. The grids should have the same origin and rotation, and SMUs should not be split between multiple panels. The panels should be large enough to provide a reliable SMU distribution within the panel and small enough to provide local precision. There is no evident optimal panel size, but panels that are one to two times the bench height and have ten to hundred SMUs within the

panel are considered reasonable (Amihere & Deutsch, 2022). The geometry of the panels should be carefully considered. The panels should be close to large volumes that could be mined. The panels should also be as homogeneous as possible; for example, if the mineralization has a strong vertical continuity, the panels should have a significant vertical extent.

2.3 Spatial Prediction Techniques

Rock samples from drilling provide information on a mine bench's composition before blasting and excavation. It is only possible to collect samples for part of the mine bench's volume, necessitating a predictive method to estimate the grade values for unsampled locations. Predictions are usually made for regular grids of data points or blocks. Grade values are obtained at the center of each block or grid at the unsampled location using a modeling technique.

An estimation framework estimates a single value for each unsampled location within the model. Estimates are usually a weighted average of samples near the unsampled location. The challenge in this methodology is determining an appropriate weighting scheme. Distance-based methods are available, such as inverse distance or inverse distance squared, but these methods do not incorporate details of data redundancy and spatial structure. Kriging, the preferred method, calculates weights using a variogram model that quantifies the spatial relationship between all locations. Many references about many forms of Kriging are available for a more detailed explanation, including (C. V. Deutsch & Journel, 1997; Isaaks & Srivastava, 1989; A. Journel & Huijbregts, 1978; Rossi & Deutsch, 2014). Probabilistic modeling techniques provide a distribution of equally probable grade values at each unsampled location. These values represent geological uncertainties due to several factors, including limited sampling.

Misclassification of mined material occurs due to limited sampling, among other factors; however, the misclassification errors and financial consequences are often asymmetric and non-linear. Kriging assumes equal penalties for underestimation and overestimation, and therefore, should be used carefully for grade control (Srivastava, 1987). Simulation provides the distribution of uncertainty in grades to permit the asymmetric consequences of grade control decisions to be considered. The following sections will review geostatistical tools for grade control.

2.3.1 Random Variables

The basic paradigm of predictive statistics is to characterize any unsampled (unknown) value z as a random variable (RV) Z, the probability distribution of which models the uncertainty about z. A Random Variable (RV) can be seen as a variable, say, Z, that can take a series of outcomes or realizations $\big(z_i, i = 1, \ldots, n\big)$ with a given set of probability occurrence $\big(p_i, i = 1, \ldots, n\big)$. When the number n of occurrences is finite, one refers to a "discrete" RV. The n probabilities of occurrences must verify the conditions. The fundamental idea of predictive statistics is to characterize any

unsampled (unknown) value z as a random variable, the probability distribution of which models the uncertainty about z. The RV model Z and its probability distribution are typically location-dependent, as represented by the notation $Z(\mathbf{u})$, with $\mathbf{u}$ being the location coordinates vector. Moreover, the RV $Z(\mathbf{u})$ is information-dependent because its probability distribution changes as more data about the unsampled value $z(\mathbf{u})$ become available. If the number of possible occurrences is infinite, say, a grade value within the interval $[0, 100\%]$, the RV Z is said to be continuous, and its probability distribution is characterized by the cumulative distribution function (cdf) defined as:

$$F(\mathbf{u}; z) = \text{Prob}\{Z(\mathbf{u}) \leq z\} \tag{2.1}$$

When the cdf is made specific to a particular information set, for example n consisting of n neighbouring data values $Z(\mathbf{u}_i) = Z(\mathbf{u}_i), i = 1 \ldots n$, the notation "conditional to n" is used, defining the conditional cumulative distribution function:

$$F(\mathbf{u}; z|(n)) = \text{Prob}\{Z(\mathbf{u}) \leq z|(n)\} \tag{2.2}$$

Equation 2.1 models the uncertainty about the unsampled value $z(\mathbf{u})$ prior to using the information set (n); Equation 2.2 models the posterior uncertainty once the information set (n) has been accounted for. The conditional cumulative distribution function $F(\mathbf{u}; z|(n))$ is a function of the location $\mathbf{u}$, the sample size and geometric configuration (the data locations $\mathbf{u}_i, i = 1 \ldots n$), and the sample values.

The expected value is the probability-weighted sum of all possible occurrences of the RV. The expected value of Z is also called the mean of Z. The mean is a central location characteristic of the RV. The variance is a characteristic of spread of that distribution around the mean.

2.3.2 Data Assembly

To ensure reliable calculations for histograms and variograms, the area of interest or domain must be of sufficient size. Although data outside of the area of interest may be utilized, it is essential to exercise caution to ensure that only relevant data are included. Utilizing an area that is too small can compromise statistical accuracy and the robustness of resulting estimates. Conversely, considering an area that is too large can compromise local accuracy. This issue is particularly relevant when working with long-term models.

Geostatistical modeling relies on a decision of stationarity, which involves the pooling of data that are considered to belong together. This decision is not an inherent property of the data but rather a choice made by the modeler. It enables the application of statistical models, such as the histogram and variogram, over the area of interest. However, when trends are present, or the area of interest includes different features, geologic controls, or rock types, the area may be considered non-stationary. In such cases, it may be necessary to divide the area of interest into several sub-areas based on geological maps or other identifying features with similar spatial and statistical

characteristics to prevent the inappropriate pooling of data. In the absence of geological maps, observing the histogram for multiple modes or peaks, creating a probability plot of the data, and looking for kinks or breaks in the distribution can also help identify sub-areas.

Inaccurate data and outliers have the potential to impact summary statistics and modeling outcomes. Therefore, it is imperative to investigate any unusual data and, if necessary, remove it from the database or cap it to some arbitrary maximum. However, not all peculiar data should be considered outliers or erroneous, and careful examination must identify them accurately. The following steps can be employed to examine data systematically:

- Generate a frequency distribution or histogram to visualize the distribution of data.
- Calculate summary statistics such as mean, median, mode, standard deviation, and variance to gain insight into the characteristics of the dataset.
- Evaluate the minimum and maximum values of the datasets to identify any outliers.
- Examine the scatter plot of the data to detect any patterns or relationships.
- Conduct a hypothesis test to evaluate whether the observed differences in the data are statistically significant.
- Investigate the source of any outliers or erroneous data to determine whether they should be removed or modified.

Sampling bias can result in non-volume representative data, mainly when preferential sampling occurs in areas of high or low value. Conventional simulation techniques aim to replicate the histogram, but if sampling bias is not considered, it can lead to the reproduction of the bias in the uncertainty model. To account for preferential sampling, data can be declustered by weighting them according to the volume each data represents. However, declustering may not always be necessary, particularly when data is collected at regular intervals, such as in blasthole spacing.

While many variables display predictable geological trends over significant distances, trend modeling may not always be necessary for grade control due to the relatively small area of interest. Instead, deterministic rock types provide hard boundaries that require direct modeling. A rock-type model can be created using field observations, exploration data, or mapping. Trend modeling involves defining a reference datum or trend and modeling the residuals after subtracting the data from the trend. However, trend modeling should not be attempted if a trend is not evident or there is doubt about its presence.

2.3.3 Variogram Modeling

The variogram, covariance, and correlation coefficient are equivalent tools for characterizing two-point correlation (assuming stationarity). The variogram measures the spatial variability between the values of the variable at different locations. It is defined as the variance of the difference between the values of the variable at two locations separated by a given lag distance. In variogram modeling, the empirical or experimental variogram is calculated from the observed data and plotted against the lag distance. The plot of the empirical variogram reveals the spatial structure of the variable, such as the range, the sill, and the nugget effect. The range is the maximum distance at which the correlation between the values of the variable is significant. The sill is the variance of the variable. The nugget effect is the variable's variance at a distance approaching zero, which represents short-scale variability, illustrated in Figure 2.3. Any error in the measurement value or the location assigned to the measurement translates to a higher nugget effect. Sparse data may also lead to a higher than expected nugget effect (Chilès & Delfiner, 1999; Pitard, 1993). The nugget effect significantly impacts estimation, simulation, and change of support. The variogram model is

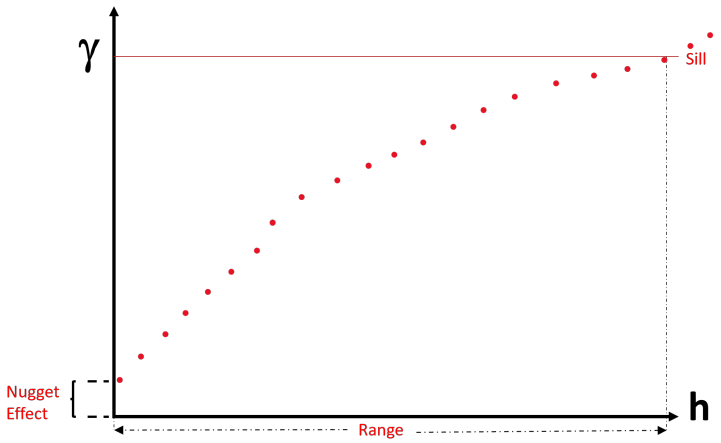

Figure 2.3: Terminologies employed for characterizing a variogram.

selected based on the shape of the empirical variogram and knowledge of the spatial process that generated the data. The most commonly used variogram models include the spherical, exponential, and Gaussian models (A. Journel & Huijbregts, 1978), see Figure 2.4. Different parameters, such as the range, the sill, and the nugget effect, characterize these models. The choice of the variogram model depends on the spatial structure of the variable, the data distribution, and the objective of the analysis. Variogram modeling is a critical step in geostatistics that allows for the quantification of the spatial structure of a variable and the selection of the appropriate spatial model. The variogram model is used to estimate the spatial correlation between the values of the variable at unsampled locations, which is essential for kriging, simulation, and risk assessment. The quality of the variogram model depends on the data quality, the model's choice, and the model's validation.

Variograms for the examples demonstrated in this thesis were calculated and modeled using the

GSLIB software. An acceptable semivariogram model for *GSLIB* consists of an isotropic nugget effect and a linear combination of the following standard semivariogram models.

1. Spherical model defined by an actual range a and positive variance contribution or sill value c.

$$\gamma(h) = c \cdot \text{Sph}\left(\frac{h}{a}\right) = \begin{cases} c \cdot \left[1.5\frac{h}{a} - 0.5\left(\frac{h}{a}\right)^3\right], & \text{if } h \leq a \\ c, & \text{if } h \geq a \end{cases}$$

2. Exponential model defined by an effective range a (integral range $a/3$) and positive variance contribution value c.

$$\gamma(h) = c \cdot \text{Exp}\left(\frac{h}{a}\right) = c \cdot \left[1 - \exp\left(-\frac{3h}{a}\right)\right]$$

3. Gaussian model defined by an effective range a and positive variance contribution value c

$$\gamma(h) = c \cdot \left[1 - \exp\left(-\frac{(3h)^2}{a^2}\right)\right]$$

Anisotropic nugget effect can also be modelled by setting some of the directional ranges of the first nested structure to a very small value. For variogram models that reach their sills c asymptotically, the effective range is defined as the distance at which $\gamma(a) == 0.95 \cdot c$ (C. V. Deutsch & Journel, 1997). To interpret the variogram, the variance which equivalent to the sill is usually plotted. There's positive correlation when the semivariogram is less than the variance, no correlation when the semivariogram is equal to the variance and negative correlation when the semivariogram points are above the variance.

2.3.4 Estimation and Probabilistic Estimations

Traditional estimation techniques can be used to assign values to blocks. Polygonal methods and Inverse Distance (ID) methods are common. For the classic polygonal method, the estimate is based on assigning estimates as the nearest borehole grade. Inverse Distance methods are a family of weighted average methods. Inverse distance methods are based on calculating weights for the samples based on the distance from the samples to the point or block of interest. The linear estimator is written as:

$$z^*(\mathbf{u}) = \frac{\sum_{i=1}^{n} \lambda_i(\mathbf{u}) \cdot z(\mathbf{u}_i)}{\sum_{i=1}^{n} \lambda_i(\mathbf{u})} \tag{2.3}$$

where $z(\mathbf{u}_i)$ is the observed value of the variable, for all sample points $(i = 1, \ldots, n)$ used in the estimation, and $z^*(\mathbf{u})$ is the estimated value of the variable at the location of interest $\mathbf{u}$. $\lambda_i(\mathbf{u})$ is the weight assigned to each observed value of the variable at a sample point (i), which is calculated as follows:

$$\lambda_i(\mathbf{u}) = \frac{1}{d(\mathbf{u}_i)^\omega} \tag{2.4}$$

where $d(\mathbf{u}_i)$ is the distance between the location of interest $\mathbf{u}$ and the sample point (i), ω is the exponent. When the weights are standardized to sum to 1 to ensure a globally unbiased estimate,

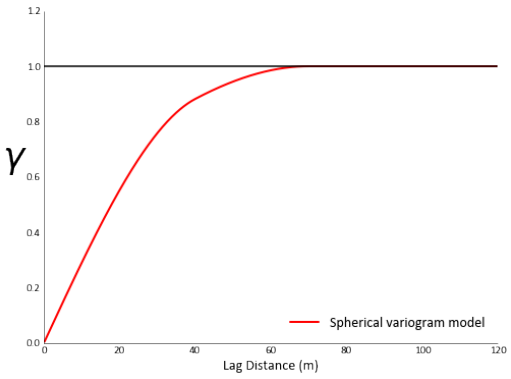

(a) Spherical variogram model.

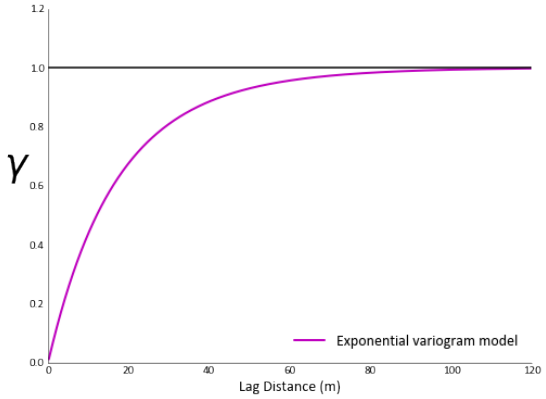

(b) Exponential variogram model.

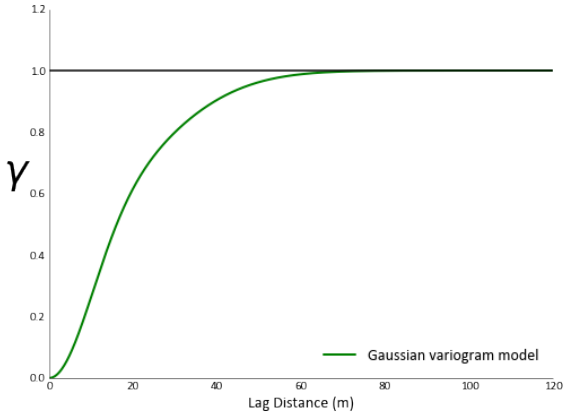

(c) Gaussian variogram model

Figure 2.4: Typical variogram structures that are combined together in nested structures to fit experimental variograms.

the formula for the weights becomes:

$$\lambda_i(\mathbf{u}) = \frac{\frac{1}{d(\mathbf{u}_i)^\omega}}{\sum_{i=1}^{n} \frac{1}{d(\mathbf{u}_i)^\omega}} \tag{2.5}$$

To estimate the value at the location of interest $\mathbf{u}$ using the standardized weights, the following formula is used:

$$z^*(\mathbf{u}) = \sum_{i=1}^{n} \lambda_i(\mathbf{u}) \cdot z(\mathbf{u}_i)$$

where $\lambda_i(\mathbf{u})$ is the standardized weight assigned to the observed value at sample point (i) and $z(\mathbf{u}_i)$ is the observed value of the variable at sample point (i).

2.3.5 Kriging

Kriging is a standard geostatistics technique for estimation and as an engine for modeling uncertainty. Kriging aims to provide the best possible estimate at the unsampled location by calculating the estimate as a weighted average for each unsampled location. The optimal weights are determined to minimize the expected error variance. There are many variations of Kriging, but the basic forms differ mostly on the assumptions they make regarding the local mean. This is expressed as conditions on the set of weights (A. Journel & Huijbregts, 1978). Despite the extensive discussion of ordinary Kriging in this thesis, various variants of Kriging exist, including:

- Simple Kriging (SK): minimizes the error variance with no constraints on the weights. The mean is a known constant (inferred from the available samples) for the entire domain.
- Ordinary Kriging (OK) : the local mean is implicitly re-estimated as a constant within each search neighborhood. OK is a common technique used to obtain interim estimates.
- Kriging with a trend model or universal kriging (KT or UK): an extension of simple kriging that assumes that the variable of interest has a deterministic trend or drift that varies spatially. Universal kriging can estimate the trend function considering the spatial correlation between sample points. It is appropriate when the variable of interest has a known trend.

In addition to these three types of Kriging methods, there are others including co-kriging, indicator Kriging, and regression Kriging. Co-kriging is used when two or more variables are spatially correlated and can be used to predict one variable from multiple variables. Indicator Kriging is used when the variable of interest is categorical, such as land use, soil type, or vegetation cover. Regression kriging is used when the variable of interest is related to other variables, such as elevation, slope, or aspect. Regression Kriging combines Kriging with regression analysis to provide more accurate estimates of the variable of interest (Isaaks & Srivastava, 1989).

The purpose of Kriging is to determine a set of optimal weights that leads to an estimate that minimizes the expected error variance. Consider the estimate of an unsampled value z($\mathbf{u}$) from neighbouring data values $\big(z(\mathbf{u}_i), i = 1, \ldots, n\big)$. The RF model Z($\mathbf{u}$) is stationary with mean m and covariance $C(h)$. In its simplest form, also known as simple Kriging (SK), considers the following linear estimator: Consider a linear estimator:

$$z^*(\mathbf{u}) = \sum_{i=1}^{n} \lambda_i(\mathbf{u}) \cdot \big[z\left(\mathbf{u}_i\right) - m\big] + m = \sum_{i=1}^{n} \lambda_i(\mathbf{u}) \cdot z\left(\mathbf{u}_i\right) + \left(1 - \sum_{i=1}^{n} \lambda_i\left(\mathbf{u}\right)\right) \cdot m \tag{2.6}$$

The weights $\lambda_i(\mathbf{u})$ are determined to minimize the error variance, also called the 'estimation variance'. (C. V. Deutsch & Journel, 1997). That minimization results in a set of normal equations (A. G. Journel, 1989):

$$\sum_{j=1}^{n} \lambda_j(\mathbf{u}) C\left(\mathbf{u}_j - \mathbf{u}_i\right) = C\left(\mathbf{u} - \mathbf{u}_i\right), \quad \forall i = 1, \ldots, n \tag{2.7}$$

The corresponding minimized estimation variance, or Kriging variance, is:

$$\sigma^2_{SK}(\mathbf{u}) = C(0) - \sum_{=1}^{n} \lambda_i(\mathbf{u}) C\left(\mathbf{u} - \mathbf{u}_i\right) \geq 0 \tag{2.8}$$

The weights differ at every location, and the final estimates are non-linear. Ordinary Kriging (OK) is the most commonly used variant of the previous simple Kriging equation, whereby the sum of the weights $\sum_{i=1}^{n} \lambda_i(\mathbf{u})$ is constrained to equal 1. This allows building an estimator $Z^*_{OK}(\mathbf{u})$ that does not require prior knowledge of the stationary mean m, yet remains unbiased in the sense that $E\left\{z^*_{OK}(\mathbf{u})\right\} = E\{Z(\mathbf{u})\}$. Non-linear Kriging is but linear Kriging performed on some non-linear transform of the z-data, e.g., the log-transform $ln\ (z)$ provided that $z > 0$.

Ordinary Kriging is based on the same minimum error variance linear estimate at a location where the true value is unknown. Contrary to SK, OK does not assume knowledge of the mean. By requiring global unbiasedness, ordinary Kriging (OK) constrains the sum of the weights to be 1.0, and as a result the mean does not need to be known. The unknown mean for the volume being estimated is assumed constant:

$$\left[z^*(\mathbf{u}) - m\right] = \sum_{i=1}^{n} \lambda_i \cdot \left[z\left(\mathbf{u}_i\right) - m\right]$$

$$z^*(\mathbf{u}) = \sum_{i=1}^{n} \lambda_i z\left(\mathbf{u}_i\right) + \left[1 - \sum_{i=1}^{n} \lambda_i\right] \cdot m \tag{2.9}$$

The condition $\sum_{i=1}^{n} \lambda_i = 1$ is the unbiasedness condition when the mean m is unknown. This is the essence of ordinary Kriging: the estimation variance is minimized because the sum of the weights is 1.0. It can be shown that ordinary kriging amounts to re-estimating, at each new location $\mathbf{u}$, the mean m as used in the SK expression. Since OK is most often applied within moving search neighborhoods, i.e., using different data sets for different locations $\mathbf{u}$, the implicit re-estimated mean denoted $m^*(\mathbf{u})$ depends on the location $\mathbf{u}$.

Kriging estimates depend on the choice of the search plan, which is the set of data used to calculate the weights of the linear combination. The search plan can be designed using criteria such as minimum variance, maximum correlation, or maximum likelihood. The choice of the search plan depends on the characteristics of the variable of interest, the sampling design, and the spatial variability of the variable.

2.3.6 Simulation

Simulation is a powerful tool used in geostatistics to generate realizations of a random variable that captures the spatial variability. Simulation can be used to explore the uncertainty associated with the variable at unsampled locations, to assess the performance of geostatistical methods, and to generate scenarios for decision-making. Simulation assumes that the variable of interest has a known covariance function that describes the spatial correlation between the values at different locations, thus allowing the generation of realizations that reproduce the variability of the underlying random function. Multiple realizations represent uncertainty about the spatial distribution of the grades. There are many simulation algorithms, and they are often nested; that is, rock types may be simulated first, then continuous grade values. The sequential Gaussian simulation (SGS) algorithm is widely used. For each location in a realization, a simulated value is drawn from the local conditional distribution and then retained to condition subsequent locations. Considering previously, simulated values preserve joint uncertainty between all locations. The realizations $z^l(\mathbf{u}), \mathbf{u} \in A, l = 1 \dots L$, represent L possible images of the spatial distribution of the attribute values $z(\mathbf{u})$ over the domain A.

Realizations are generated at the data scale, and averaging to blocks is applied to represent the SMU scale uncertainty. Sequential Gaussian Simulation requires all variables to be transformed to a standard normal (Gaussian) distribution. The conditional distribution for a variable at an unsampled location is calculated in Gaussian units. The normal equations (simple kriging) are utilized to compute the local mean and variance that define the local distribution. The conditioning includes all original data and previously simulated values available within a neighborhood. A value is drawn randomly from this distribution and retained as the simulated realization. This simulated value is also incorporated into the data set available for conditioning future distributions. This process is repeated for the entire grid, retaining a simulated value at each location to complete a realization.

2.3.7 Uniform Conditioning

This technique estimates the tonnage and grade at an SMU scale that could be extracted from larger panels. The key steps in the UC procedure include (1) fitting the data scale distribution by a series of Hermite polynomials, (2) inferring global SMU scale and panel scale distributions using the data scale distribution and the volume averaged variogram values within the SMU scale and panel scale, (3) ordinary kriging at the panel scale, (4) transforming the panel scale estimates to Gaussian units, (5) extract the distribution of Gaussian SMU values from the bivariate distribution of Gaussian panel and Gaussian SMU values, and (6) back transform the Gaussian SMU distribution at each location to original grade units. The key assumption of UC is that the bivariate distribution of the Gaussian panel and Gaussian SMU values is bivariate Gaussian defined by a stationary correlation

coefficient. This assumption requires stationarity and uniform conditioning. The ore tonnage at the SMU scale and the grade of the recoverable tonnage are calculated from the local distributions without specifying the position of the ore grade SMU blocks. To arrive at one SMU grade per SMU location, Localized Uniform Conditioning (LUC) was proposed by Abzalov (2006) to locate the SMU grades determined by the UC technique spatially. The SMU distributions within each panel are a direct input to localization.

2.3.8 Localization

Recoverable resources for both surface and underground mining at a chosen mining selectivity must be predicted from sparse exploration drill hole data. Grade control sampling at the time of mining provides orders of magnitude more data and much better estimates than possible with exploration data. Probabilistic methodologies anticipate this information effect with distributions of possible outcomes. Managing the uncertainty represented by these models is a challenge. Many mine planning operations require a single deterministic model as input. Localization creates a single model from the distribution of possible values for the unsampled locations. Localization was initially proposed as an extension of Uniform Conditioning (Abzalov, 2006), but can be straightforwardly extended to Multiple Indicator Kriging (MIK) (Hardtke, Allen, & Douglas, 2011), MultiGaussian Kriging (Daniels & Deutsch, 2014) and simulation (Boisvert & Deutsch, 2012). This thesis provides an overview of the localization process and discusses the pros and cons of the approach. An alternative to localization is to estimate a single resource model with ordinary kriging or inverse distance. The search or other estimation parameters would be restricted to calibrate the smoothing to a change of support model, as described in Chapter 3. Comparing a probabilistic model with a single resource model generated by estimation can be challenging (Amihere & Deutsch, 2022). Localizing probabilistic results, however, generates a single model consistent with the source probabilistic models.

The first step in localization is to assemble a distribution of SMU grades within each panel. Local SMU distributions within the panel are combined to form a single distribution for each panel; see Figure 2.5 for a schematic illustration. As mentioned, panels are often defined as a rectangular volume containing 10s to 100s of SMUs. The panel size does not depend on details of the mining operation, the mine plan, the equipment size, or other considerations. The SMUs should nest neatly within the chosen panel grid. Ultimately, localization aims to have one SMU grade for each SMU grid location. The second step is to discretize each panel's combined distribution of SMU grades. The aim is to extract the exact number of grades from the distribution as there are in the panel. The number of SMUs in each panel can vary because of intersecting geological boundaries. In any case, the number of discretization classes considered equals the number of SMUs within a panel. Each grade class is of equal probability. The mean, median, or randomly drawn values are kept

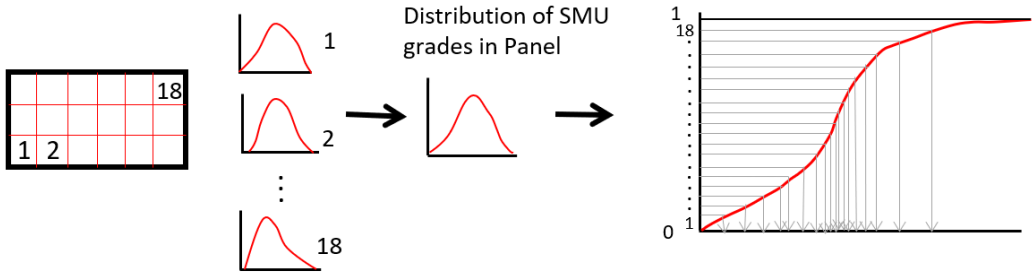

Figure 2.5: The local distribution of each SMU within the panel is combined to a panel scale CDF,then discretized by grade class, a regularly defined panel containing eighteen SMUs is used in this example. Modified after Boisvert and Deutsch (2012)

.

from each grade class. Using the mean is straightforward and unbiased. This step results in a set of SMU grades for each panel - the exact number required for each panel is illustrated in Figure 2.6. The third and final step is to assign each of the chosen SMU grades to an SMU in the panel. Each panel is processed one at a time. It would be a bad idea to assign the SMU grades to random SMUs in the panel; the result would be very noisy. It would be a bad idea to assign the SMU grades in a regular order starting from the bottom left corner; the result would look very odd with artifact stripes. The central idea of localization is to place the low values in lower grade areas of the panel and the high values in high grade areas of the panel. A ranking or localizing variable achieves this purpose. Commonly, ordinary kriging at the SMU block scale is used to determine the ranking Hardtke et al. (2011), or for simulation, the e-type model could be used. This necessitates performing a kriging run separately from the determination of SMU uncertainty. The final model does not directly include the kriged grades, avoiding smoothing the histogram. The lowest SMU value determined in step two is placed in the lowest SMU from the localized kriged grade in the panel. The value from the second grade class is assigned to the SMU ranked second according to the kriged grade. This is repeated until each SMU has a grade. The result is a single localized model considered representative of the SMU distributions within each panel (Boisvert & Deutsch, 2012), as portrayed in Figure 2.7. The localized model shows a similar grade distribution configuration compared to the localized realizations. One of the main disadvantages of localization is the noticeable abrupt changes in values at the boundaries of adjacent panels. These discontinuities occur because each panel is processed independently of the information from the surrounding panels. Suppose there is a pattern or trend that extends across multiple panels. In that case, the highest values in one panel will likely be next to lower values in an adjacent panel, resulting in these irregularities at the boundaries.

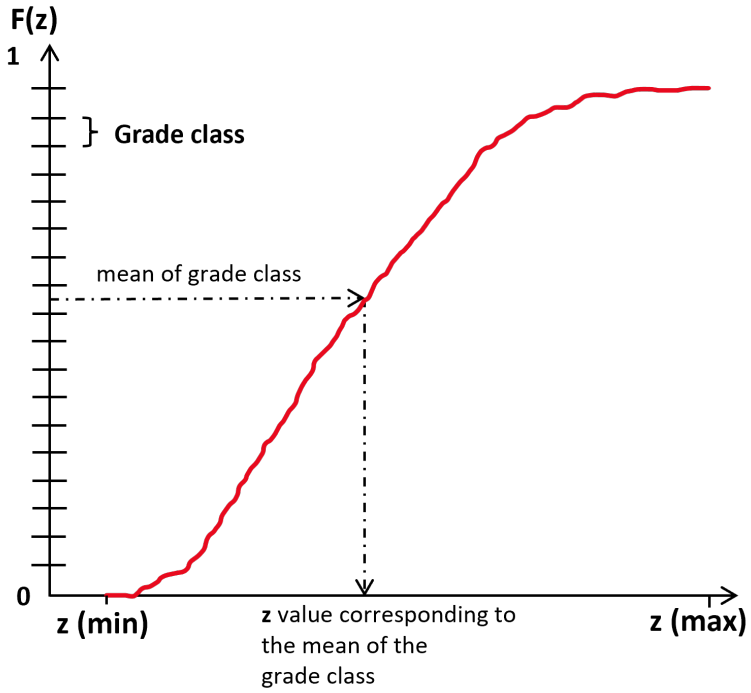

Figure 2.6: The CDF illustrated represents a panel containing 18 SMUs. The appropriate value from each grade class is assigned to an SMU based on its relative rank within the panel. Ranking is usually determined by ordinary kriging. Modified after (Daniels & Deutsch, 2014)

.

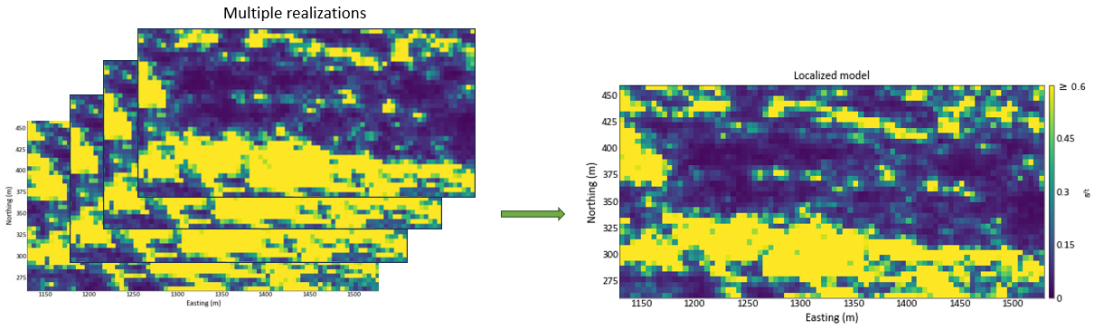

Figure 2.7: An example of a set of realizations localized to a single model. Units are arbitrary for this synthetic example.

2.4 Volume Variance Relation

The data collected for estimation only represents a small volume relative to the relevant volume at the time of mining. There is grade variability at any scale within a deposit. At the data support, the variance of the distribution is greater than the variance of the block distribution for the same attribute or variable. A change of support model forecasts how grade distributions alter with varying volume support, considering only the data and statistical information from the composited drill hole data. As defined earlier, the SMU may be considered the smallest volume on which ore or waste classification is made for a mining operation. A typical three meter long diamond drill core sample represents 5-25 kg of material. In contrast, an open pit SMU of, say, $5m \times 5m \times 10m$ may represent 675 tonnes of material with a specific gravity of 2.7. This significant increase in support from the data and the SMU is an important consideration when estimating long-term resources. To test the volume variance relation for different SMU sizes, a synthetic dataset, as seen in Figure 2.8 (left), is used to perform ordinary Kriging using Equation 2.10, a spherical variogram model with a maximum range of 305m in the principal direction and a maximum range of 47m in the minor direction. The azimuth of the principal direction is 100°. Figure 2.8 (right) illustrates the modeled variograms.

$$\gamma(\mathbf{h}) = 0.3 + 0.384 \cdot \underset{\substack{a_{hmin}=9.07}}{\text{Sph}_{a_{hmax}=12.1756}} + 0.316 \cdot \underset{\substack{a_{hmin}=47.84}}{\text{Sph}_{a_{hmax}=305.43}} \tag{2.10}$$

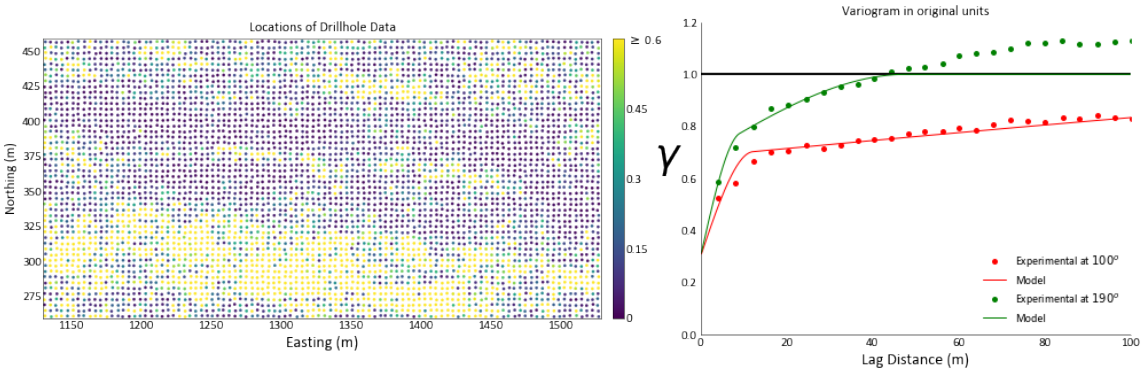

Figure 2.8: location map of data (left), Variogram plot of data (right)

Figure 2.9 shows the resulting grade distribution for the ordinary kriged models for two SMU supports. The black curve represents the distribution of the data support, indicating the variability in grades. The shaded portions in represent regions under the probability density functions (PDFs) of the distributions. The red curve represents a smaller SMU support with reduced variability, while the green curve represents a larger SMU support with even less variance. If the cutoff grade(z_{c2}) is below the mean grade of 0.468 g/t, the estimated tonnage above this cutoff will increase as support size increases. Conversely, when the cutoff grade (z_{c1}) is set above the mean grade of 0.468 g/t, the estimated tonnage exceeding this cutoff will decrease as the support increases, see Table 2.1. Thus, accurately anticipating the appropriate change of support is crucial for estimating resources at an

SMU support level.

Cutoff	Small SMU size Tonnage(tonnes)	Large SMU size Tonnage(tonnes)
0.2 g/t (z_{c2})	1263384	1339200
1.0 g/t (z_{c1})	254880	248400

Table 2.1: Impact of support size on estimated tonnage at different cutoff grades.

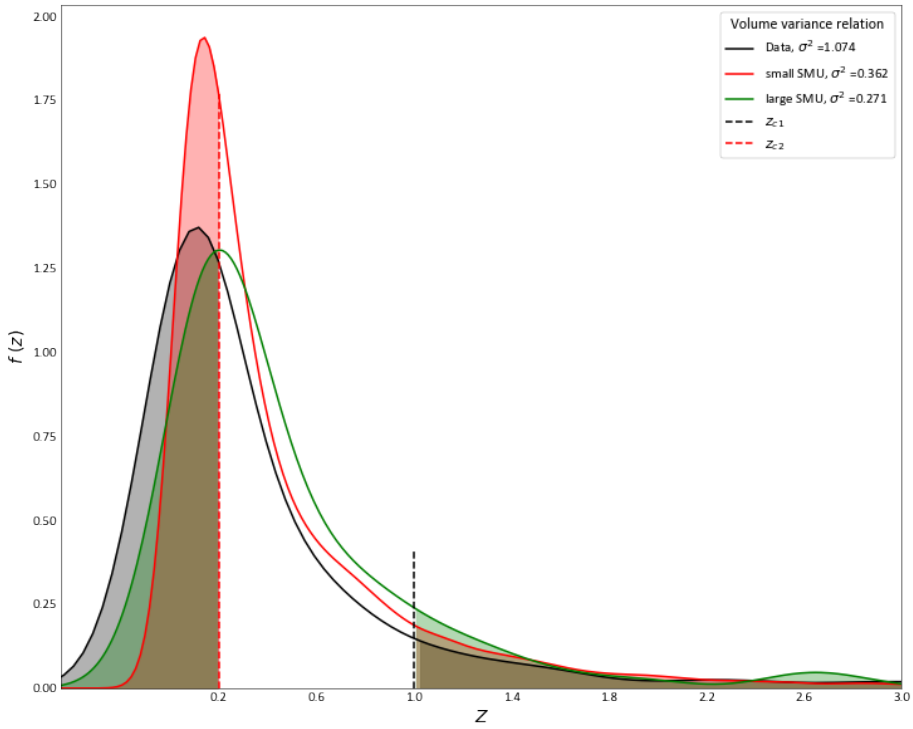

Figure 2.9: As support increases, the variance of the distribution decreases, which influences the total proportion above or below a defined cutoff.

Understanding how a grade distribution will change when scaled up to a larger support level is essential in evaluating recoverable resources. Krige's relation and the additivity of variances provide insights into how variance changes with support (Harding & Deutsch, 2019). The average variogram, $\overline{\gamma}(\mathbf{V}, \mathbf{V})$ is the expected variance of points inside a volume V and can be calculated from the variogram model and the SMU geometry. By incorporating the volume variance relation, it becomes possible to derive a grade distribution that accurately represents what will be mined. This information serves as a valuable target for estimating the recoverable reserves.

2.5 Grade Control Decision Making

The errors associated with an estimate can be defined as $e(\mathbf{u}) = z^*(\mathbf{u}) - z(\mathbf{u})$, where $z^*(\mathbf{u})$ is an estimated value and $z(\mathbf{u})$ is the true value at a location $\mathbf{u}$ in a domain A. Then, the loss from this error can be defined by a loss function (A. G. Journel, 1989). The quadratic loss function is well-known:

$$L(e(\mathbf{u})) = e^2(\mathbf{u}) \tag{2.11}$$

Where $e(\mathbf{u})$ is the variance of estimation at a location $\mathbf{u}$. The mean of a distribution minimizes the quadratic loss function regardless of the distribution shape. Simple kriging computes a conditional mean and theoretically minimizes the quadratic loss function between the true and estimated values. Also, the mean value of multiple realizations at a location $\mathbf{u}$ minimizes the quadratic loss function (Glacken, 1996). A. G. Journel (1984) proves that if the loss function is linear and asymmetric, the optimal estimate decision will be a p quantile of a distribution instead of the median. This can be understood as if, for example, underestimation is penalized more than overestimation, the value minimizing the estimation error is above the mean. An example of such a loss function is in Figure 2.10. The p quantile can be calculated using the following expression (A. G. Journel, 1984):

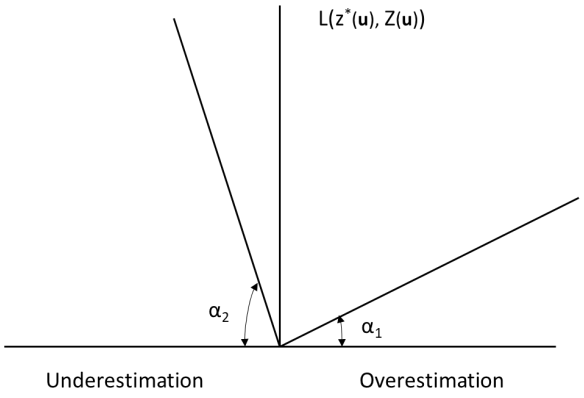

Figure 2.10: Angles determining the rates for the overestimation and underestimation errors, respectively for an asymmetric loss function modified after A. G. Journel (1984).

$$p = \frac{\alpha_1}{\alpha_1 + \alpha_2} \tag{2.12}$$

Where α_1 and α_2 represent the angles determining the rates for the penalty of overestimation and underestimation errors, respectively. It is impossible to correctly classify all unsampled locations because of sparse sampling and geologic variability. The idea is to maximize the expected profit. Estimation methods like kriging and inverse distance are extensively used in grade control, as they are shown to be reasonable estimators. However, they do not account for uncertainty, possible non-linearity of recovery, and asymmetry in the profit function (e.g., more profit assigned to a correct ore or waste decision). This is achievable by assessing the uncertainty in profit through a proper profit function. Minimum expected loss and maximum expected profit yield the same classification

of mined material in a risk-neutral situation. Since we are mining for profit, using expected profit for selection is correct.

2.6 Codes

The appendix section illustrates a comprehensive collection of codes utilized in various stages of data analysis, modeling, simulations, and any other relevant calculations. These codes have been appropriately referenced and documented to ensure transparency and reproducibility. Some of these codes were obtained from external sources, while others were personally developed for this research. These self-authored codes were created to address specific requirements and contribute to the overall methodology of this thesis. These codes were included to provide a detailed understanding of the computational procedures involved in this research and enable readers to replicate and verify the results obtained.

Chapter 3

Grade Control

To ensure efficient mining operations and maximize profitability, grade control becomes a crucial aspect that involves several technical processes and methodologies. Geological modeling is a significant element of grade control, which involves constructing three-dimensional models of the ore deposit using geological data obtained from drilling, sampling, and mapping. The geological model helps identify the boundaries of the deposit and the variations in ore grade. After establishing the geological model, miners can create mine plans considering the ore grade variations, rock type, mining method, and equipment selection. During the mining process, techniques such as drilling and blasting, sampling and assaying, and geostatistical analysis are used for grade control. Drilling and blasting break up the rock to access the orebody, while sampling and assaying determine the ore grade.

3.1 Sampling for Grade Control

To ensure the accuracy of grade control samples, they should be collected in a reproducible, unbiased, safe, and timely manner. The sampling strategy should be designed to provide reliable information about the mineral grade. Different methods for grade control sampling are discussed in (Dominy, 2010). Data collection and quality depend highly on the mining method and, to some extent, the geometry of the orebody being mined. The needs of the orebody and practicality determine the spacing of grade control samples. A small-scale operation that deals with coarse-gold and high-nugget mineralization usually requires a closely spaced sampling to capture small-scale variations. When enough sample data are available, variograms can be constructed to determine the optimal sample spacing. Open pit mines commonly use blast holes as the primary data source for grade control while occasionally using reverse circulation drilling. In contrast, underground mining methods typically provide little to no flexibility for ore and waste selection during extraction. Once a stope is designated as ore, the entire stope is typically considered ore, including planned and unplanned dilution (Rossi & Deutsch, 2014).

3.2 Modeling Grade Control Data

The process of modeling grade control data can be carried out using conventional or geostatistical methods. To minimize errors, grade control methods should consider all possible sources of error, not just the prediction error of the in-situ grade. The grade control process involves three fundamental aspects: data collection and quality assessment, grade control modeling to determine ore and waste boundaries, and consideration of operational procedures and constraints. Mineral resource estimates are subject to ongoing modifications based on new information, and precision requirements may change as mining operations commence. Selecting ore versus waste is a crucial geological determination that is final and unalterable. Kriging-based methods can fail if not implemented correctly, and using minimum-variance estimation methods with a symmetric loss function may be inappropriate since sending waste to the plant generally has a different cost compared to sending ore to the waste dump (A. G. Journel, 1989; Srivastava, 1987). The effectiveness of grade control models depends on mining practices and methods. It is essential to consider whether a mining operation can use more advanced grade control methods before implementing them. While these methods may offer improved ore/waste selection, if the mining method and operational practices cannot utilize the additional detail, it may not be worth the effort. Examples are provided in this chapter, where various methods, such as ordinary Kriging with different search plans, sequential Gaussian simulation, localized uniform conditioning, and localized sequential simulation, are applied to demonstrate their effectiveness.

In order to ensure that these models are accurate and reliable, it is important to use a range of statistical measures to assess their precision and accuracy. Here are some of the ways we can measure the accuracy and precision of geostatistical modeling techniques:

- K-fold: The basic idea of k-fold cross-validation is to divide the available data into k subsets of equal size, or as close to equal as possible. One of the subsets is then held out as a validation set, while the remaining k-1 subsets are used to train the prediction model. This process is repeated k times, with each subset serving once as the validation set, and the results are averaged over the k iterations to obtain an overall estimate of model performance (Hengl, 2009).

- Mean Square Error (MSE): Due to sampling and short scale variability, there will always be differences between predicted values and the true values. The MSE is commonly used to measure this difference. It calculates the average of the squared differences between the predicted and actual values. The coefficient of determination (R^2) is also a measure closely related to the MSE, and it can be utilized to assess the proportion of variation in the dependent variable that can be predicted from the independent variable. A high R^2 value indicates a strong correlation between the predicted and actual values, while a low R2 value indicates that

the model is not accurate (Montgomery, Peck, & Vining, 2012).

- Variogram analysis: Variogram analysis is used to assess the spatial correlation between data points. By comparing the spatial correlation of the modelled data against actual data, we can assess the accuracy of the model and identify areas of potential error.

Using these and other statistical measures, we can assess the accuracy and precision of geostatistical modeling techniques and identify areas where improvements can be made. Figure 3.1 shows a plot of the estimated grades and the true grades based on a specified cutoff grade, allowing distinguishing between two destinations: ore and waste. This defines four scenarios for a location being estimated: correct acceptance (CA), false positive (FP), correct rejection (CR), and false negative (FN). The cutoff grade is shown as a vertical dashed line. The correct acceptance region corresponds to the cases where both the estimated and true values are above the cutoff grade, and the material is classified as ore. The correct rejection region corresponds to the cases where both the estimated and true values are below the cutoff grade, and the material is classified as waste. The false positive region corresponds to the cases where the estimated value is above the cutoff grade. However, the true value is below the cutoff grade, resulting in waste being incorrectly classified as ore. The false negative region corresponds to the cases where the estimated value is below the cutoff grade. However, the true value is above the cutoff grade, resulting in ore being incorrectly classified as waste. The goal of grade control is to minimize the number of points in the false positive and false negative regions while maximizing the correct classifications. This can be achieved through the use of appropriate estimation techniques. In practice, we do not know the true grades, but techniques can be calibrated with synthetic true models.

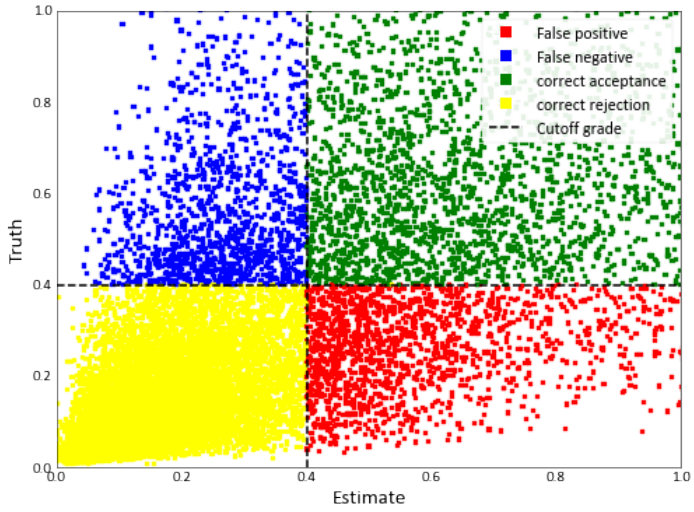

Figure 3.1: An illustration depicting four scenarios for ore and waste decisions, which classify an estimate when compared to a reference model.

3.3 Profit Conversion

The primary objective of a mining company is to maximize profit. However, this can be a challenging task due to the inherent uncertainty in the spatial distribution of variables. Traditionally, mines have relied on cutoff grades or probability of ore thresholds for their grade control. To enable a grade control program that utilizes profit as a metric, it is necessary to convert the uncertainty in grade into uncertainty in profit. Classification should account for the risk of misclassifying the material. Transforming the distribution of uncertainty in grade to a distribution of uncertainty in profit accounts for this risk. The cutoff based grade to profit conversion requires some parameters:

- Grade ($z(\mathbf{u})$): the observed value of the variable at a location $\mathbf{u}$
- Recovery of grade (r) : in most mines the recovery varies with grade. Often, the recovery increases with increasing grade.
- Selling price (p): the selling price per unit of mineral or metal produced.
- Cost of processing (c_p)
- Cost of mining (c_m)
- Cutoff grade (z_c) : in general the cutoff grade is defined as the grade at which the cost/profit is equal for the mine to process the material as ore or mine it as waste. Market conditions, the plant recovery, mining costs, administration costs, and contract obligations dictate the cutoff grade. The cutoff grade is calculated using the following expression:

$$z_c = \frac{c_p}{r \cdot p}$$

Two separate profit functions can be computed for a simple case of grade control estimates being converted to profits based on a specified cutoff grade and two possible destinations for mined material, either to be sent to the plant or waste dump. One function determines the profitability of sending material to the ore destination; the other determines the decision to send it to the waste destination. Figure 3.2 illustrates the slope of the profit functions. With this, grades can be converted to profit as follows. The constant is the maximum absolute value between the C_T and C_w. This is added to ensure all profit values are positive.

$$P(\boldsymbol{u}) = \begin{cases} C_t + (\frac{C_w - C_t}{z_c}) * z(\mathbf{u}) + constant & \text{value for ore destination; based on estimates} \\ C_w + constant, & \text{value for waste destination ; regardless of the estimates} \end{cases} \tag{3.1}$$

Classified as ore if the expected profit of ore, $EP(\mathbf{u})_{ore}$ is greater than the expected profit of waste, $EP(\mathbf{u})_{waste}$ otherwise waste. Considering a stationary domain A, there are $g = 1, \ldots, G$ true grade

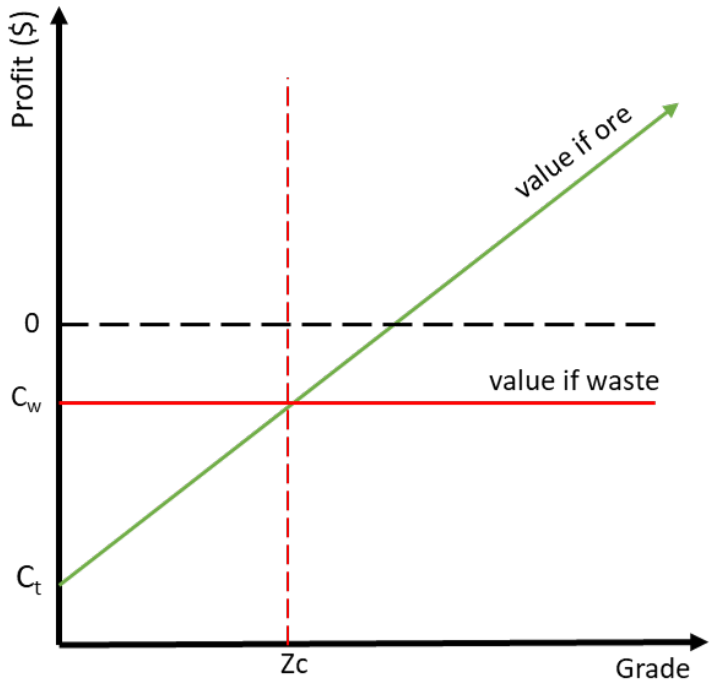

Figure 3.2: Profit function model for a scenario with two destinations for mined material

values associated with each location $\mathbf{u} \in A$. It should be noted that there is a single true grade of the variable at any point in time, but limited geologic information leads to uncertainty in the true grades. Of course, the true grades and true profit values are inaccessible. A carefully applied geostatistical framework would provide L realizations of grades that accurately and precisely represent uncertainty in the true values. The number of possible true grades $z_{\text{true}}(\mathbf{u})$ that can be observed at a location $\mathbf{u}$ in the domain A is expressed as:

$$z_{\text{true}}(\mathbf{u}; g), g = 1, \ldots, G, \mathbf{u} \in A \tag{3.2}$$

The true grades permit calculating true profit for every destination $k = 1, \ldots, K$ through a profit function P :

$$P_{\text{true}}(\mathbf{u}; k) = P\left(z_{\text{true}}(\mathbf{u}; g), g = 1, \ldots, G; k\right), k = 1, \ldots, K, \mathbf{u} \in A \tag{3.3}$$

The true optimal destination at each location is the one that maximizes the true profit:

$$d_{\text{true}}(\mathbf{u}) = \max k \text{ of } \left(P_{\text{true}}(\mathbf{u}; k), k = 1, \ldots, K\right), \mathbf{u} \in A \tag{3.4}$$

The true cumulative profit over the domain is written as:

$$CP_{\text{true}} = \sum_{\mathbf{u} \in A} P_{\text{true}}\left(\mathbf{u}; d_{\text{true}}(\mathbf{u})\right) \tag{3.5}$$

In the case of SGS, it could provide L realizations that accurately and precisely predicts uncertainty

in the true grades.

$$z^l_{true}(\mathbf{u};g), \mathbf{u} \in \mathrm{A}, g = 1, \ldots, G, l = 1 \ldots, L \tag{3.6}$$

The expected profit for each destination at each location could be calculated as follows:

$$EP(\mathbf{u};k) = \frac{1}{L}\sum_{l=1}^{L} P\left(z^l(\mathbf{u};g), g = 1, \ldots, G; k\right) \tag{3.7}$$

The optimal destination for each location would be calculated from the expected profit:

$$d_{\mathrm{opt}}\ (\mathbf{u}) = \max k \text{ of } (EP(\mathbf{u};k), \mathrm{k} = 1, \ldots, k), \mathbf{u} \in \mathrm{A} \tag{3.8}$$

The cumulative profit based on these optimal destinations maximizes the expected profit (a sum of maximum values is the maximum of the sum).

$$CP_{\mathrm{opt}} = \sum_{\mathbf{u}\in\mathrm{A}} EP\left(\mathbf{u}; d_{\mathrm{opt}}(\mathbf{u})\right) \tag{3.9}$$

Given unavoidable uncertainty and differences between $\mathrm{d_{opt}}\ (\mathbf{u})$ and $\mathrm{d_{true}}\ (\mathbf{u})$ at some locations, the optimized cumulative profit must be less than the true cumulative profit:

$$CP_{opt} < CP_{true} \tag{3.10}$$

Various numerical metrics can be used to express the performance of estimators, including total misclassification, total profit loss or loss from a mine bench, mean squared error, maximum attainable profit, and others. The profit function regulates the expected profit with each grade control decision. Provided the geostatistical realizations are truly accurate and precise, the expected profit should be close to the true profit over multiple locations. There will be differences due to incomplete sampling and short-scale variability. A measure of error could be written as:

$$MSE_{\mathrm{profit}}\ = E\left\{\left(EP(\mathbf{u};k) - P_{\mathrm{true}}\ (\mathbf{u};k)\right)^2\right\} > 0, \mathbf{u} \in A, k = 1, \ldots, K \tag{3.11}$$

As written, this MSE is across all locations and destinations. The mean squared error would depend on the amount of local data and the quality of the geostatistical approach. Percentage of misclassified errors (PME) is also calculated as:

$$PME = \frac{\text{number of } \mathbf{FN} \text{ blocks } + \text{ number of } \mathbf{FP} \text{ blocks}}{\text{total number of blocks}} \times 100\% \tag{3.12}$$

Maximum attainable profit for each model is calculated as the cumulative profit for ore divided by the cumulative maximum profit.

$$\frac{\sum P\left(z(\mathbf{u}); k = 1\right)}{\sum \max k \text{ of } \left(P\left(z(\mathbf{u}); \mathbf{k} = 1, \ldots, k\right)\right.} \tag{3.13}$$

This calculation indicates the highest profit that can be achieved by the model, considering the total profit generated from the available resources. By comparing the cumulative profit with the cumulative maximum profit, the analysis allows for assessing the efficiency and performance of each model in terms of profit generation.

3.4 Dig Limits

Dig limit optimization is a component of short-term mine planning as it is implemented daily on the grade control model. Recognizing that block models provide a deeper understanding of deposit characteristics, it is established that generating dig limits based on these block models constitutes the optimal approach. A computational algorithm can develop semi-automatically dig lines (Neufeld, Norrena, & Deutsch, 2005). While all issues are unlikely to be addressed, defining dig lines can be sped up. It is expected, though, that a degree of manual intervention and validation will always be required. The process of automatically defining dig limits is based on pre-defined operational and selection criteria. The optimal dig limits can be posed as an optimization problem. Sequential annealing could be applied by defining the objective function as:

$$O_{\text{global}} = O_{\text{profit}} - O_{\text{digability}} \tag{3.14}$$

The initial profit is calculated as the sum of all fractional blocks that are considered ore (profitable):

$$O_{profit} = \sum_{ix=1}^{nx} \sum_{iy=1}^{ny} \text{frac}_{(ix,iy)} \cdot \bar{P}_{(ix,iy)} \tag{3.15}$$

Where $\bar{P}$ represents the profit assigned to each block in the model, and "frac" represents the volume within each profitable block.

The initial digability is calculated based on the characteristics of the mining equipment, taken for example from an equipment curve, and interpreted as the sum of the penalties for each angle in the ore/waste polygon, see Figure 3.3:

$$O_{\text{digability}} = \sum_{iv=1}^{nv} \text{pen}_{iv} \tag{3.16}$$

Using simulated annealing, the vertices and angles can be moved within a small circle (tolerance) to change the angle that it defines, and thus changing the penalty and overall profitability.

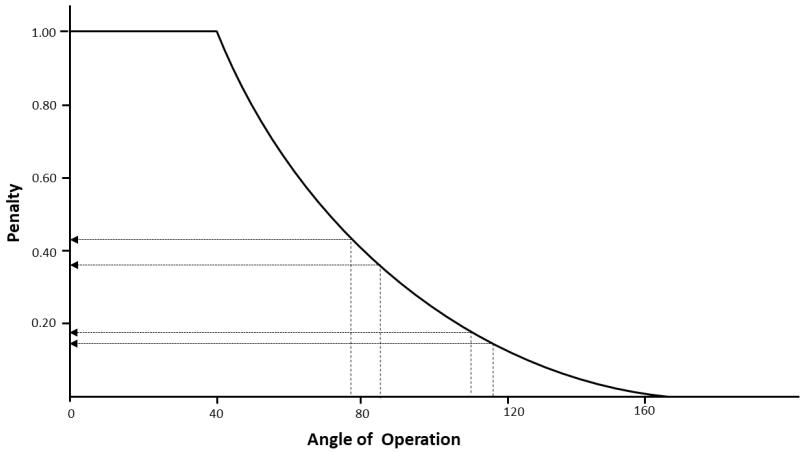

Figure 3.3: An example of how penalties can be assigned based on the angle of operation of the shovel, Modified after Rossi and Deutsch (2014).

3.5 Optimal Grid Size Relative to Data Spacing

In order to develop a practical methodology to determine a maximum reasonable 'Kriging grid size/sampling data spacing' ratio, a theoretical experiment has been conducted. The fundamental paradigm relating to grid size and sample spacing holds that while finer or high resolution kriging grid sizes improves estimation quality, it also results in a large increase in processing time. The common practice has always been based around one third of the sample spacing. The goal of this theoretical experiment will be to calculate the impact of the kriging grid size / data spacing ratio on the amount of estimation errors. An initial study is developed that consists of the following steps:

- Simulate a high-resolution realization accounting for all regional geological controls, trends, and available data. The resolution of the realization is at a $1m \times 1m \times 10m$ grid that spans a domain size of $400m \times 200m \times 10m$.
- Sample the realization at a regular spacing of $4m \times 4m$. Some reasonable error can be added to the values sampled from the reference distribution constructed in Step 1 to mimic the influence of sampling errors. A 1% sampling error is added.
- Calculate and model the experimental variograms for the sampled data .
- Perform ordinary Kriging conditional to the sampled data using $kt3dn$ with sequentially varying grid sizes. Twenty four grid sizes varying between $1m \times 1m \times 10m$ and $15m \times 15m \times 10m$ is observed.
- Convert the estimates to profits using an appropriate profit function. The profit function described in Equation 3.1 is used.
- Perform re-gridding the estimated values to the initial grid size of the reference distribution ($1m \times 1m \times 10m$). As the estimation is performed on a coarser grid than the reference distribution, in order to check each block of an estimate on the matter of false negatives and false positives based on a cutoff grade of 0.2g/t, the Kriging estimates should be re-gridded to $1m \times 1m \times 10m$ grid size.
- Calculate the percentages of the misclassified errors in profits based on Equation 3.12.

Figure 3.4 illustrates a map of the kriged estimates for some selected grid sizes. As depicted in the graph presented in Figure 3.5(a), the minimum PME value was from OK using a grid/ block size of 1m. There is no clear pattern observed in PME values for grid sizes larger than 2 meters. It can be suggested that further reducing grid sizes below the minimum 1-meter block size may lead to even lower PME values. However, it's important to note that geostatistical models are designed at suitable scales, as using excessively small block sizes can introduce fine-scale variations in grades, making it difficult to discern trends or deposits. Additionally, mining operations are conducted at

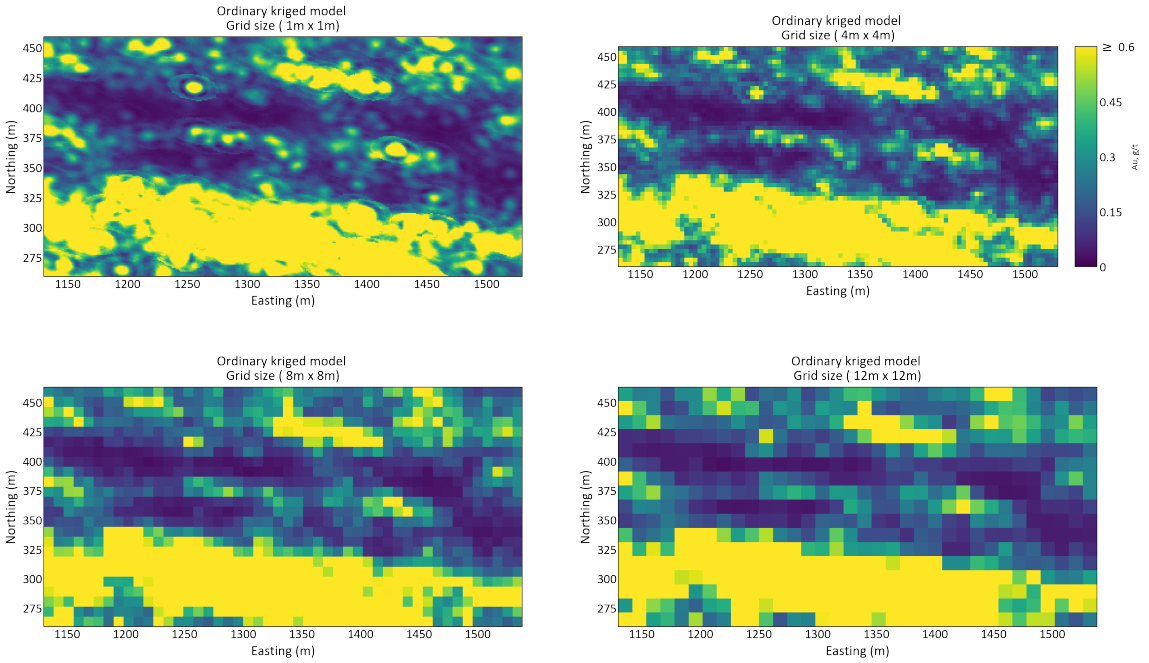

Figure 3.4: Map of ordinary Kriging estimates for different grid sizes.

an appropriate SMU size, which is often influenced by the equipment bucket size. In this case, a 1-meter block size proves sufficient to avoid excessive small-scale grade variability. Since the sample spacing is 4m, the conclusion is that the minimum PME values are evident within the range of 1/4 to 1/2 of the kriging grid size to data spacing ratio, Figure 3.5(b). Larger grid sizes results in an increase in the PME values and hence there's the need to choose an appropriate grid size.

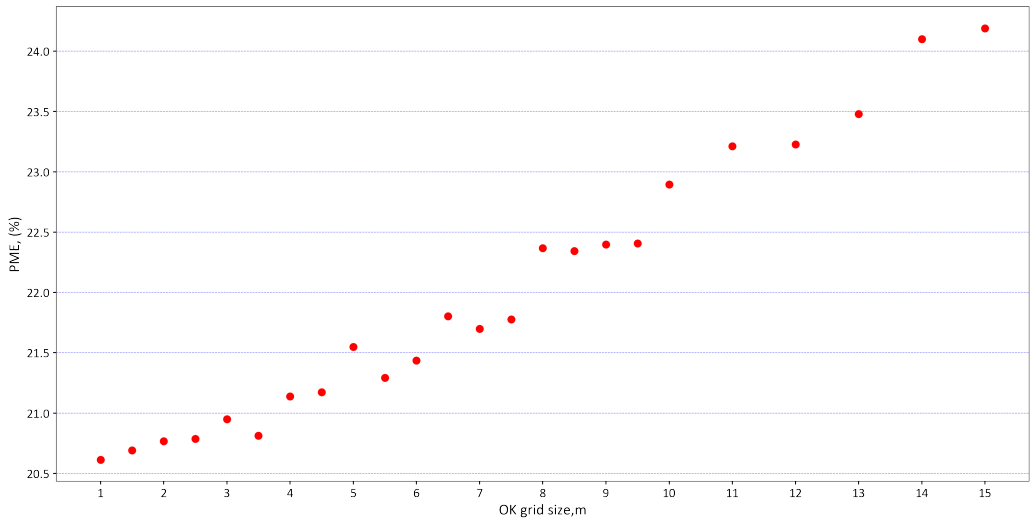

(a) PME versus OK grid size.

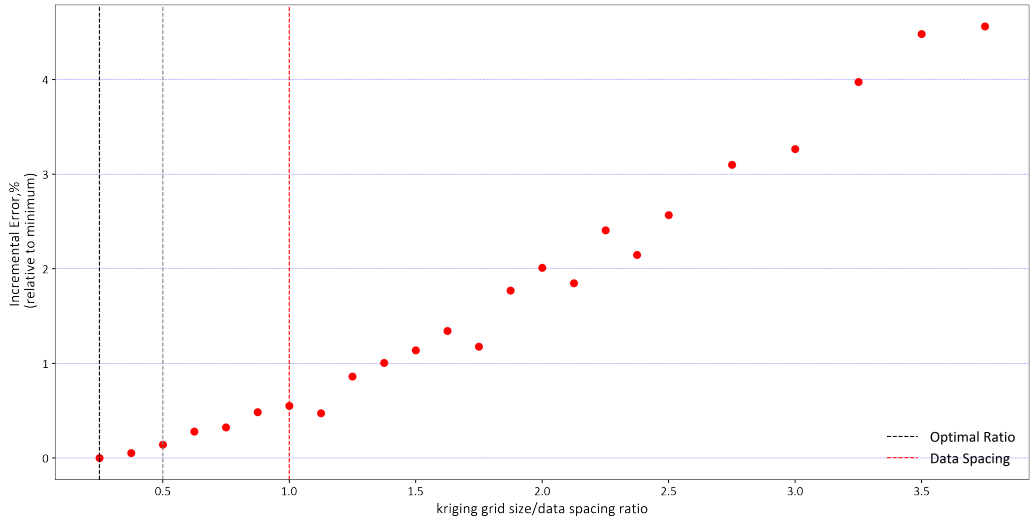

(b) Incremental error versus Kriging grid size/ data spacing ratio.

Figure 3.5: Experimental results for error with different grid size.

3.6 Generating Reference Distributions

In order to develop a practical methodology to review techniques used to create models for estimation, an initial study is developed that consists of the following:

- Simulate a high-resolution realization accounting for all regional geological controls, trends, and available data. The resolution of the realization is at a $1m \times 1m \times 10m$ grid that spans a domain size of $400m \times 200m \times 10m$. Two hundred realizations are generated using $SGSIM$. By generating two hundred realizations, uncertainty in grades are accounted for the set of influencing factors.

- Sample the reference realization at the anticipated grade control spacing. In this case the sample spacing is $4m \times 4m$. Some reasonable errors can be added to the values sampled from the reference distribution constructed in Step 1 to mimic the influence of sampling errors. A 1% sampling error is added.

- Calculate and model experimental variograms for each sampled dataset.

- Perform ordinary Kriging with different search plans, sequential Gaussian simulation, localized uniform conditioning, and localized sequential Gaussian simulation.

- Convert the estimates to profits using an appropriate profit function. The profit function described in Equation 3.1 is used.

- Perform re-gridding the estimates from the reference distribution to the initial grid size of the grade control models. As the estimation is performed on a coarser grid than the reference distribution, the reference distribution is re-gridded in order to check each block of an estimate on the matter of false negatives, false positives, mean square error, percentage of maximum attainable profit, and percentage of misclassified errors based on specified cutoff grades.

- Plot the grade control results using different estimation techniques in a series of graphs of grade tonnage curves, percentage of maximum attainable profits, mean squared errors, and total misclassification.

- Review each of the methods and apply recommendations made in a practical setting.

Figure 3.6 outlines the workflow employed for the executed examples aimed at evaluating the effectiveness of estimators for grade control modeling.

To implement the methodology, dataset containing 881 gold values, having a mean of 0.425 and a standard deviation of 1, is utilized to generate 200 realizations that are conditional on the data. The location map and histogram of the conditioning data are displayed in Figure 3.7. This data is available in the CCG data repository, which is used for research purposes. Equation 3.17 outlines the

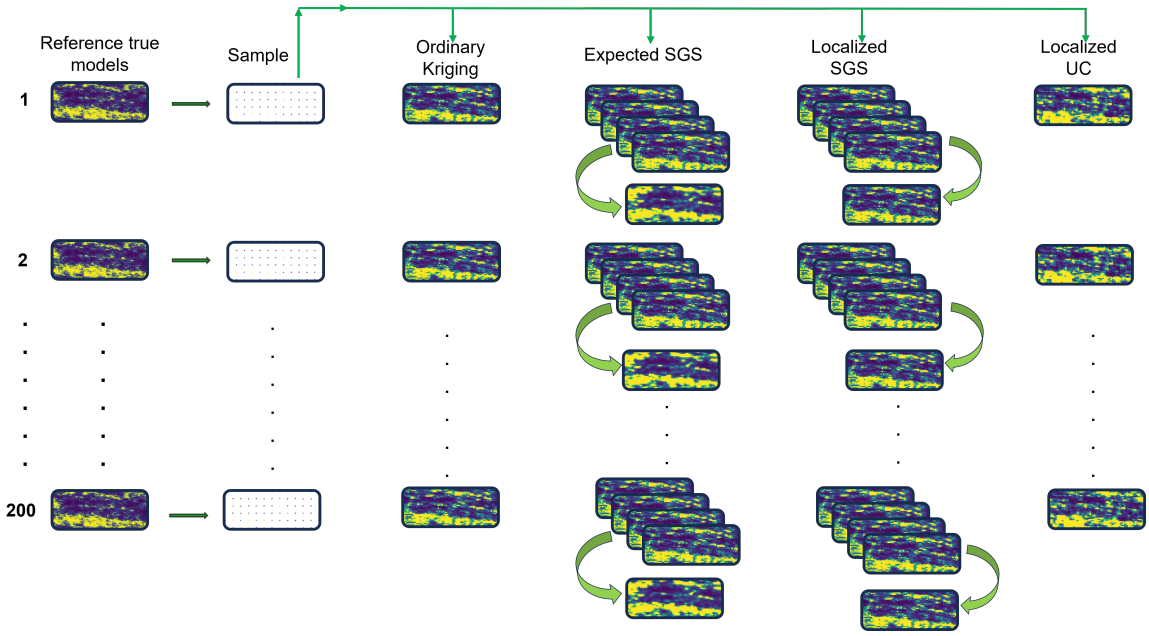

Figure 3.6: Illustration of workflow to generate grade control models.

parameters employed to model the experimental variograms. Variograms are calculated and modeled in two directions: a major direction with an azimuth of 100 degrees and a minor direction with an azimuth of 190 degrees. Two spherical variogram structures are utilized for the major direction, with a minimum range of 40m and a maximum of 325m. Similarly, the minor direction requires two spherical variogram structures, with a minimum range of 13m and a maximum range of 22m. Figure 3.8 visually represents the variogram map and depicts a plot of the modeled experimental variograms derived from the original data. The variogram of the dataset in Gaussian space is utilized for simulation in Gaussian units using the GSLIB *SGSIM* program. The resulting simulated values are then transformed back to lognormal units and checked for histogram reproduction, as shown in Figure 3.9.

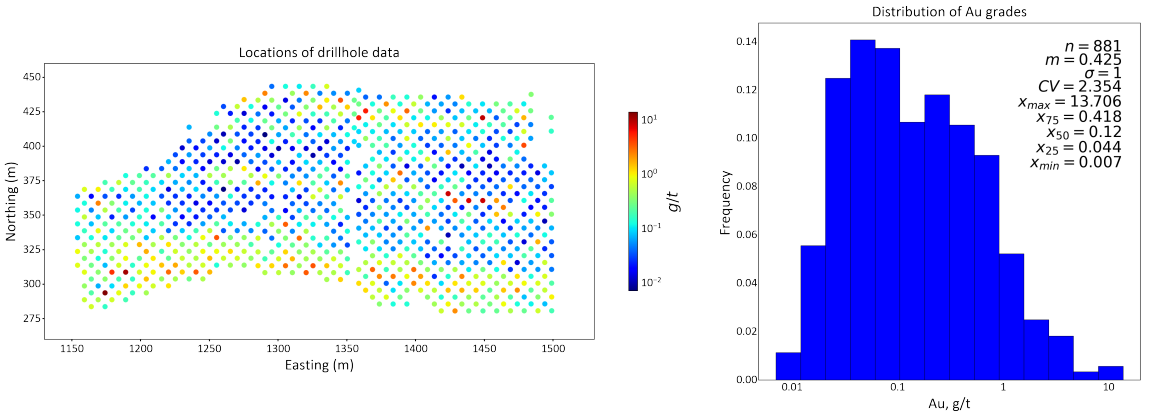

Figure 3.7: Location map and histogram of conditioning data used to generate the reference realizations. Units for grade values are in g/t

$$\gamma(\mathbf{h}) = 0.28 + 0.325 \cdot \underset{\substack{a_{hmax}=22 \\ a_{hmin}=13}}{\text{Sph}} + 0.395 \cdot \underset{\substack{a_{hmax}=325 \\ a_{hmin}=40}}{\text{Sph}} \tag{3.17}$$

The 200 realizations are generated at a resolution of $1m \times 1m \times 10m$ that spans an area of $400m \times$

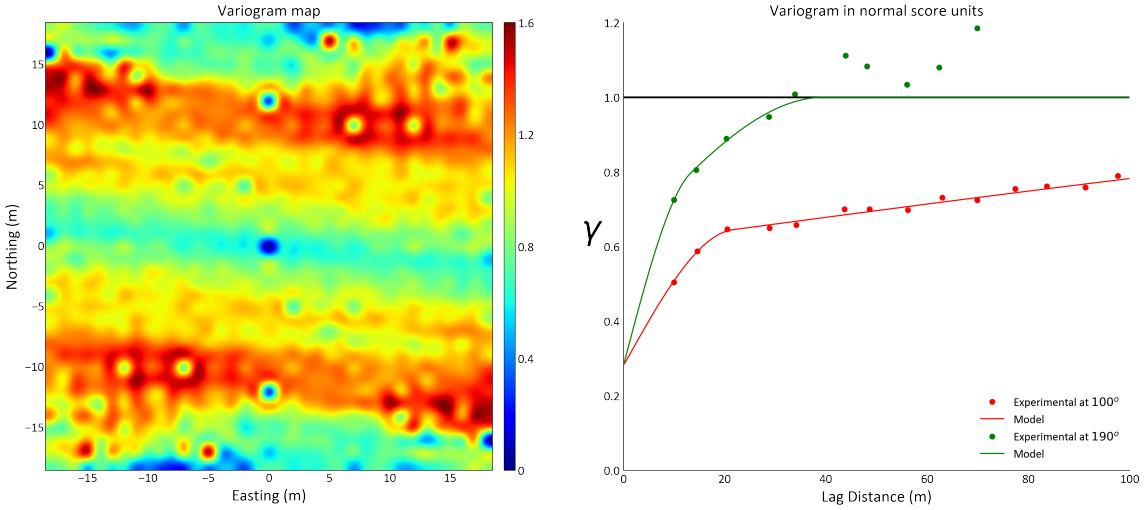

Figure 3.8: Variogram map of conditioning data (left), Modelled variograms of conditioning data (right)

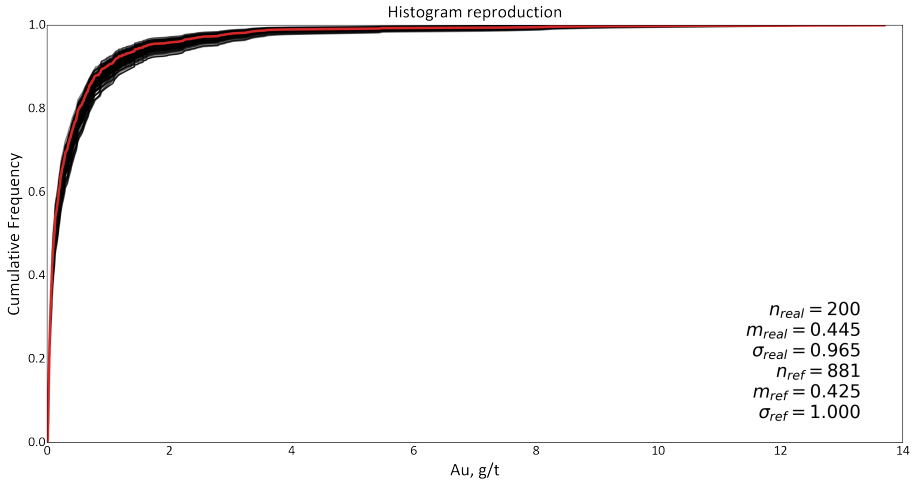

Figure 3.9: Distributions of two hundred realizations plotted against the conditioning data. This serves a simulation check

$200m$. The block height corresponds to an arbitrary 10m bench. Assuming a specific gravity of 2.7, this volume corresponds to a production volume of 2,160,000 tonnes. Figure 3.10 shows four realizations from the set of two hundred plotted against their respective histograms.

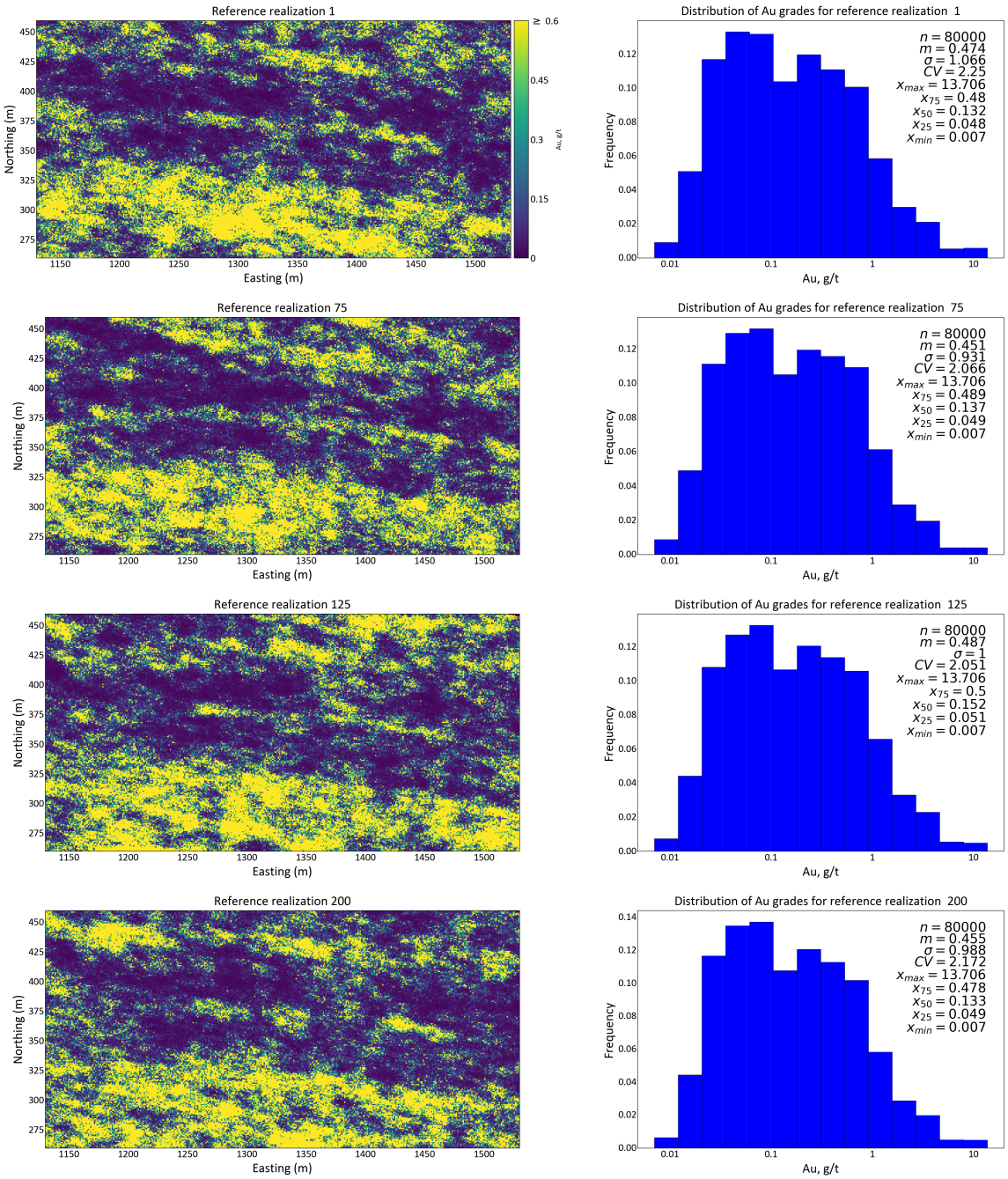

Figure 3.10: Some selected realizations from the set of two hundred along with their histograms.

3.7 Case Study

Examples have been developed to show the effectiveness of the estimators used for grade control. These examples consist of two hundred realizations generated through conditional simulation, as depicted in Figure 3.10, serving as reference or 'true' models against which the performance of implemented techniques will be evaluated. The realizations are sampled at regular intervals of $4m \times 4m$. In order to replicate real-world sampling conditions, a 1% sampling error is introduced.

On each of the sampled datasets from the 200 reference realizations, four different geostatistical modeling techniques—ordinary Kriging with two different search plans, Expected Sequential Gaussian Simulation (ExpSGS), Localized Uniform Conditioning (LUC), and Localized Sequential Gaussian Simulation (LocSGS), are applied. As a result, 200 ordinary Kriging models for each search plan, 200 ExpSGS models, 200 LUC models, and 200 LocSGS models are generated. The expected values or mean obtained from the distribution of these models are then graphed for analysis. Figure 3.11 displays a location map illustrating three of the two hundred newly sampled datasets resulting from applying the $4m \times 4m$ sampling configuration to each realization. For all final models generated to evaluate the performance of estimators for grade control, a grid size of $2m \times 2m \times 10m$ is considered. This means the reference realizations at $1m \times 1m \times 10m$ resolution are also scaled to the grid volume to be used as a reference for model validation. Details on factors that influence the choice of an grid size is discussed in Chapter Two. If panels are required, grids can be grouped to form panels of size $20m \times 20m \times 10m$.

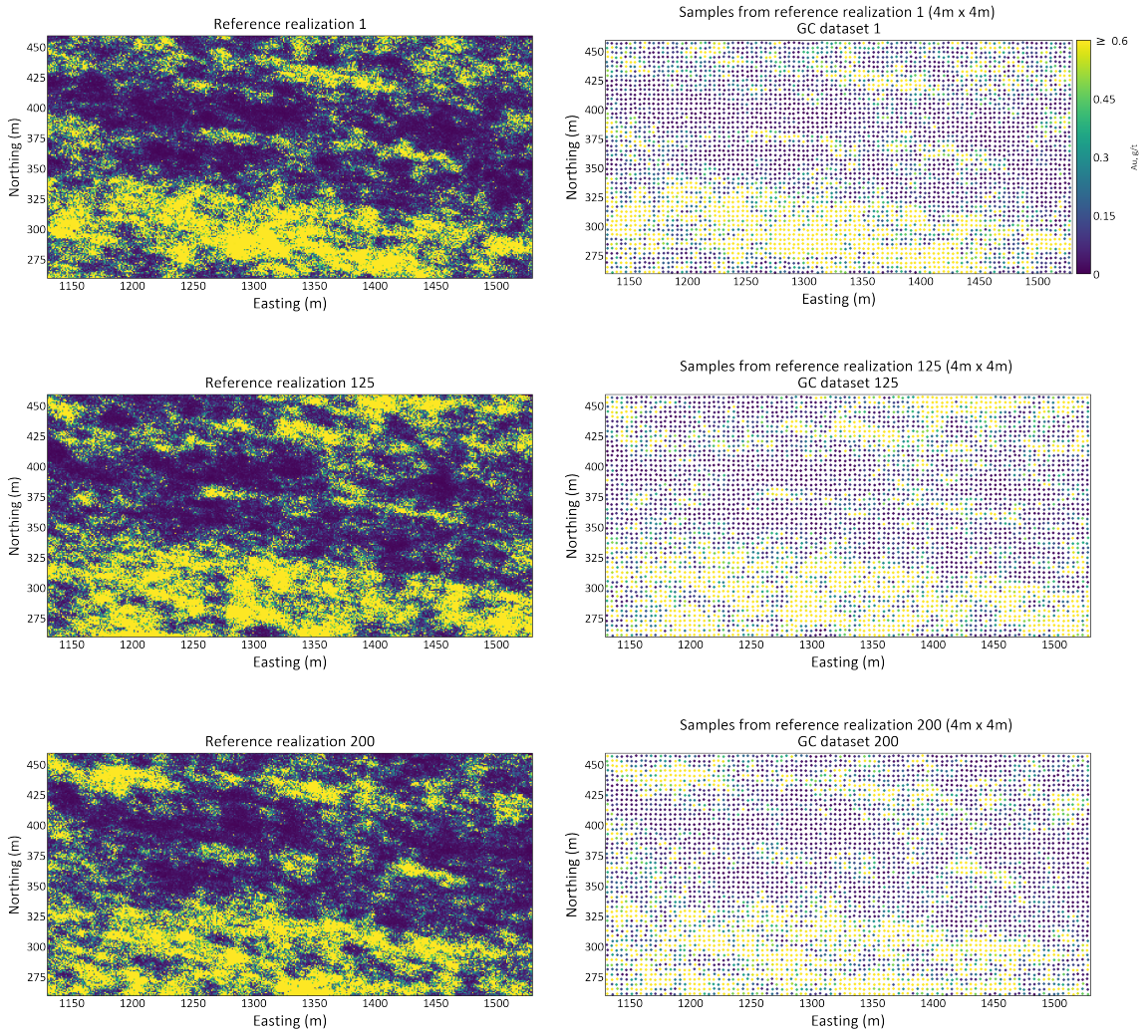

Figure 3.11: Reference realizations and their sampled datasets from a $4m \times 4m$ sampling configuration. Unit of grade values are in g/t.

3.7.1 Variography

The spatial correlation of samples is quantified by the variogram, although there are other ways, such as using covariance and correlation coefficient. Variograms are calculated in both original and Gaussian units. The original units variogram is required for ordinary kriging in original units. The variogram in Gaussian units is required for SGS. For both cases, the variograms are modeled in two directions in the horizontal plane following Equation 3.18. The variograms are constructed with a major direction of continuity at 100 degrees from the north and a minor direction at 190 degrees from the north. For all the 200 sampled datasets derived from the 200 reference realizations, the variograms are calculated with consistent directions of continuity and modeled using two nested spherical variogram structures. The range of parameters for the two hundred variograms is described in Equation 3.18.

$$\gamma(\mathbf{h}) = (0.1:0.3) + (0.1:0.7)\cdot \underset{\substack{a^1_{hmax}=0:80\\ a^1_{hmin}=0:50}}{\mathrm{Sph}} + (0.1:1)\cdot \underset{\substack{a^2_{hmax}=90:400\\ a^2_{hmin}=0:100}}{\mathrm{Sph}} \tag{3.18}$$

The nugget effect for all the variograms falls within the range of 0.1 to 0.3. The first spherical structure has a variance contribution ranging from 0.1 to 0.7, a minimum range from 0 to 50m, and a maximum range from 0 to 80m. The second spherical structure has a variance contribution ranging from 0.1 to 1, a minimum range between 0 and 100m, and a maximum range between 90 and 400m. More detailed parameters for some selected datasets derived from the two hundred realizations are provided in Table 3.1. Figure 3.12 presents a plot illustrating six of the 200 variograms computed and modeled in original units.

GC dataset	Nugget effect	Structure types	Variance contribution (cc)	Range		
				a_{hmax}	a_{hmin}	a_{vert}
1	0.300	spherical	0.384	12	9	10
		spherical	0.316	305	48	10
30	0.300	spherical	0.445	15	9	10
		spherical	0.255	296	42	10
65	0.300	spherical	0.463	12	8	10
		spherical	0.237	211	37	10
100	0.300	spherical	0.387	14	10	10
		spherical	0.313	308	41	10
150	0.300	spherical	0.424	13	8	10
		spherical	0.276	263	34	10
200	0.300	spherical	0.430	12	8	10
		spherical	0.270	222	40	10

Table 3.1: Variogram model parameters for a few chosen reference datasets in their original units. All variograms were calculated in two directions with a major and minor azimuth of 100° and 190° respectively. Please note that each GC dataset is obtained by sampling from the corresponding realization. GC dataset one is derived from sampling reference realization one.

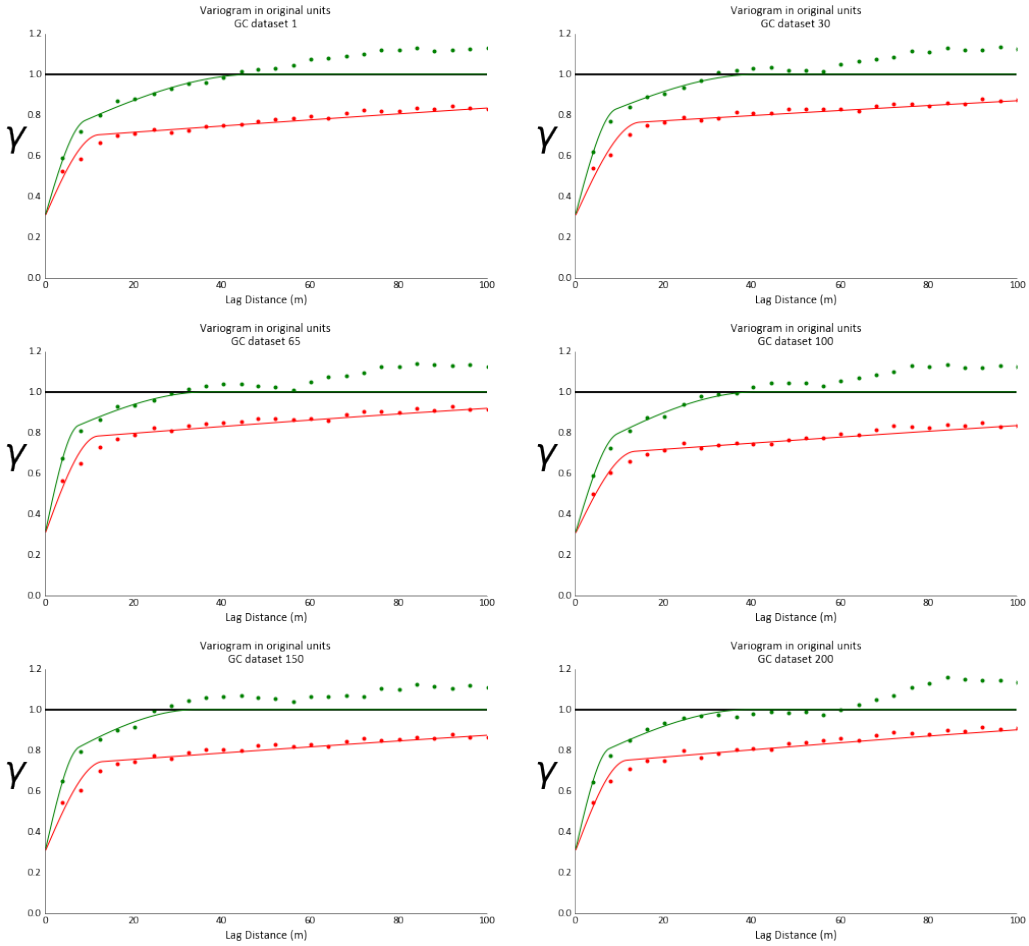

Figure 3.12: Standardized variograms calculated and fitted with two spherical structures for GC datasets (minor direction -green, major direction red).

Modeling in Gaussian space requires an additional set of variograms calculated using the normal scores of the sampled data. The range of parameters for the two hundred normal score variograms is described in Equation 3.19.

$$\gamma(\mathbf{h}) = (0.1:0.3) + (0.1:0.7)\cdot \mathrm{Sph}_{\substack{a^1_{hmax}=0:80 \\ a^1_{hmin}=0:50}} + (0.1:1)\cdot \mathrm{Sph}_{\substack{a^2_{hmax}=90:400 \\ a^2_{hmin}=0:150}} \tag{3.19}$$

The nugget effect for all the variograms falls within the range of 0.1 to 0.3. The first spherical structure has a variance contribution ranging from 0.1 to 0.7, a minimum range from 0 to 50, and a maximum range from 0 to 80. The second spherical structure has a variance contribution ranging from 0.1 to 1, a minimum range between 0 and 150, and a maximum range between 90 and 400. More detailed parameters for selected datasets are provided in Table 3.2. Figure 3.13 presents a plot illustrating six of the two hundred normal score variograms for the sampled data in Gaussian units.

GC dataset	Nugget effect	Structure types	Variance contribution (cc)	Range a_{hmax}	a_{hmin}	a_{vert}
1	0.300	spherical	0.267	22	15	10
		spherical	0.433	397	56	10
30	0.300	spherical	0.345	23	15	10
		spherical	0.355	369	46	10
65	0.300	spherical	0.371	21	11	10
		spherical	0.329	293	42	10
100	0.284	spherical	0.291	23	18	10
		spherical	0.425	382	44	10
150	0.300	spherical	0.335	22	12	10
		spherical	0.365	297	37	10
200	0.300	spherical	0.336	22	12	10
		spherical	0.364	343	60	10

Table 3.2: Parameters of variogram model in Gaussian units. Variograms were calculated in two directions with a major and minor azimuth of 100° and 190° respectively.

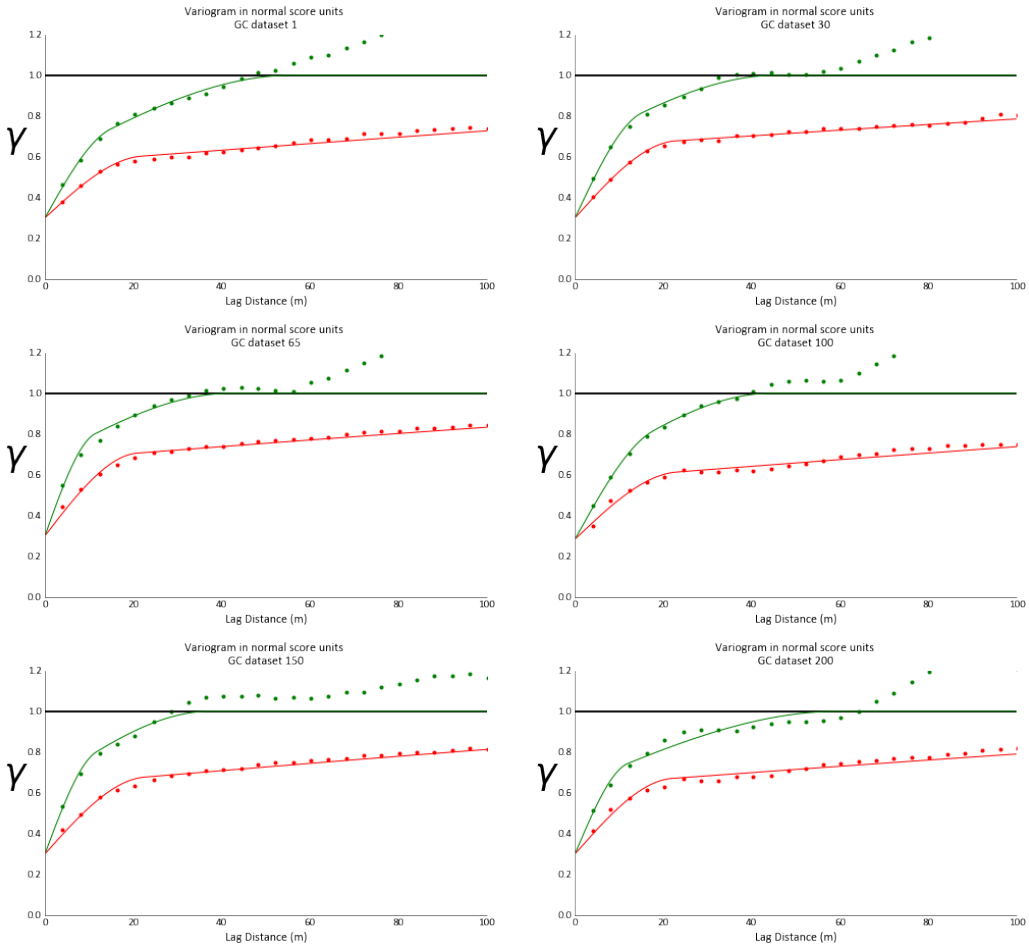

Figure 3.13: Normal score variograms calculated and fitted with two spherical structures for GC datasets (minor direction -green, major direction red).

3.7.2 Ordinary Kriging

The blasthole data is collected by sampling from each of the two hundred reference realizations at a regular interval of $4m \times 4m$, illustrated in Figure 3.11. To simulate potential errors in the field, a small random sampling error is introduced to the coordinates of the sampled data. These sampled data are utilized for grade estimation at a $2m \times 2m \times 10m$ SMU scale using ordinary kriging with two different search plans. The kriging process is performed using the software program $kt3dn$. Driven by the need to manage CPU and memory requirements, many kriging algorithms consider a limited number of nearby conditioning data. The time it takes to solve a kriging system using the CPU grows significantly as the number of conditioning data increases. Additionally, utilizing a global search neighborhood would demand accurate knowledge of covariance for the longest separation distance between the data. However, such covariance values are typically uncertain for distances exceeding half or one-third of the domain size (C. V. Deutsch & Journel, 1997).

Two search plans are employed - the first plan uses a minimum of 4 and a maximum of 5 data. This is referred to as the small search plan, while the second uses a minimum of 25 and a maximum of 45 data and is referred to as the large search plan. A maximum search radius of $200m$ is used for the major and minor direction of continuity, and $10m$ is used for the vertical direction. This ensures that the required maximum data are met when estimating the unsampled locations. Figure 3.14 shows a map of the kriged estimates for both search plans.

To convert the ordinary kriging estimates to profit values, arbitrary values that are reasonable and consistent with the case of real costs are used. $C_T = -10\$/t$, $C_w = -1.5\$/t$. Where C_T is the total cost of processing, administration, mining, etc. C_w is waste mining cost. z_c is the cutoff grade. Some cutoff grades are also considered to determine the cutoff grade's influence on the percentage of maximum attainable profit. The cutoff grades are 0.2, 0.4, 0.8, 1.0, 1.2, 1.4, 1.6, 1.8 and 2.0 g/t.

From the profit functions defined in Equation 3.1, there are only two destinations for mined material: waste dump (waste) and processing plant (ore). Equation 3.7-3.8 calculates the profits for the kriged estimates and corresponding optimal destinations. In this instance, the L for ordinary Kriging will be one since we only have one realization or model from Kriging. However, this procedure for the profit calculation will be repeated 200 times for the 200 models generated from each borehole data. Figure 3.15 shows a numerical model of profits for some selected ordinary Kriging models.

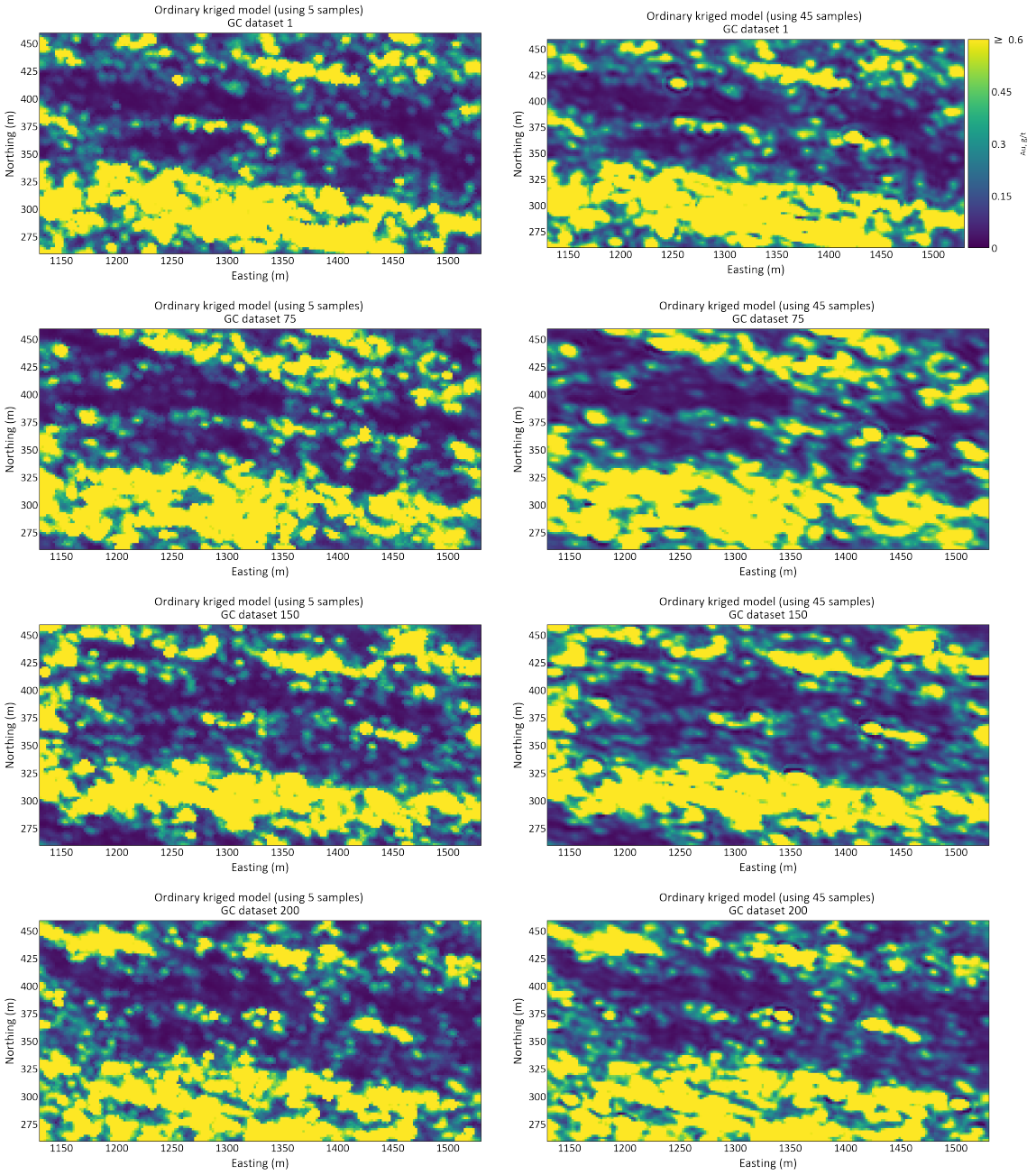

Figure 3.14: Some selected ordinary Kriging models for grade control using a different search plans. Unit of grade values are in g/t

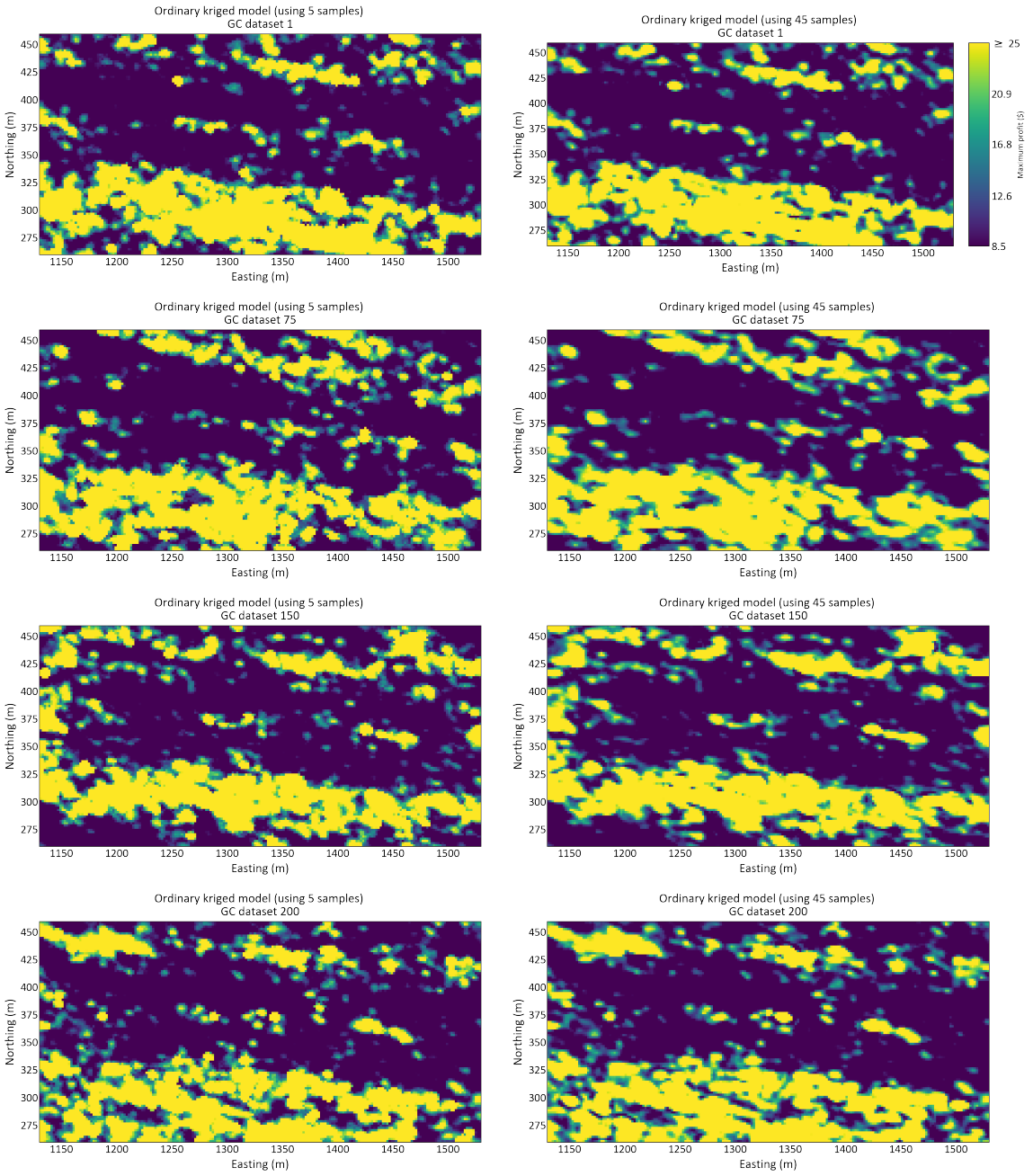

Figure 3.15: Some selected numerical models of profits from ordinary kriged models using different search plans. Unit of profit values are in $.

The models were compared to the reference realizations to assess the accuracy of these two kriging techniques. For instance, the OK model from GC dataset 1, using both the small and large search plans, was compared to reference realization 1. Table 3.3 presents the expected percentage of misclassified errors, maximum attainable profit, and mean squared error for the two hundred OK models evaluated against the reference realizations for a 0.2 g/t cutoff grade and 0.8 g/t.

Model	False positive FP(%)	False negative FN(%)	Misclassified errors (%)	Maximum attainable profit(%)	Mean squared error ($)
Cutoff grade of 0.2					
OK (using 5 samples)	9.98	7.22	17.20	80.34	515
OK (using 45 samples)	10.85	6.36	17.21	80.88	476
Cutoff grade of 0.8					
OK (using 5 samples)	5.52	5.20	10.72	26.89	41
OK (using 45 samples)	5.48	5.02	10.50	26.35	38

Table 3.3: Expected percentage of misclassified errors, maximum attainable profit and mean squared error of the two hundred models for both the small and large search plan.

Figure 3.16 displays the MSE in profits for all 200 ordinary kriging models using different search plans for a low and high cutoff grade. It was observed that when using a large search plan, the OK model consistently produced lower MSE compared to the corresponding kriged model using a small search plan. At a cutoff of 0.2g/t, the difference in expected MSE is $ 39.656; at a cutoff of 0.8g/t, the difference in expected MSE is $ 2.891. A relatively higher 75th percentile for Figure 3.16 (a) when using five samples for ordinary kriging, $568.132, suggests that the top 25% of models had larger errors, impacting profit predictions. From Figure 3.17 (a), the difference in the expected percentage of maximum attainable profit is 0.536%.

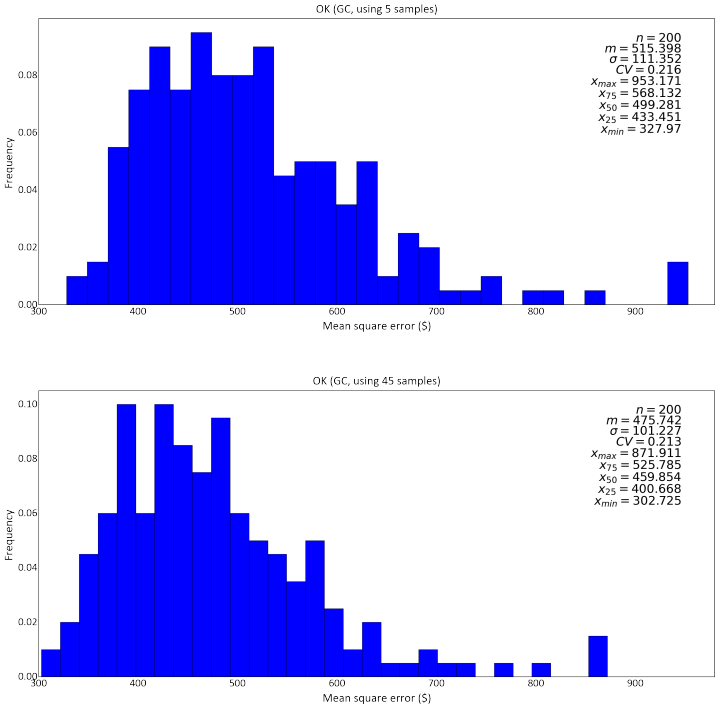

(a) Summary statistics of MSE in profits for 200 ordinary kriging models with different search plans at a cutoff of 0.2 g/t. The expected MSE is the average MSE of all the models.

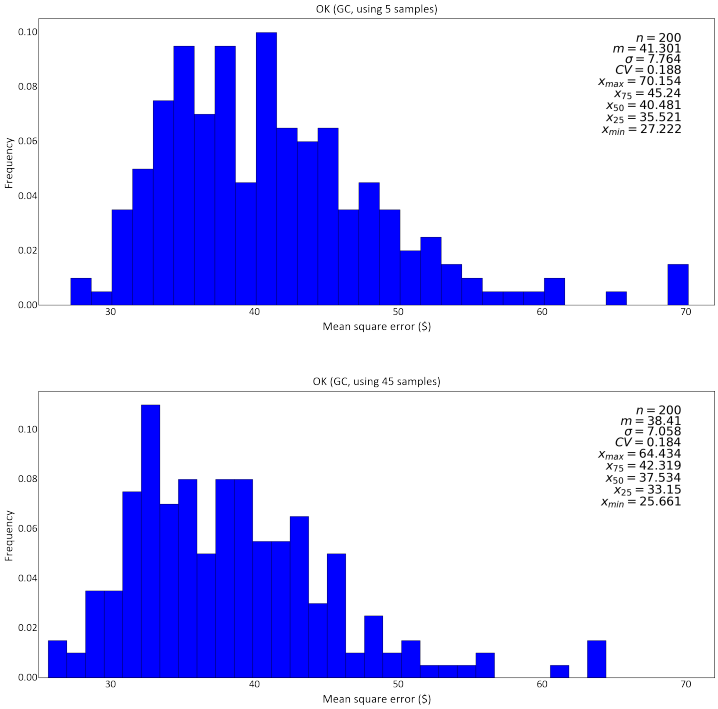

(b) Summary statistics of MSE in profits for 200 ordinary kriging models with different search plans at a cutoff of 0.8 g/t. The expected MSE is the average MSE of all the models.

Figure 3.16: Comparison of MSE in profits for 200 ordinary kriging models with different search plans.

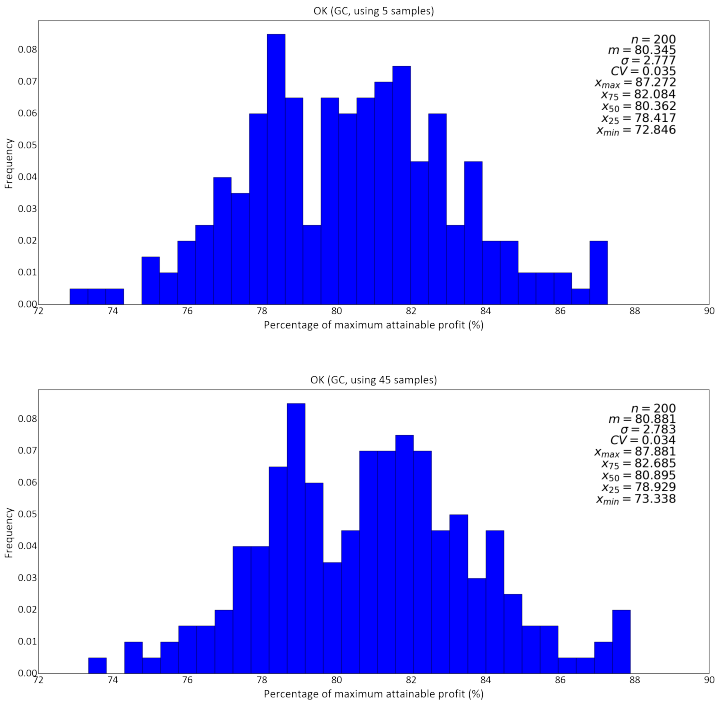

(a) Summary statistics of percentage maximum attainable profit for 200 ordinary kriging models with different search plans at a cutoff of 0.2 g/t. The expected MSE is the average MSE of all the models.

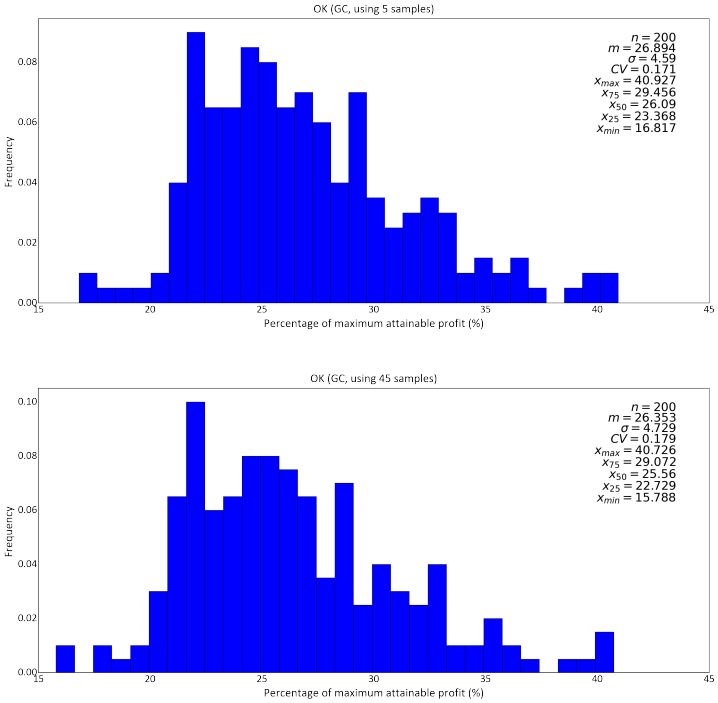

(b) Summary statistics of percentage maximum attainable profit for 200 ordinary kriging models with different search plans at a cutoff of 0.8 g/t.

Figure 3.17: Comparison of MSE in profits for 200 ordinary kriging models with different search plans.

3.7.3 Expected Sequential Gaussian Simulation

The second technique considered is expected sequential Gaussian simulation (ExpSGS), performed based on the literature discussed in Chapter 2. SGS is used to create a model of uncertainty, then compared to models generated using ordinary Kriging, localized uniform conditioning, and localized SGS. The same set of normal-scored sampled data values modeled by Gaussian variograms described by Equation 3.19 and illustrated in Figure 3.11 are used. These normal scored data values are obtained by transforming the original sampled data sets used for generating the ordinary kriging models. Each of the 200 sampled GC datasets is transformed to have a mean of zero and a standard deviation of one using the *nscore* program. The parameters for conditional simulation include a search radius of $400m$ in the major direction of continuity, $200m$ in the minor direction of continuity, and $10m$ in the vertical direction. The number of conditioning data used for simulation varies between 0 and 40. A large search radius ensures that a sufficient amount of data is used for each estimate. The simulation is performed at the data scale, which can be time-consuming and computationally expensive, especially when multiple realizations are generated. Realizations are generated at a $1m \times 1m \times 10m$ grid resolution to mitigate these issues. This provided adequate discretization to average results to the larger $2m \times 2m \times 10m$ grid size. In each unsampled location, 40 previously simulated values are incorporated into the dataset for conditioning future distributions. This means that 40 simulated values are included as part of the dataset at each location where data was not initially sampled. The $SGSIM$ program is used for the conditional simulation.

For each of the 200 normal score transformed GC datasets, 100 realizations are generated conditional to the datasets. These realizations are then back-transformed to the original units using their respective transformation tables. The program *backtr* is used for this task. As a result, 20,000 files need to be managed for post-processing. The histogram reproduction of the 100 realizations generated checked against the conditioning data is shown in Figure 3.18. All realizations from each sampled dataset are then scaled to the grid size used for all the grade control models. Visualizing each realization is not practical because each realization is equiprobable. Realization 1 has the same chance of having the same grade variability as realization 20, 50, or any other realization in the total set generated. Therefore, instead of displaying all 100 realizations, a single realization from the 100 generated for GC dataset 1 is chosen.

The plot in Figure 3.19 (a) shows a more realistic variability of grades for realization one at the point scale compared to the same realization but this time averaged to the grid scale, Figure 3.19 (b). This indicates that the sequential Gaussian simulation (SGS) technique captures the inherent variability in the data more effectively, resulting in a more realistic representation of the spatial distribution of grades. Figure 3.19 (c) shows the expected SGS model from the 100 realizations for GC dataset 1. The calculated mean values for all locations $\mathbf{u}$ from the 100 realizations generated through conditional simulation of dataset each sampled dataset is the expected SGS (ExpSGS)

model for that dataset. Some of the ExpSGS models from selected datasets are shown in Figure 3.20.

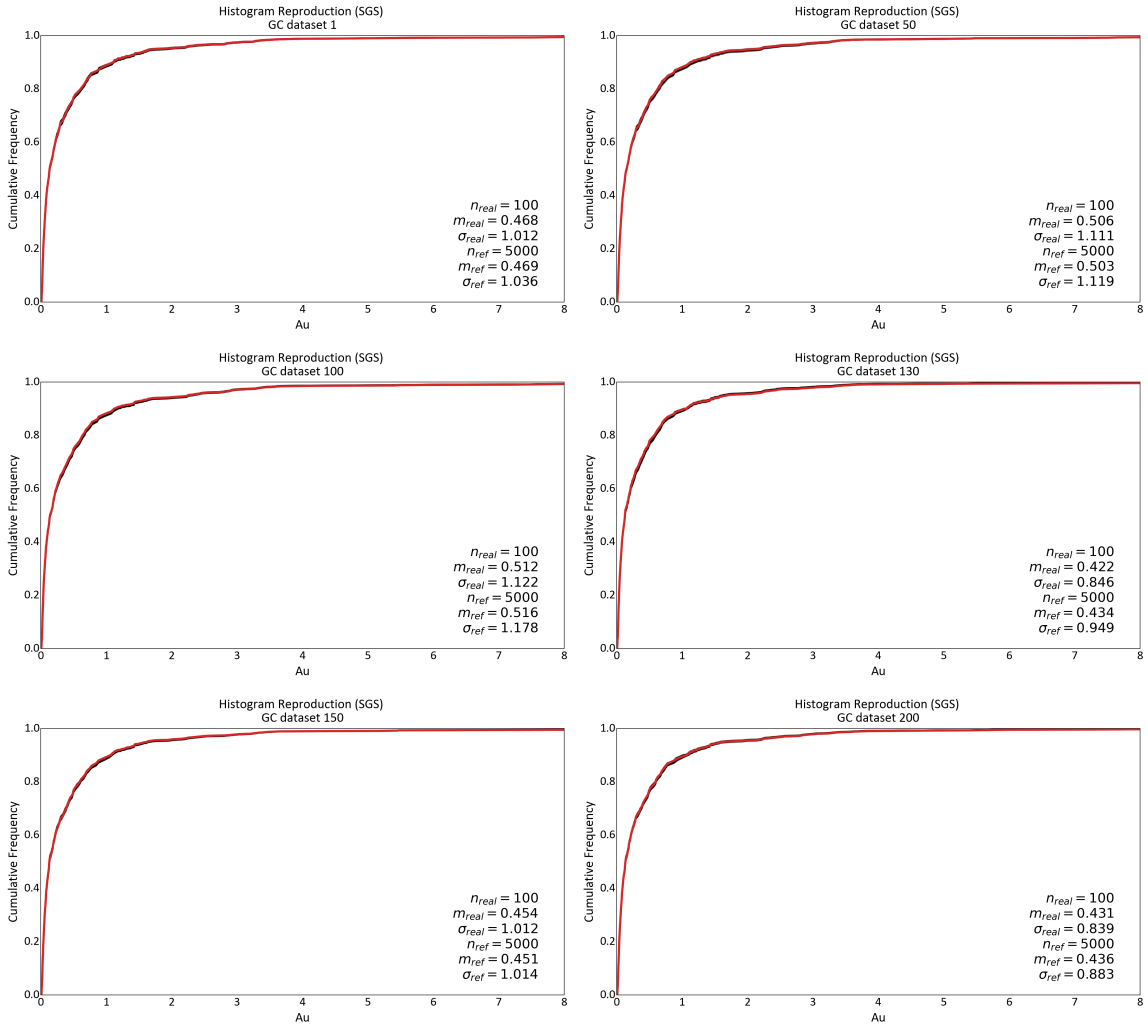

Figure 3.18: Histogram reproduction of the realizations generated for expected SGS. The overlaid red CDF represents the original distribution of the GC dataset used for the conditioning.

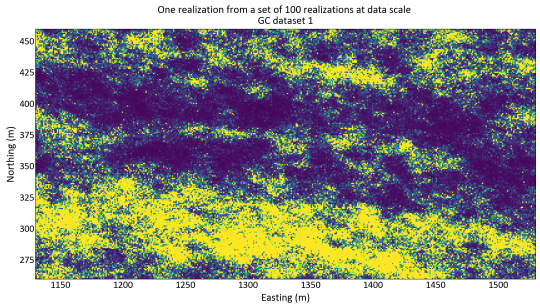

(a) A single realization at the point scale out of the 100 generated from GC dataset 1

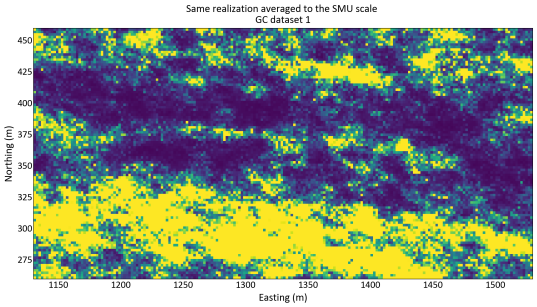

(b) A single realization averaged to the grid volume.

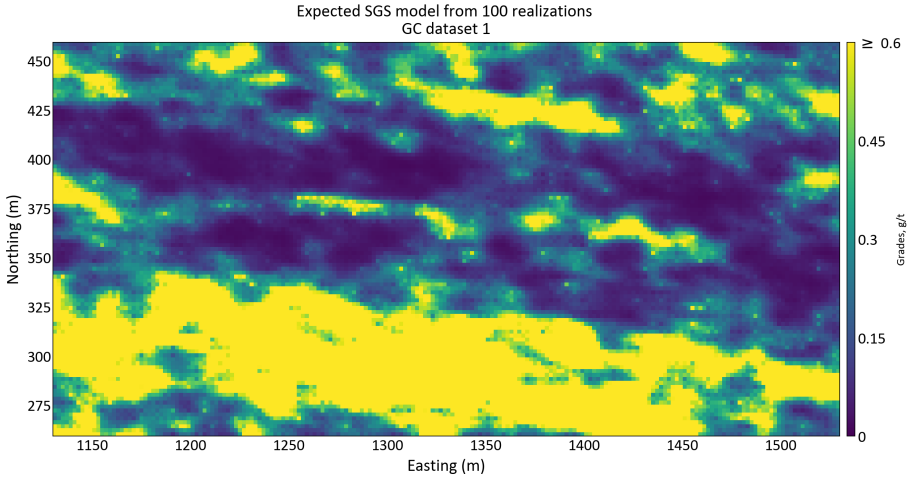

(c) Expected SGS model from the average of the 100 realizations for GC dataset 1.

Figure 3.19: Comparison of grade variability: Point Scale vs. SMU Scale.

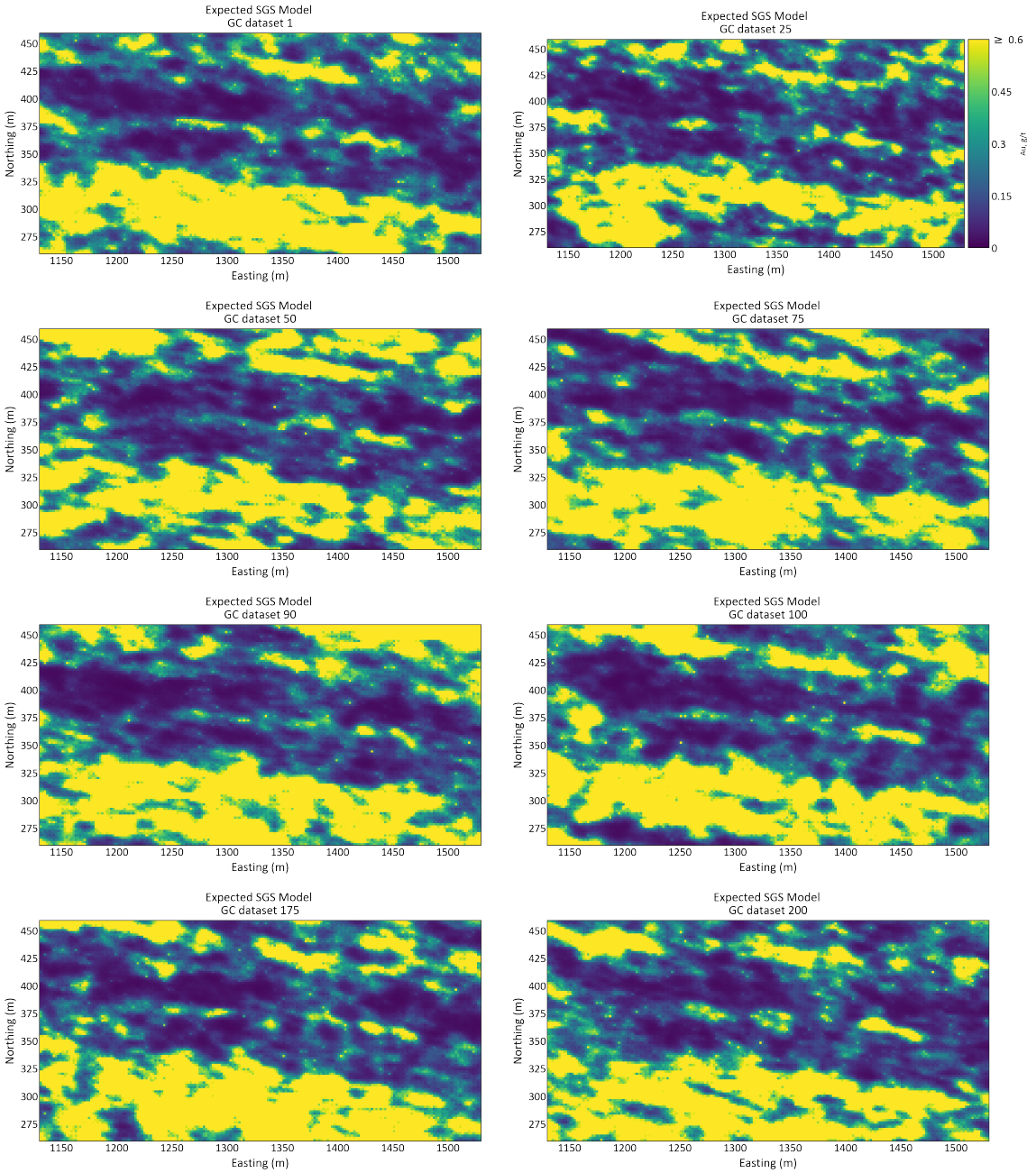

Figure 3.20: Some selected expected SGS map. Each expected SGS map displayed here is an average of one hundred realizations.

3.7.4 Expected Profits

The same arbitrary values used to convert the ordinary kriging estimates are also used here. This ensures consistency for a better evaluation of performance. From the profit functions defined in Equation 3.1, there are only two destinations for the mined material: the waste dump (waste) and the processing plant (ore). Equations 3.7 and 3.8 are used to calculate the profits for the Expected SGS models. In this case, the value of L for expected SGS is 100 since there are only 100 realizations from conditional simulation of each reference sampled dataset. However, this procedure for profit calculation will be repeated 200 times for the 200 GC datasets used to generate the conditional SGS models shown in Figure 3.18. Figure 3.21 presents a numerical model illustrating the expected profits for some selected ExpSGS models. Table 3.4 details the expected values of some performance measures for all the 200 models generated.

Model	False positive FP(%)	False negative FN(%)	Misclassified errors (%)	Maximum attainable profit(%)	Mean squared error ($)
Cutoff grade of 0.2					
OK (using 5 samples)	9.98	7.22	17.20	80.34	515
OK (using 45 samples)	10.85	6.36	17.21	80.88	476
Expected SGS	6.67	8.66	15.33	85.88	409
Cutoff grade of 0.8					
OK (using 5 samples)	5.52	5.20	10.72	26.89	411
OK (using 45 samples)	5.48	5.02	10.50	26.35	38
Expected SGS	2.55	6.84	9.39	30.51	31

Table 3.4: Expected percentage of misclassified errors, maximum attainable profit and mean squared error of the 200 expected SGS and OK models.

Figure 3.22 illustrates the mean square error in profits across all 200 ExpSGS models at 0.2 g/t and 0.8 g/t cutoff grades. The findings indicate that the ExpSGS models exhibit significantly lower expected MSE values than their corresponding kriged counterparts. Notably, at a low cutoff grade of 0.2 g/t, there exists a substantial difference of $66.801 in the MSE between ExpSGS and ordinary kriging using 45 samples and a substantial difference of $106.457 in MSE between ExpSGS and ordinary kriging using 5samples. Furthermore, ExpSGS achieves an expected percentage of maximum attainable profit of 85.88%, outperforming the values achieved by OK(SSP) (80.34%) and OK(LSP) (80.88%) for the same 0.2 g/t cutoff grade. These findings underscore the superior performance of ExpSGS in terms of minimizing error and optimizing profit expectations, particularly evident at the lower cutoff grade of 0.2 g/t.

Figure 3.23 shows a distribution of maximum attainable profits for the 200 ExpSGS models at 0.2 g/t and 0.8 g/t cutoff grade.

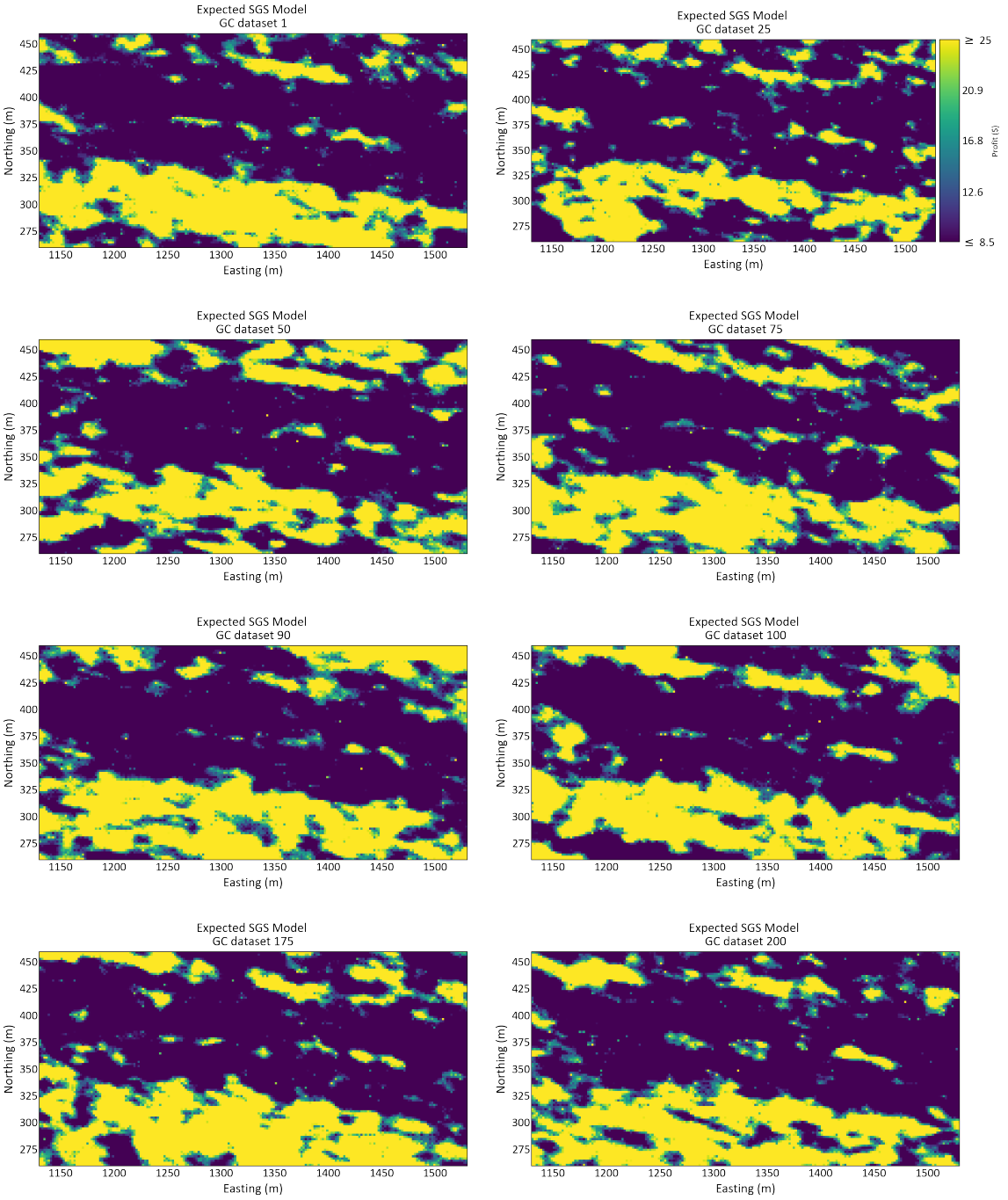

Figure 3.21: Some selected numerical models in expected profits from expected SGS.

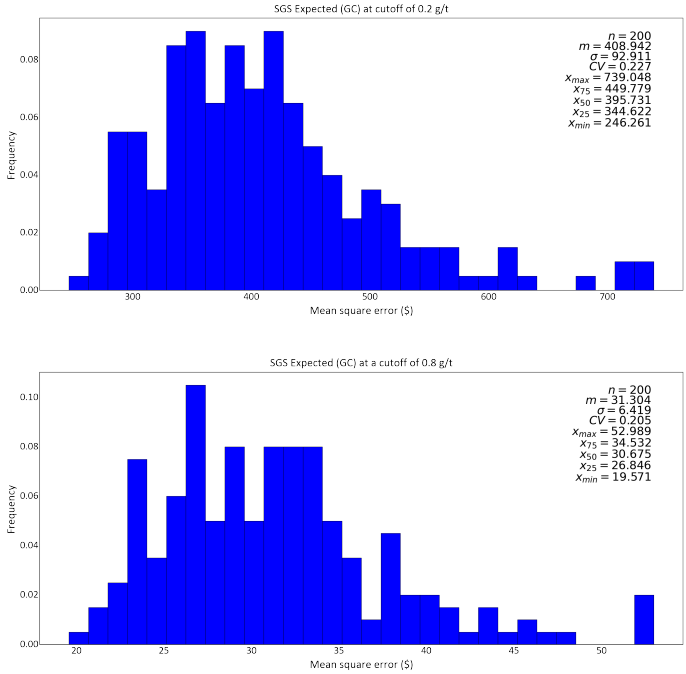

Figure 3.22: Summary statistics of MSE in profits for 200 ExpSGS models at different cutoff grades.

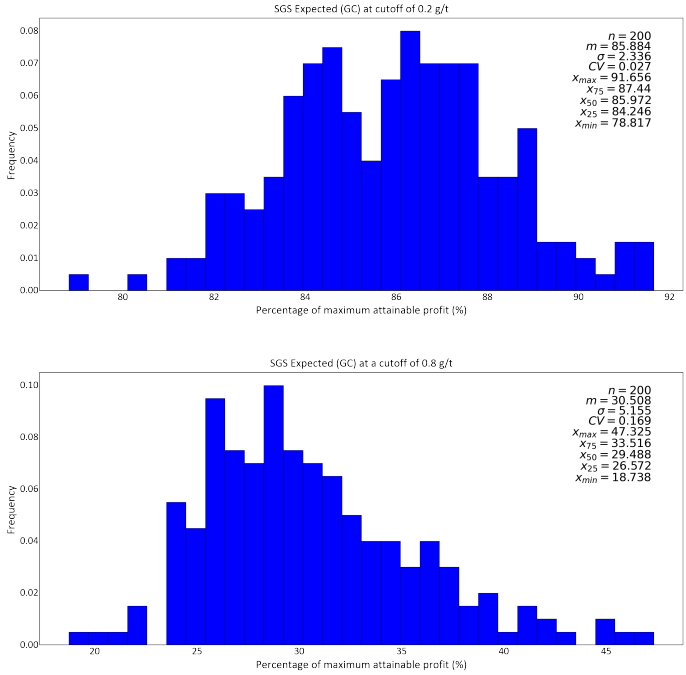

Figure 3.23: Summary statistics of percentage maximum attainable profits for 200 ExpSGS models at different cutoff grades.

3.7.5 Localized Uniform Conditioning

Uniform conditioning (UC) is a method used to obtain grade-tonnage relationships at the SMU scale by using a Discrete Gaussian model (DGM) to calculate the change of support coefficients for larger scales (Rivoirard, 1987), refer to Chapter 2. UC does not provide information on the local distribution of SMU grades within a panel, but this can be overcome by using Localized Uniform Conditioning (LUC). LUC assigns the average grade of each grade-tonnage class to the SMUs ranked within the panel. The ranking is performed with ordinary Kriging or other methods using available geological information. The *LUC* program by C. V. Deutsch and Journel (1997) is used following the workflow from (Neufeld, 2005). The panel grid is $10m \times 10m \times 10m$. All kriging and average variogram calculations use the variograms in original units.

The panel grades were estimated using ordinary Kriging over the panel grid defined above. The variogram models from equation 3.18 were used as the basis for the Kriging. A minimum and maximum of 20 and 45 data were used in the search neighborhood of $200m$ in both major and minor directions of continuity and $10m$ in the vertical direction. The order of Hermite polynomials fitted to blasthole data is 1000. The SMU estimates from the OK large search plan in Section 3.2.2 are used as the localizing variable to rank the SMU blocks within a panel. After the result for each panel was localized following the localization workflow discussed in Chapter 2. The distribution of panel scale estimates used for uniform conditioning is shown in Figure 3.24. The panel estimates reveal a decrease in variability, with a value of 0.291, in contrast to the 0.476 variance observed for the localizing variable at the SMU scale. This reduction in variability can be attributed to the amplified scale and the smoothing impact achieved through kriging with a large search radius. The LUC estimate is shown in Figure 3.25.

To convert the grades to profit values, consistent parameters as used for the profit conversion of ordinary kriged estimates are used here, including $C_T = -10\$/t$, $C_w = -1.5\$/t$. Where C_T is the total cost related to processing, administration, mining , etc. C_w is waste mining cost. z_c is the cutoff grade. The cutoff grades are 0.2, 0.4, 0.8, 1.0, 1.2, 1.4, 1.6, 1.8 and 2.0 g/t.

From the profit functions defined in Equation 3.1, there are only two destinations for mined material: waste dump (waste) and processing plant (ore). Equation 3.7-3.8 calculates the profits for the LUC models. In this instance, the L for LUC will be one since we only have one realization or model from localized uniform conditioning. However, this procedure for the profit calculation will be repeated 200 times for the 200 models generated from each GC dataset. Figure 3.26 shows a numerical model of profits for some selected LUC models. Table 3.5 details the expected values of misclassified errors, false negatives, false positives, maximum attainable profit and mean squared error for all the 200 models generated via OK, ExpSGS and LUC. Figure 3.27 illustrates the mean square error in profits across all 200 LUC models at 0.2 g/t and 0.8 g/t cutoff grades. The findings indicate that the LUC models exhibit significantly higher expected MSE values than their corre-

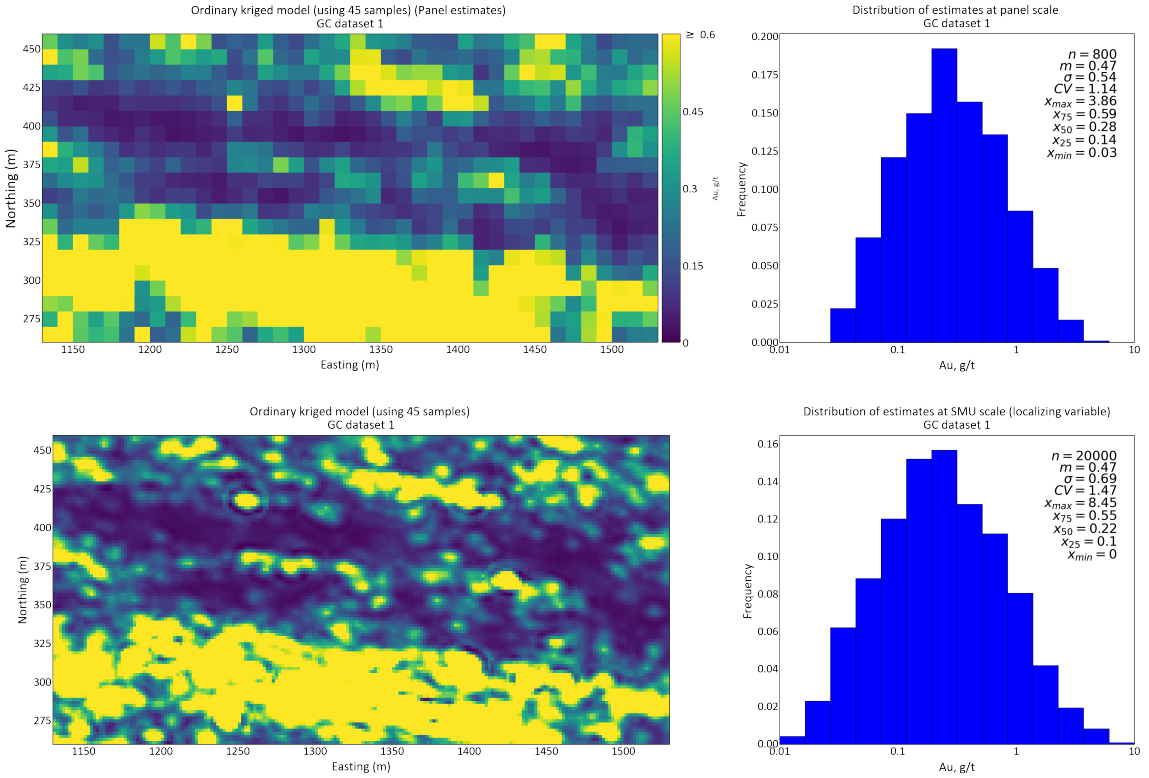

Figure 3.24: Distribution of panel scale and SMU scale estimates used for localized uniform conditioning (GC dataset 1).

Model	False positive FP(%)	False negative FN(%)	Misclassified errors (%)	Maximum attainable profit(%)	Mean squared error ($)
Cutoff grade of 0.2					
OK (using 45 samples)	10.85	6.36	17.21	80.88	476
Expected SGS	6.67	8.66	15.33	85.88	409
LUC	13.90	6.34	20.24	81.97	507
Cutoff grade of 0.8					
OK (using 45 samples)	5.48	5.02	10.50	26.35	38
Expected SGS	2.55	6.84	9.39	30.51	31
LUC	6.0	5.41	11.41	25.49	40

Table 3.5: Expected percentage of misclassified errors, maximum attainable profit and mean squared error of the two hundred models for OK, expected SGS and LUC.

sponding kriged and ExpSGS counterparts. Notably, at a low cutoff grade of 0.2 g/t, there exists a substantial difference of $98.5 in the expected MSE between ExpSGS and LUC and a difference of $31.699 in expected MSE between LUC and ordinary kriging using 45 samples. Furthermore, LUC achieves an expected percentage of maximum attainable profit of 81.97%, outperforming the values achieved by OK (SSP) (80.34%) and OK (LSP) (80.88%) for the same 0.2 g/t cutoff grade.

Figure 3.28 shows a distribution of maximum attainable profits for the 200 LUC models at 0.2g/t and 0.8g/t cutoff grade.

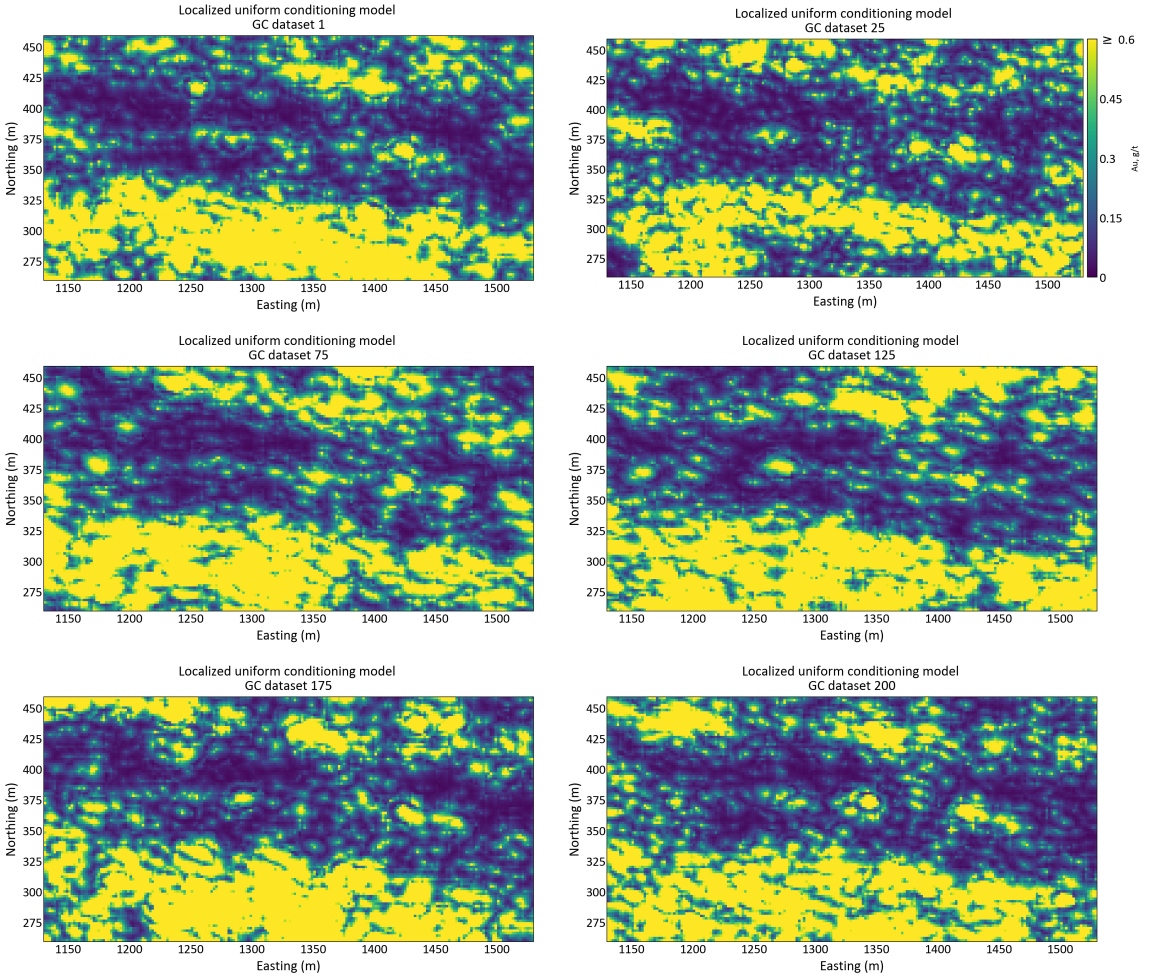

Figure 3.25: Localized uniform conditioning map.

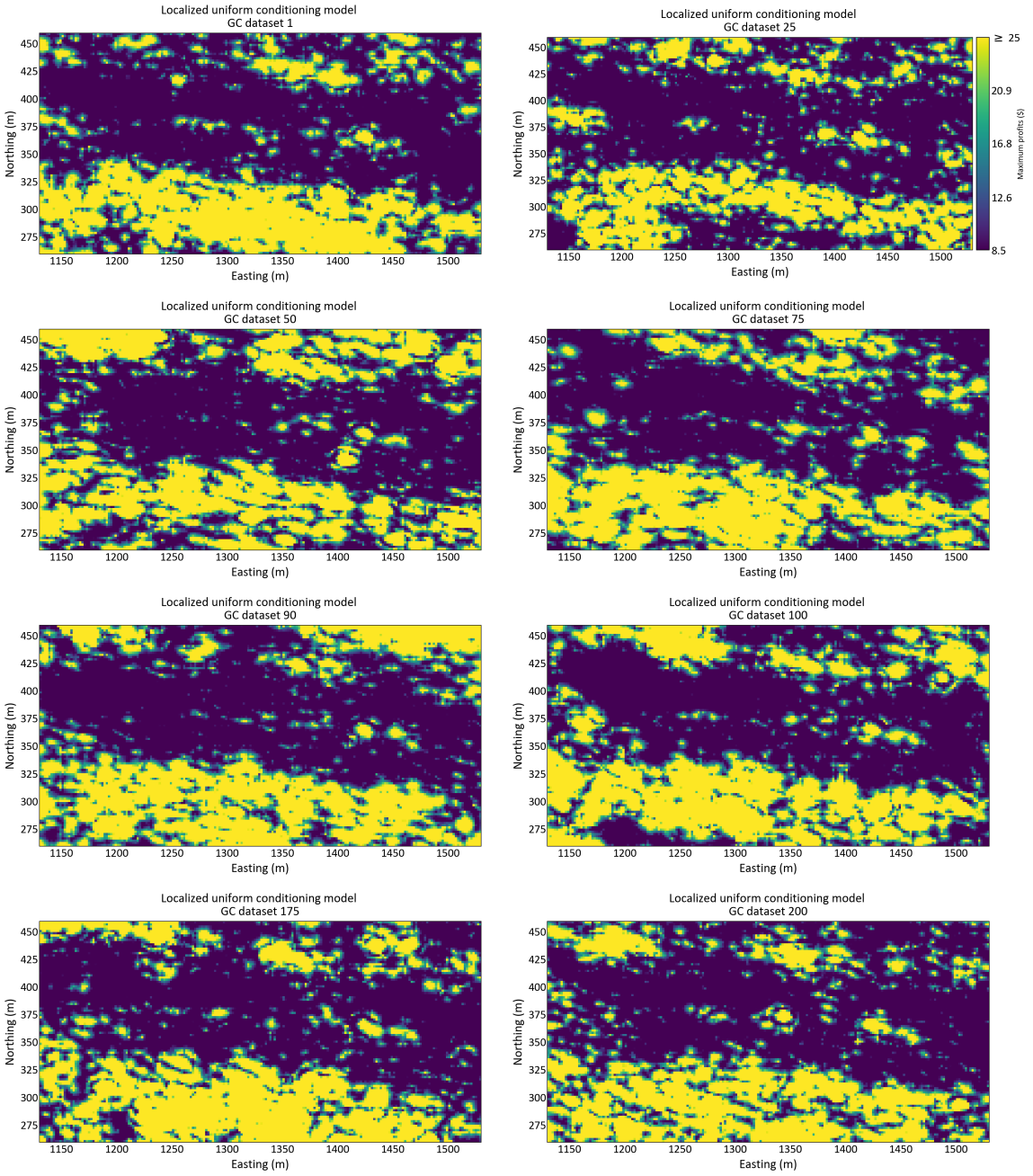

Figure 3.26: Numerical model in profits for some selected LUC models.

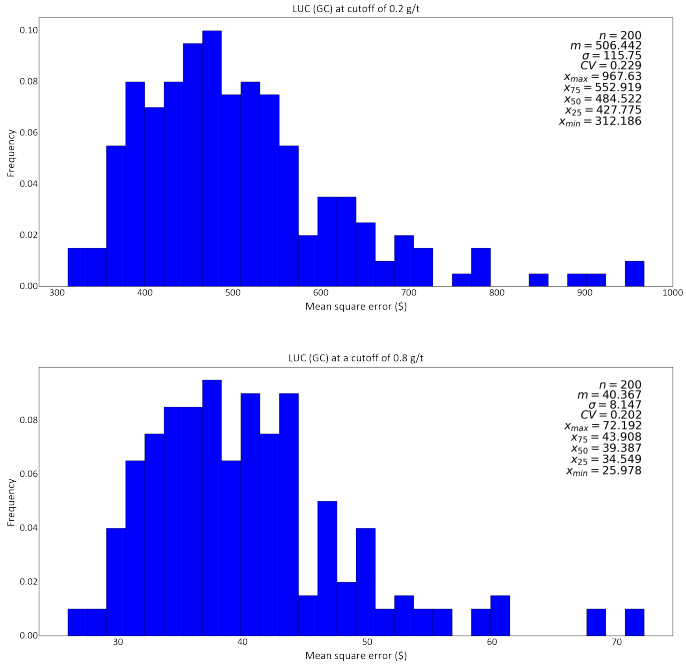

Figure 3.27: Summary statistics of MSE in profits for 200 LUC models at different cutoff grades.

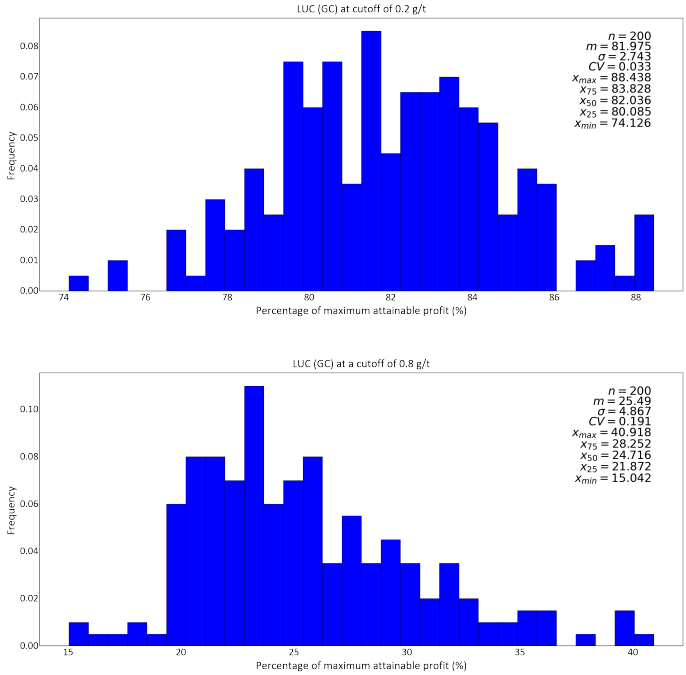

Figure 3.28: Summary statistics of percentage maximum attainable profits for 200 LUC models at different cutoff grades.

3.7.6 Localized Sequential Gaussian Simulation

After generating and checking 100 simulated realizations for each GC dataset, the data was back-transformed to the original units for localization. For proper assignment of grades at the SMU scale, a localizing variable is required to rank each SMU within a panel. The localizing variable is the SMU estimates from the ordinary kriging using 45 samples. Figure 3.29 shows a map of kriged estimates at the SMU volume, which is used as the localizing variable to localize the 100 realizations generated via conditional simulation of GC dataset 1. The panel scale is defined at $10m \times 10m \times 10m$, which nests properly with the smaller scale SMU grid, resulting in 25 SMUs within each panel. The simulated SMU grades falling within each panel (for all 100 realizations) are compiled to form a single distribution for each panel. This distribution is discretized into 25-grade classes, and the mean of each grade class is calculated and assigned to an SMU based on the kriged estimate of that SMU. This process is repeated for each panel in the model and is performed 200 times for the 200 different GC datasets. The *localization* program by Daniels (2015) is utilized for this purpose. The localized SGS models are shown in Figure 3.30.

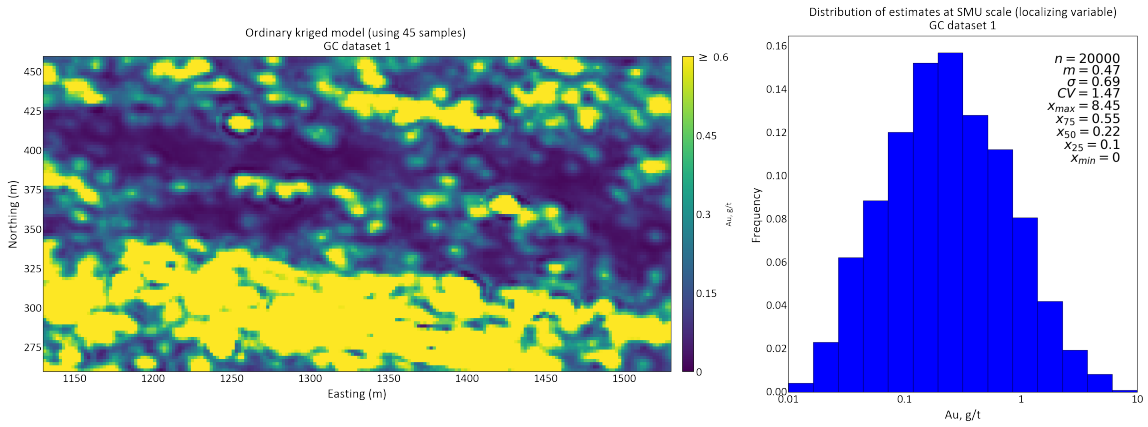

Figure 3.29: Distribution of localizing variable at the SMU scale.

As before, $C_T = -10\$/t$, $C_w = -1.5\$/t$. Where C_T is the total cost of processing, administration, mining, etc. C_w is waste mining cost. z_c is the cutoff grade.

From the profit functions defined in Equation 3.1, there are only two destinations for mined material: waste dump (waste) and processing plant (ore). Equation 3.7-3.8 calculates the profits for the LocSGS models. In this instance, the L for LocSGS will be one since we only have one realization or model from localized SGS. However, this procedure for the profit calculation will be repeated 200 times for the 200 models generated from each GC dataset. Figure 3.31 shows a numerical model in profits for some selected localized SGS models. Table 3.6 details the expected values of misclassified errors, false negatives, false positives, maximum attainable profit, and mean squared error for all the 200 models generated via OK, ExpSGS, LUC, and LocSGS. Figure 3.32 illustrates the mean square error in profits across all 200 localized SGS models at 0.2 g/t and 0.8 g/t cutoff grades. The

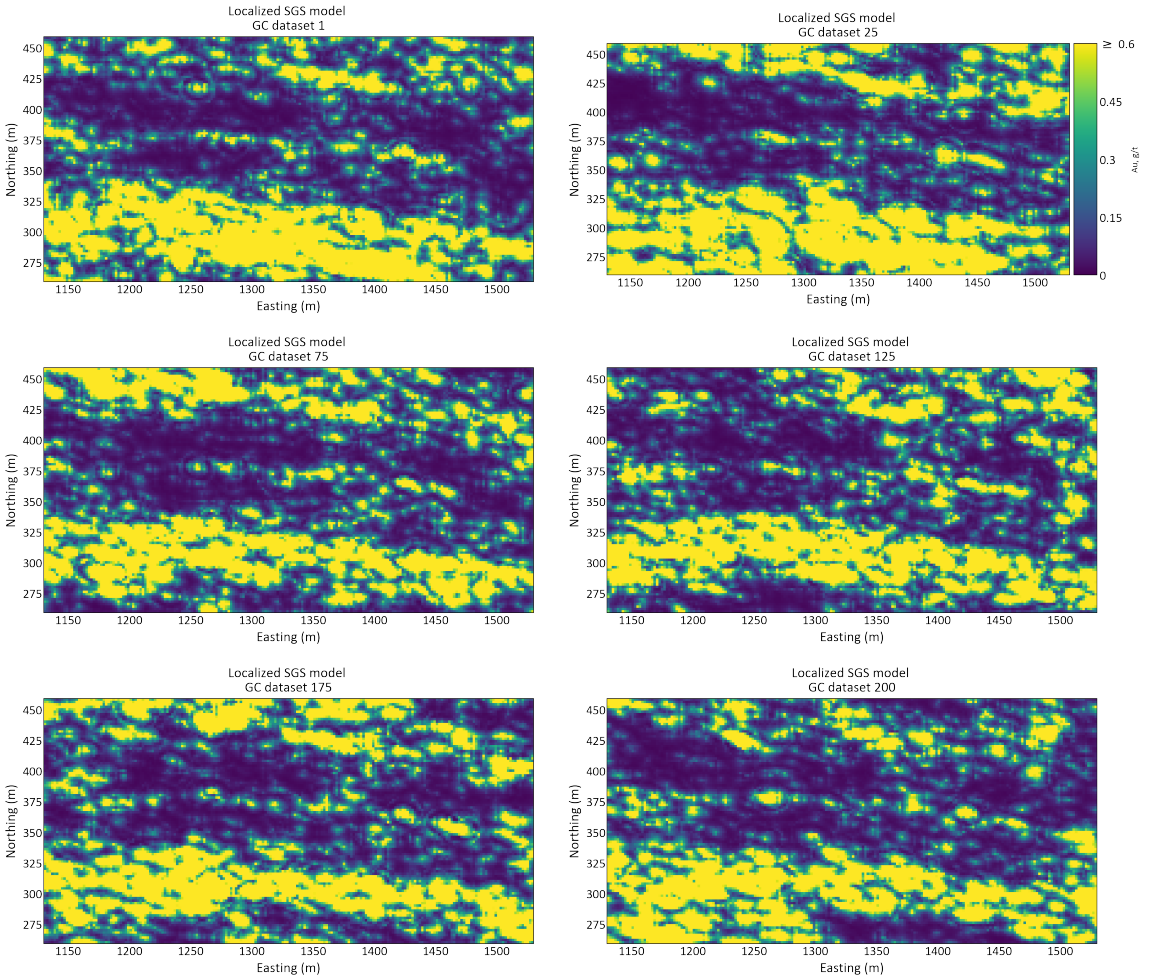

Figure 3.30: Some selected Localized SGS models. Each localized SGS model is generated from localizing 100 realizations.

findings indicate that the localized SGS models exhibit significantly higher expected MSE values than their corresponding kriged and ExpSGS counterparts but a lower expected MSE than LUC. Notably, at a low cutoff grade of 0.2 g/t, there exists a substantial difference of $94.613 in the expected MSE between ExpSGS and LocSGS and a difference of $27.812 in expected MSE between LocSGS and ordinary kriging using 45 samples. Furthermore, LUC achieves an expected percentage of the maximum attainable profit of 78.50%, demonstrating a performance below that of OK (SSP) (80.34%), OK (LSP) (80.88%), ExpSGS (85.88%) and LUC (81.97%) for the same 0.2 g/t cutoff grade.

Figure 3.33 shows a distribution of maximum attainable profits for the 200 LocSGS models at 0.2g/t and 0.8g/t cutoff grade.

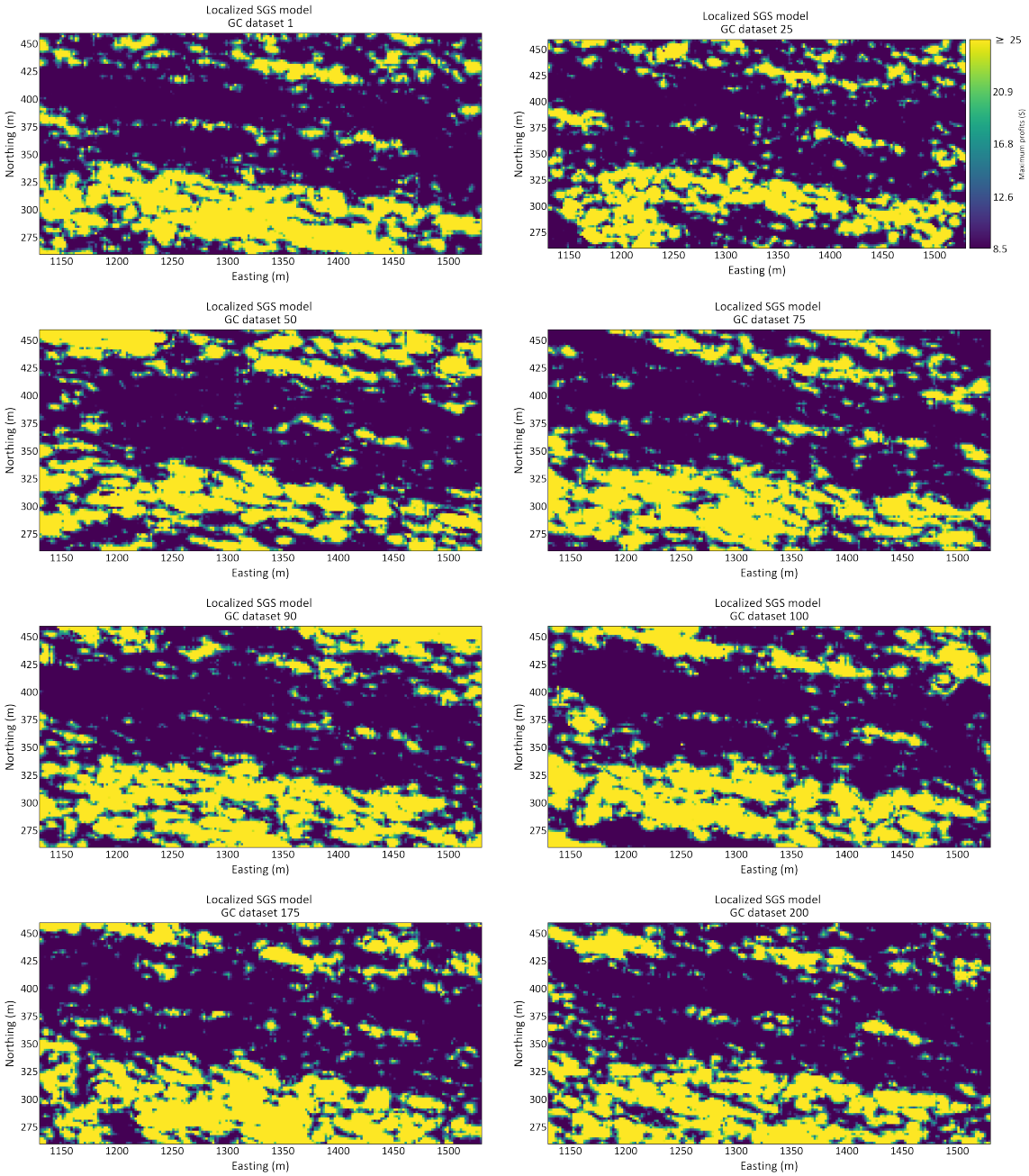

Figure 3.31: Numerical model in profits for some selected localized SGS models.

Model	False positive FP(%)	False negative FN(%)	Misclassified errors (%)	Maximum attainable profit(%)	Mean squared error ($)
Cutoff grade of 0.2					
OK (using 45 samples)	10.85	6.36	17.21	80.88	476
Expected SGS	6.67	8.66	15.33	85.88	409
LUC	13.90	6.34	20.24	81.97	507
LocSGS	8.95	8.67	17.62	78.50	504
Cutoff grade of 0.8					
OK (using 45 samples)	5.48	5.02	10.50	26.35	38
Expected SGS	2.55	6.84	9.39	30.51	31
LUC	6.0	5.41	11.41	25.49	40
LocSGS	5.09	5.57	10.66	25.36	40

Table 3.6: Expected percentage of misclassified errors, maximum attainable profit and mean squared error of the two hundred models for OK, expected SGS, LUC and LocSGS.

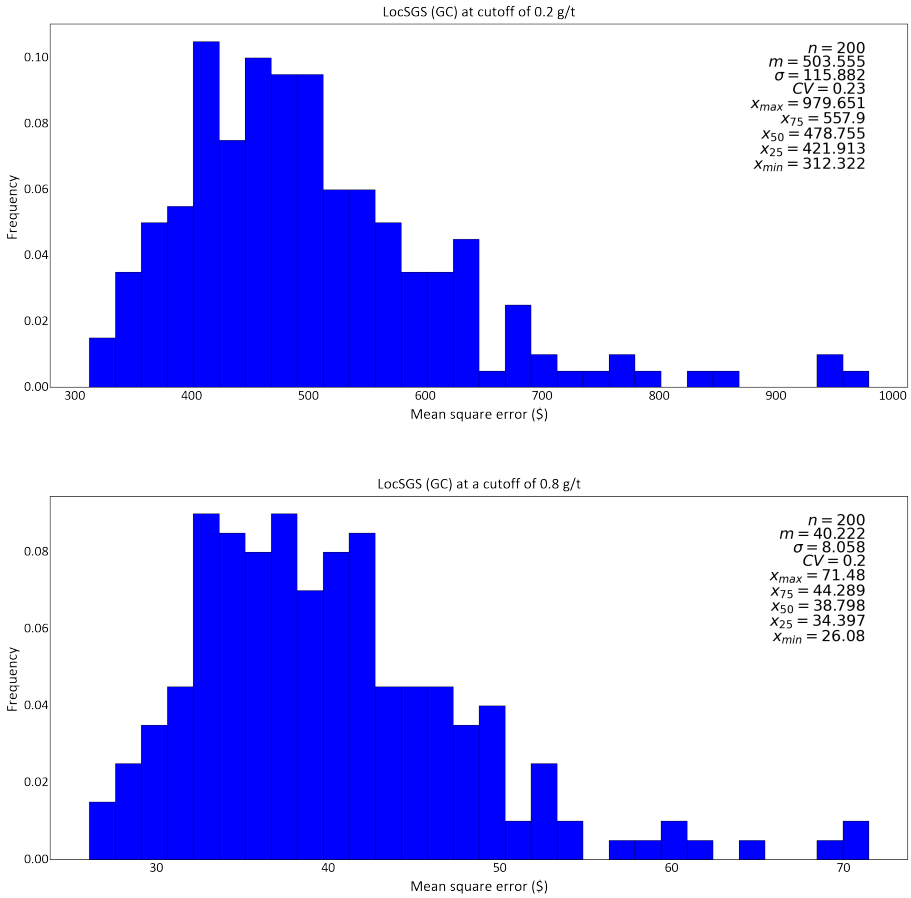

Figure 3.32: Summary statistics of MSE in profits for 200 LocSGS models at different cutoff grades.

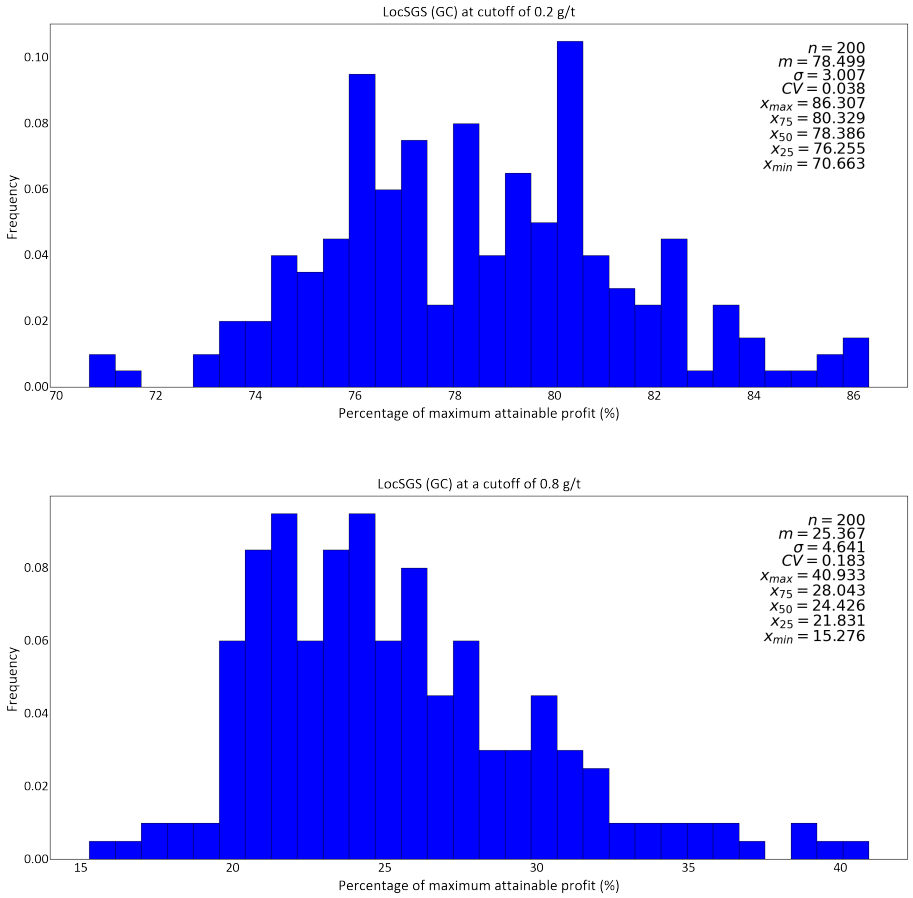

Figure 3.33: Summary statistics of percentage maximum attainable profits for 200 LocSGS models at different cutoff grades.

3.7.7 Dig Limits

Hand-drawn dig limits, a traditional practice, delineate ore and waste boundaries based on equipment capabilities. These manual drawings are subjective, don't directly maximize profit, and often exhibit significant inconsistencies. Determining the optimal destination for material in a mine based on expected profit at a cutoff involves considering uncertainty in grade distribution. While the maximum profit destination may seem like the best choice, it may not always be correct due to the possibility of true grades indicating a different destination. The decision must be based on expected profit values, a risk-neutral approach. To achieve the highest profit, selecting the destination that maximizes expected profit is necessary. Figure 3.34 shows the expected maximum profit destination and mineable destination determined autonomously.

The optimal dig limit for the mine would have the lowest equipment factor possible and still be easy to mine. One way to compare the effectiveness of the different limits is to calculate the amount of ore and waste within the limits and the amount of ore lost. A mining professional can select an appropriate equipment factor that results in a dig limit polygon with the best balance, maximum profit, and digability. Table 3.7 shows the values of maximum profit with free selection and profit with mining selection.

Description	Maximum profit with free selection	Profit with mining selection	Percentage of maximum profit
Cutoff grade of 0.2			
OK (using 5 samples)	$ 376280	$ 375713	99.84 %
OK (using 45 samples)	$ 376016	$ 375551	99.87 %
Expected SGS	$ 372897	$ 372493	99.89 %
Localized UC	$ 372212	$ 371647	99.84 %
Localized SGS	$ 358745	$ 358009	99.79 %
Cutoff grade of 0.8			
OK (using 5 samples)	$ 160909	$ 160425	99.69 %
OK (using 45 samples)	$ 160730	$ 160241	99.69 %
Expected SGS	$ 160103	$ 159804	99.81 %
Localized UC	$ 158898	$ 158494	99.74 %
Localized SGS	$ 160562	$ 159922	99.60 %

Table 3.7: Summary table for dig limit performance.

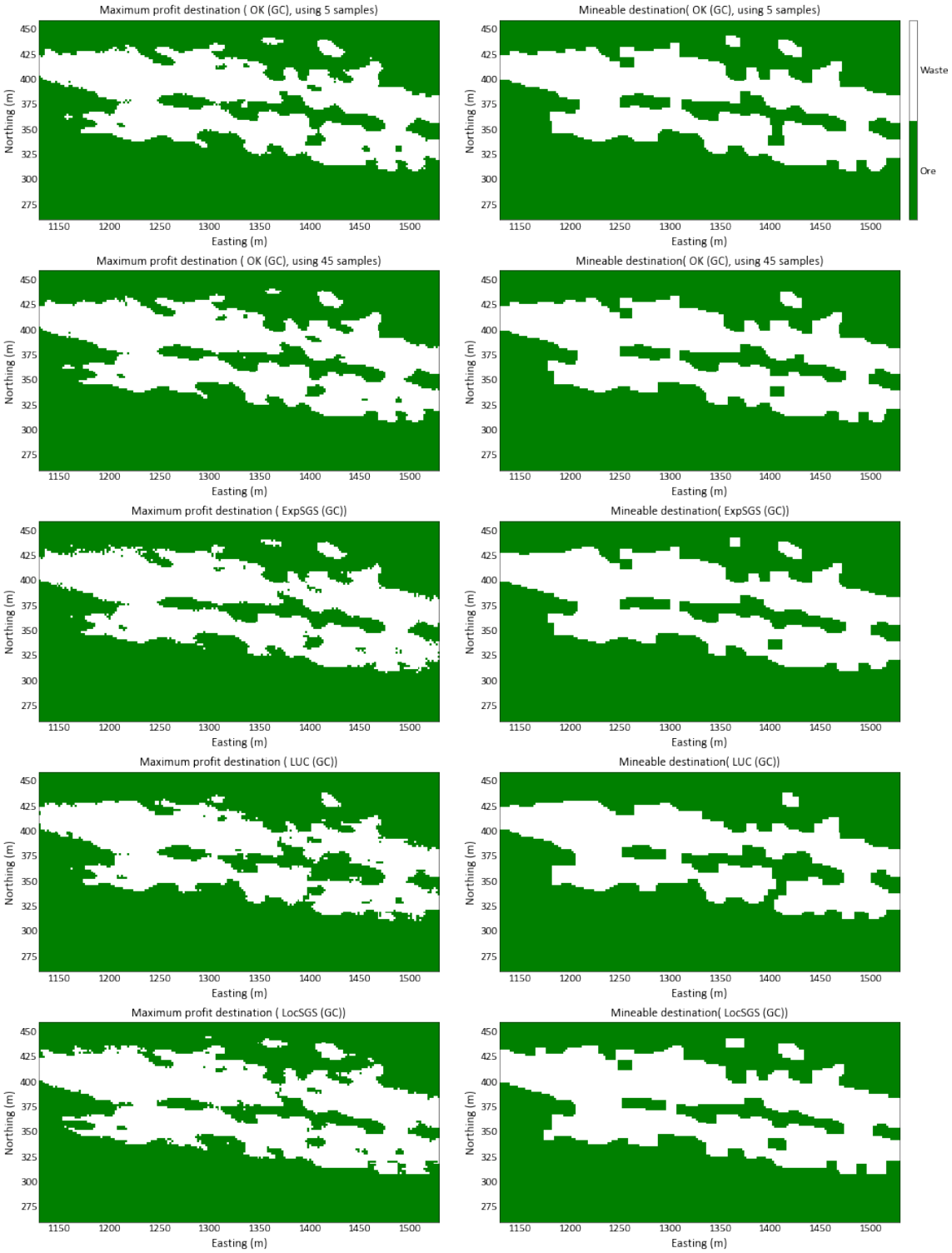

Figure 3.34: Dig limits for grade control models.

3.7.8 Conclusion

In this case study, each modeling technique has generated an estimate at the SMU scale for each location within the area of interest. In this instance, where we have a reference true model with an estimate for each location, the model checking approach will evaluate the global histogram reproduction, mean squared error, expected false negatives and false positives, and percentage of maximum attainable profits. First, an overview of the results from each model is given, followed by a look at the local results for select locations. Table 3.8 shows the expected values of the global results of the 200 grade control models at the SMU scale.

Description	**Mean Au (g/t)**	**Variance**
Upscaled reference models	0.445	0.557
OK (using 5 samples)	0.445	0.456
OK (using 45 samples)	0.445	0.406
Expected SGS	0.442	0.338
Localized UC	0.446	0.334
Localized SGS	0.420	0.421

Table 3.8: Expected values of the global results of the 200 grade control models at the SMU scale.

Model	False positive FP(%)	False negative FN(%)	Misclassified errors (%)	Maximum attainable profit(%)	Mean squared error profit($)
Cutoff grade of 0.2					
OK (using 5 samples)	9.98	7.22	17.20	80.34	515
OK (using 45 samples)	10.85	6.36	17.21	80.88	476
Expected SGS	6.67	8.66	15.33	85.88	409
Localized UC	13.90	6.34	20.24	81.97	507
Localized SGS	8.95	8.67	17.62	78.50	504
Cutoff grade of 0.8					
OK (using 5 samples)	5.52	5.20	10.72	26.89	41
OK (using 45 samples)	5.48	5.02	10.50	26.35	38
Expected SGS	2.55	6.84	9.39	30.51	31
Localized UC	6.00	5.41	11.41	25.49	40
Localized SGS	5.09	5.57	10.66	25.36	40

Table 3.9: Expected percentage of misclassified errors, maximum attainable profit and mean squared error of the two hundred models for OK, expected SGS, LUC and LocSGS.

The mean and variance of estimates reported for each technique demonstrate a similar overall trend. However, when considering ordinary kriging (OK) with a small search plan, a notable increase in the variance of 0.101 is observed compared to the expected variance estimates derived from the reference true models. This decrease in variance for OK (using 45 samples) can be attributed to the

smoothing effect caused by using more samples. Nevertheless, despite these differences, the expected mean and expected variance suggest that all five techniques effectively represent the deposit. Table 3.9 details the expected percentage of misclassified errors, maximum attainable profit, and mean squared error of the LocSGS, LUC, expected SGS, and OK model. At both a low and high cutoff grade, ExpSGS outperforms the other techniques in terms of the percentage of misclassified errors, percentage of maximum attainable profit, and mean square error. LocSGS outperforms OK (using 5 samples) regarding the MSE by a \$11.844 improvement and LUC by a \$3.887 improvement. LocSGS returned the lowest expected percentage of maximum attainable profit, 7.38% less than ExpSGS. It can also be seen from Table 3.9 that using fewer data is not enough to obtain optimal kriging results. Generally, using 24-60 data is enough to obtain optimal Kriging results. Figure 3.35 illustrates the sensitivity of kriging results to the number of data points used for estimation. It showcases the mean squared error (MSE) and estimates variance obtained through kriging for varying data sizes, ranging from 1 to 60 samples. Typically, increasing the number of data used for the Kriging enhances the quality of the estimation, reaching a threshold where further data inclusion primarily prolongs computational time without significantly altering the estimation results. It is impractical to directly compare and contrast the distributions across an entire domain for all models generated using different geostatistical techniques. To assess the variation between the five techniques at a local scale, estimates from three specific Selective Mining Units (SMUs) within each model have been chosen for analysis. These SMUs include a high-value SMU located at grid coordinates $x = 1353.0$, $y = 303.0$, and $z = 5$; a medium-value SMU at $x = 1397.0$, $y = 287.0$, and $z = 5$; and a low-value SMU at $x = 1370.0$, $y = 261.0$, and $z = 5$. Figure 3.36 illustrates the spatial positions of these SMUs and how each technique classifies them as ore or waste based on a cutoff grade of 0.2 g/t. For a comprehensive description of these SMUs across all five implemented techniques, refer to Table 3.10. This table provides detailed information about each SMU, including its grade values and the classification assigned by each technique. The results shows that Kriging with 5 samples produced estimates with better local accuracy for the three SMU values.

Description	High Value SMU			Medium Value SMU			Low Value SMU		
	grade	maximum profit	classification	grade	maximum profit	classification	grade	maximum profit	classification
Upscaled reference model	1.186	\$50.417	Ore	0.427	\$18.156	Ore	0.049	\$8.500	Waste
OK (using 5 samples)	1.279	\$54.385	Ore	0.616	\$26.210	Ore	0.098	\$8.500	Waste
OK (using 45 samples)	1.267	\$53.863	Ore	0.789	\$33.548	Ore	0.212	\$9.021	Ore
Expected SGS	1.322	\$56.207	Ore	0.659	\$27.420	Ore	0.148	\$6.460	Waste
Localized UC	1.366	\$58.055	Ore	1.371	\$58.267	Ore	0.268	\$11.390	Ore
Localized SGS	1.325	\$56.320	Ore	0.634	\$26.945	Ore	0.188	\$8.500	Waste

Table 3.10: Results for some specific SMU locations across implemented techniques. Note: Ore & waste classification is based on a cutoff grade of 0.2g/t. These results are based on models generated from dataset 1.

Figure 3.37 presents the mean square error in profits for all 200 models generated via each

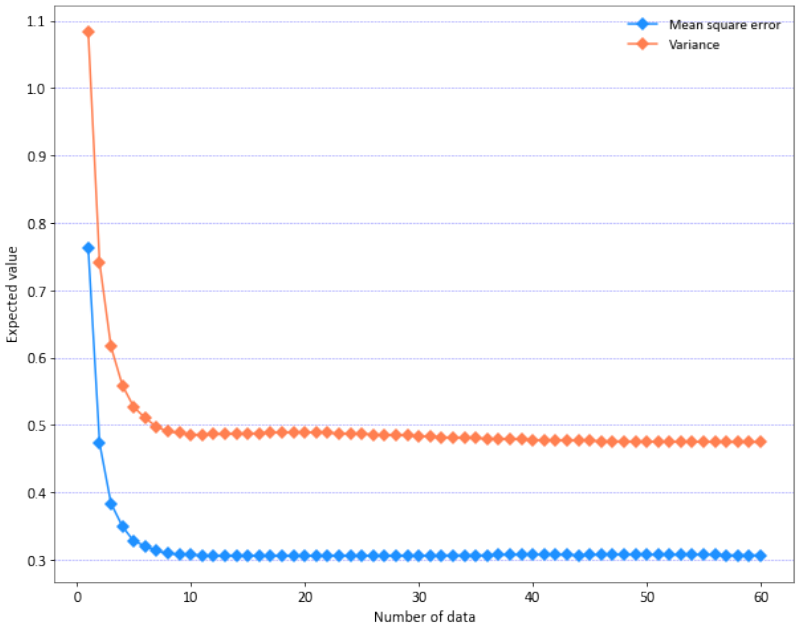

Figure 3.35: Effect of data size on ordinary kriging performance.

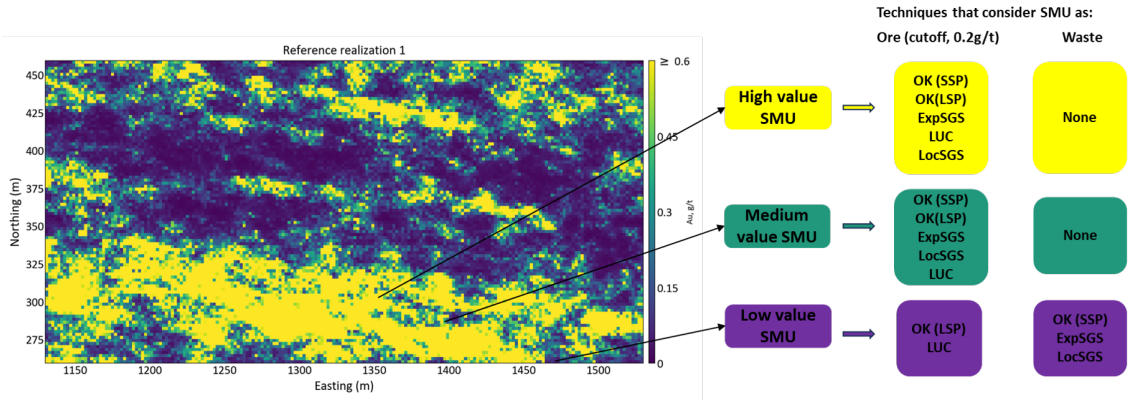

Figure 3.36: spatial positions of these SMUs and how each technique classifies them as ore or waste based on a cutoff grade of 0.2 g/t.

technique. It was consistently observed that the ExpSGS models yielded lower MSE compared to the corresponding kriged models, LUC, and LocSGS models for each GC dataset. More errors will translate to lower profits. Additionally, it is noticed from Figure 3.38(b) that the percentage of false negatives (FN) for the ExpSGS models is consistently higher than the percentage of FN for the corresponding models generated via OK, LUC, and LocSGS. Conversely, the percentage of false positives (FP) for the ExpSGS models was consistently lower than the percentage of FP for the other techniques, Figure 3.38(a). When dealing with false positives, which are blocks estimated as ore but are actually waste according to the true model, it is preferable to aim for a lower expected false positive rate. This is because false positives entail additional costs related to transporting material to the mill and processing it, even though it does not contain valuable ore. Figure 3.39 shows the relations between the cutoff grades, maximum attainable profit and MSE for ordinary

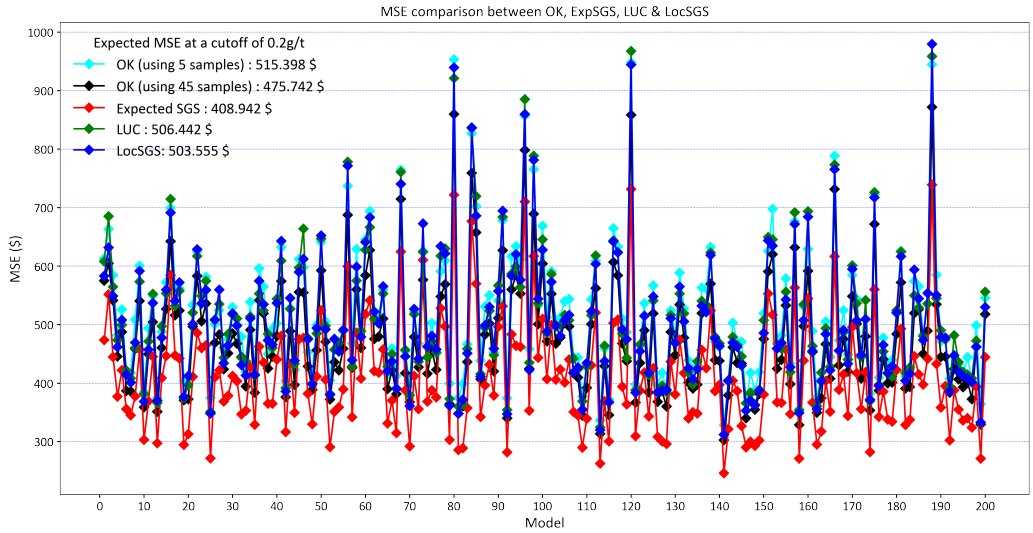

(a) Comparison of MSE in profits for all 200 models generated via OK, ExpSGS, LUC and LocSGS at a cutoff of 0.2 g/t.

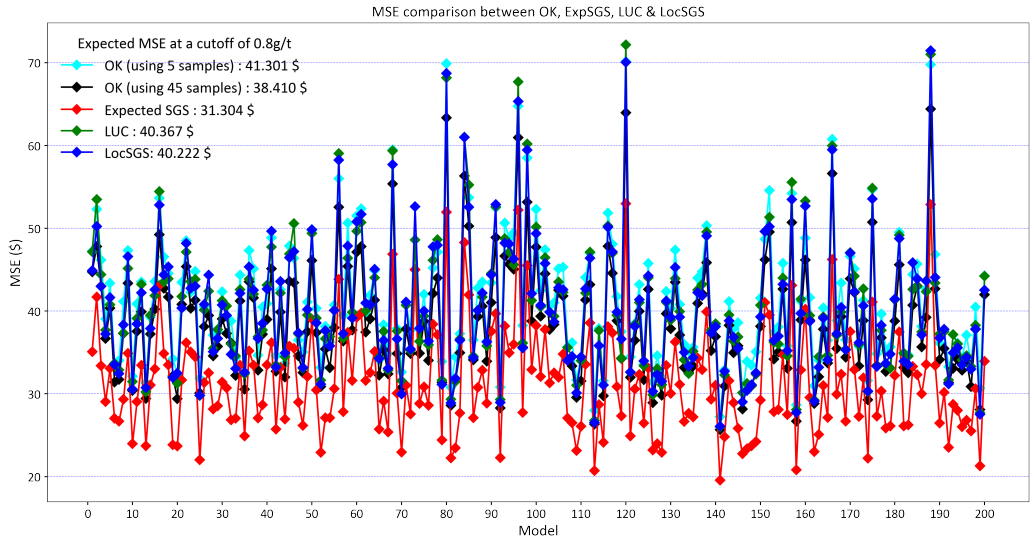

(b) Comparison of MSE in profits for all 200 models generated via OK, ExpSGS, LUC and LocSGS at a cutoff of 0.8 g/t.

Figure 3.37: Comparison of MSE in profits for all 200 models generated via OK, ExpSGS, LUC and LocSGS.

kriging, ExpSGS, LUC and LocSGS. Figure 3.40 shows the relations between the cutoff grades, false positives and false negatives for ordinary kriging, ExpSGS, LUC and LocSGS. Figure 3.41 and 3.42 shows a distribution of MSE and maximum attainable profits for the 200 OK, ExpSGS, LUC and LocSGS models.

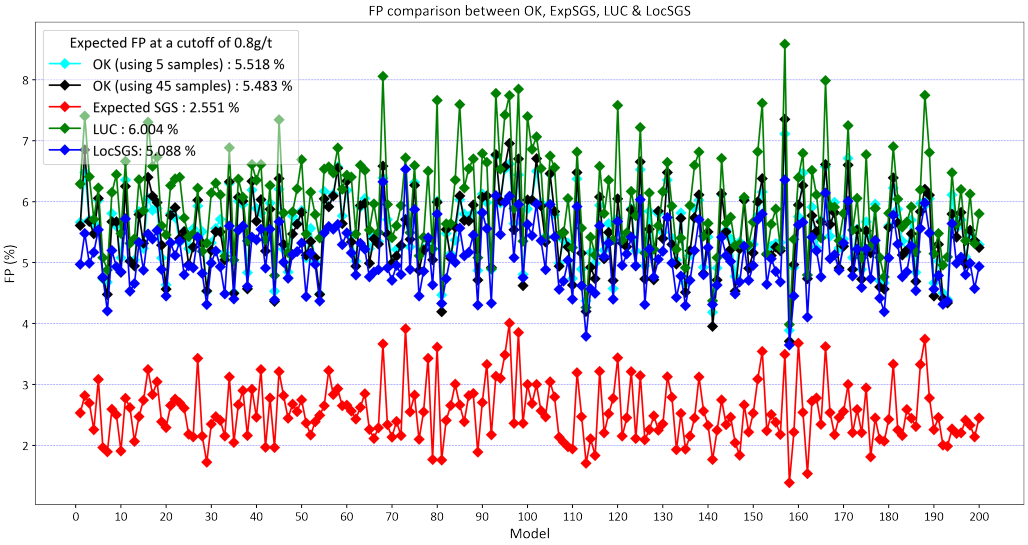

(a) Comparison of false positives for all 200 models generated via OK, ExpSGS, LUC and LocSGS at a cutoff of 0.8 g/t.

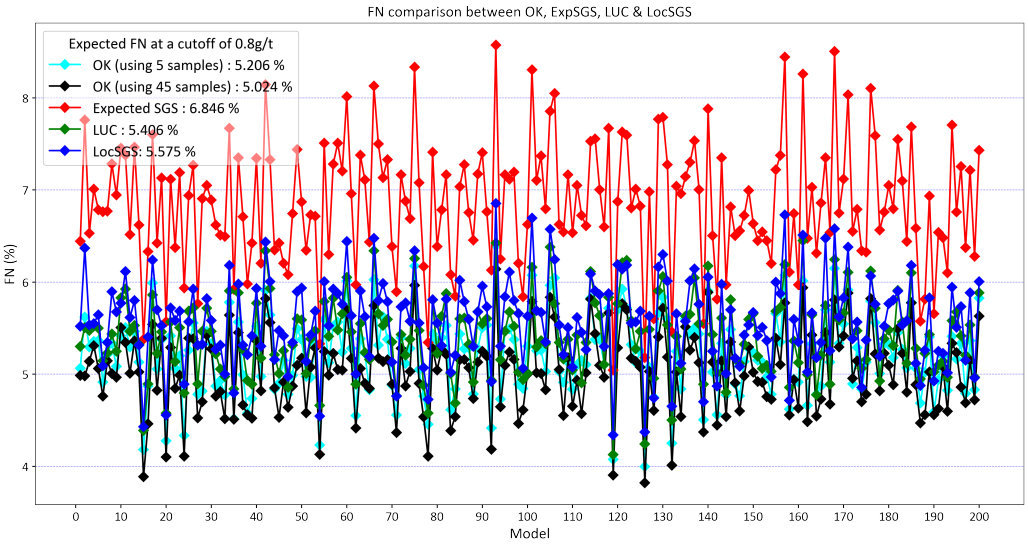

(b) Comparison of false negatives for all 200 models generated via OK, ExpSGS, LUC and LocSGS at a cutoff of 0.8 g/t.

Figure 3.38: Comparison of false negatives and false positives for all 200 models generated via OK, ExpSGS, LUC and LocSGS.

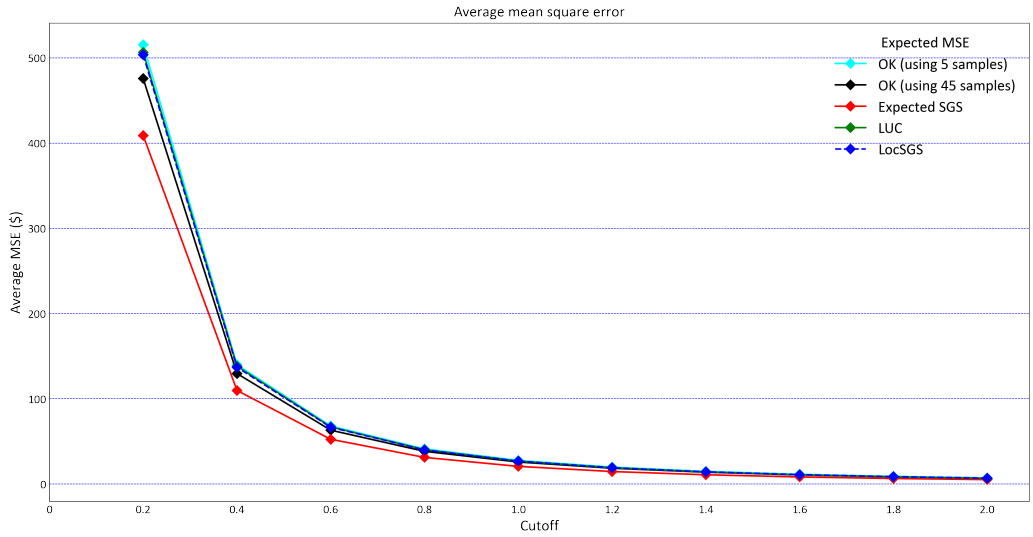

(a) Expected mean square error for OK, ExpSGS, LUC and LocSGS at different cutoff grades.

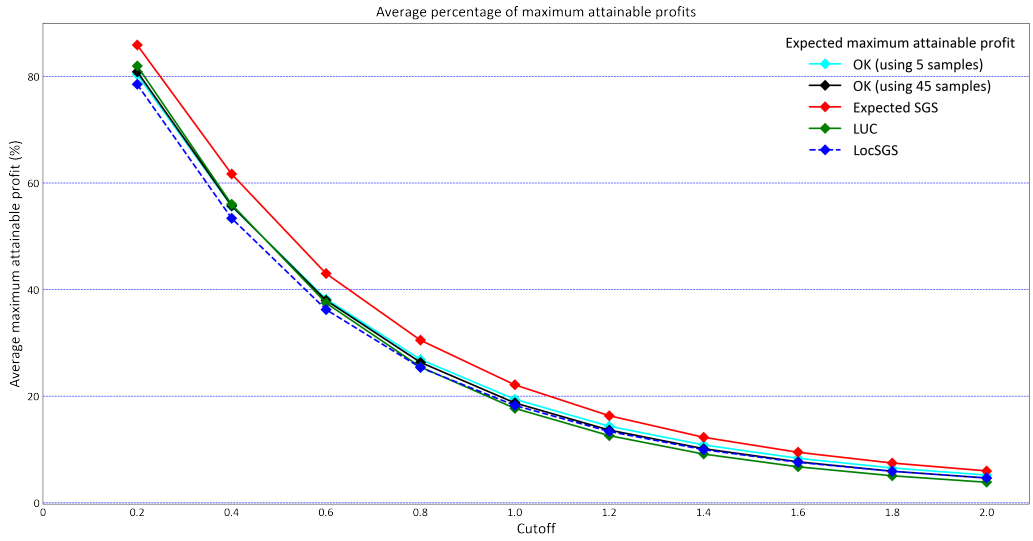

(b) Expected percentage of maximum attainable profit for OK, ExpSGS, LUC and LocSGS at different cutoff grades.

Figure 3.39: Expected percentage of maximum attainable profit and mean squared error of grade control models at different cutoff grades.

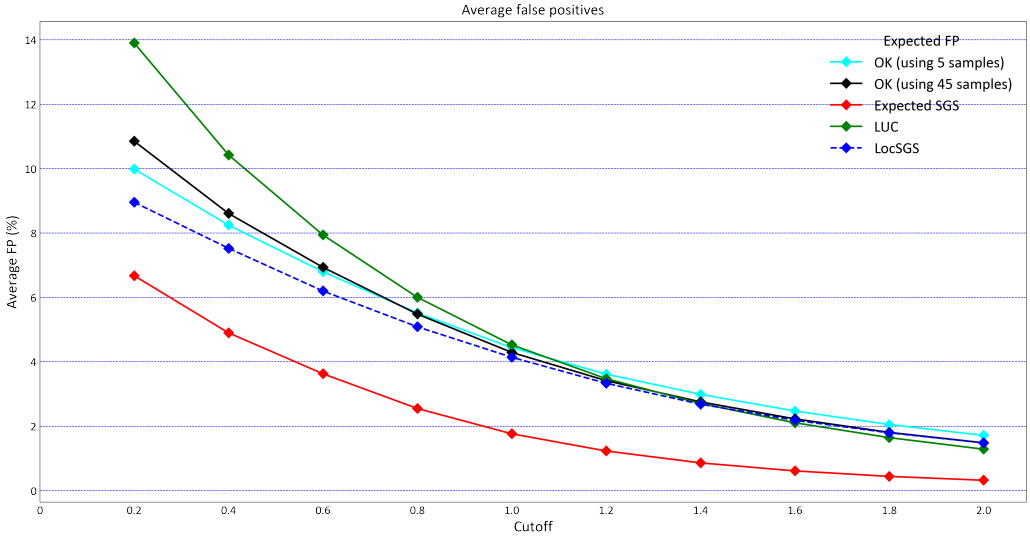

(a) Expected FP for OK, ExpSGS, LUC and LocSGS at different cutoff grades.

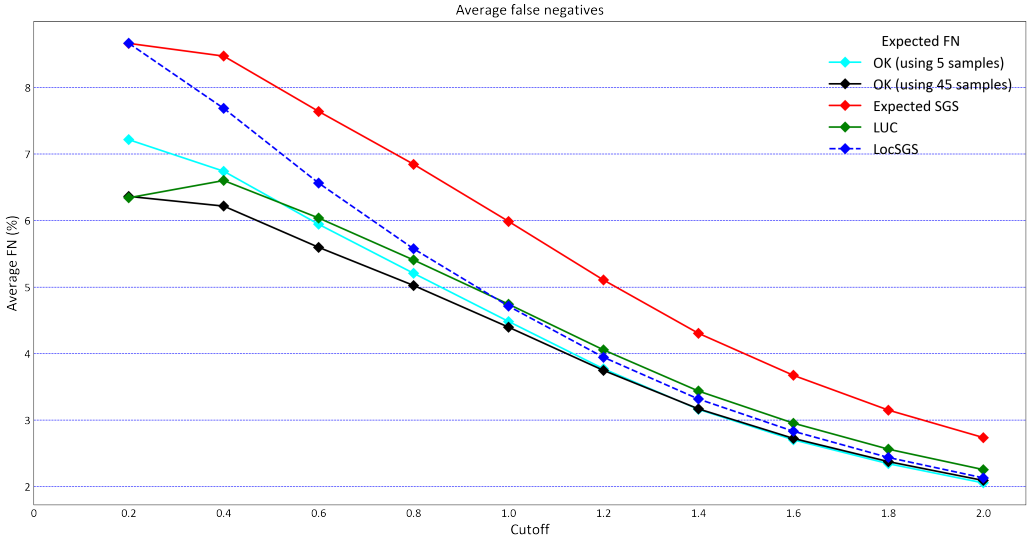

(b) Expected FN for OK, ExpSGS, LUC and LocSGS at different cutoff grades.

Figure 3.40: Comparative analysis of expected performance metrics for techniques used to model grade control data.

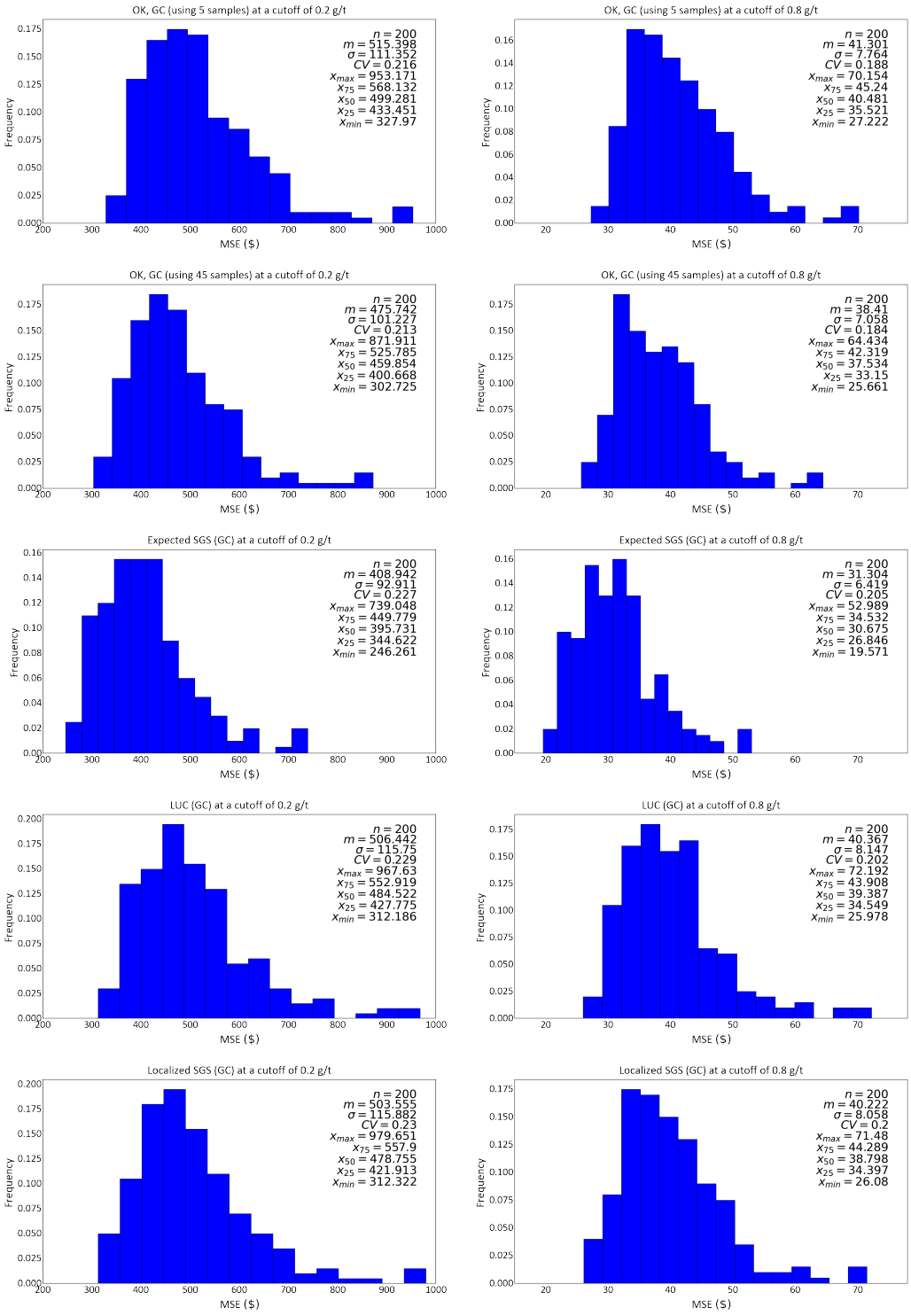

Figure 3.41: Summary statistics of MSE in profits for OK, ExpSGS, LUC and LocSGS models at a cutoff grade of 0.2 g/t and 0.8 g/t.

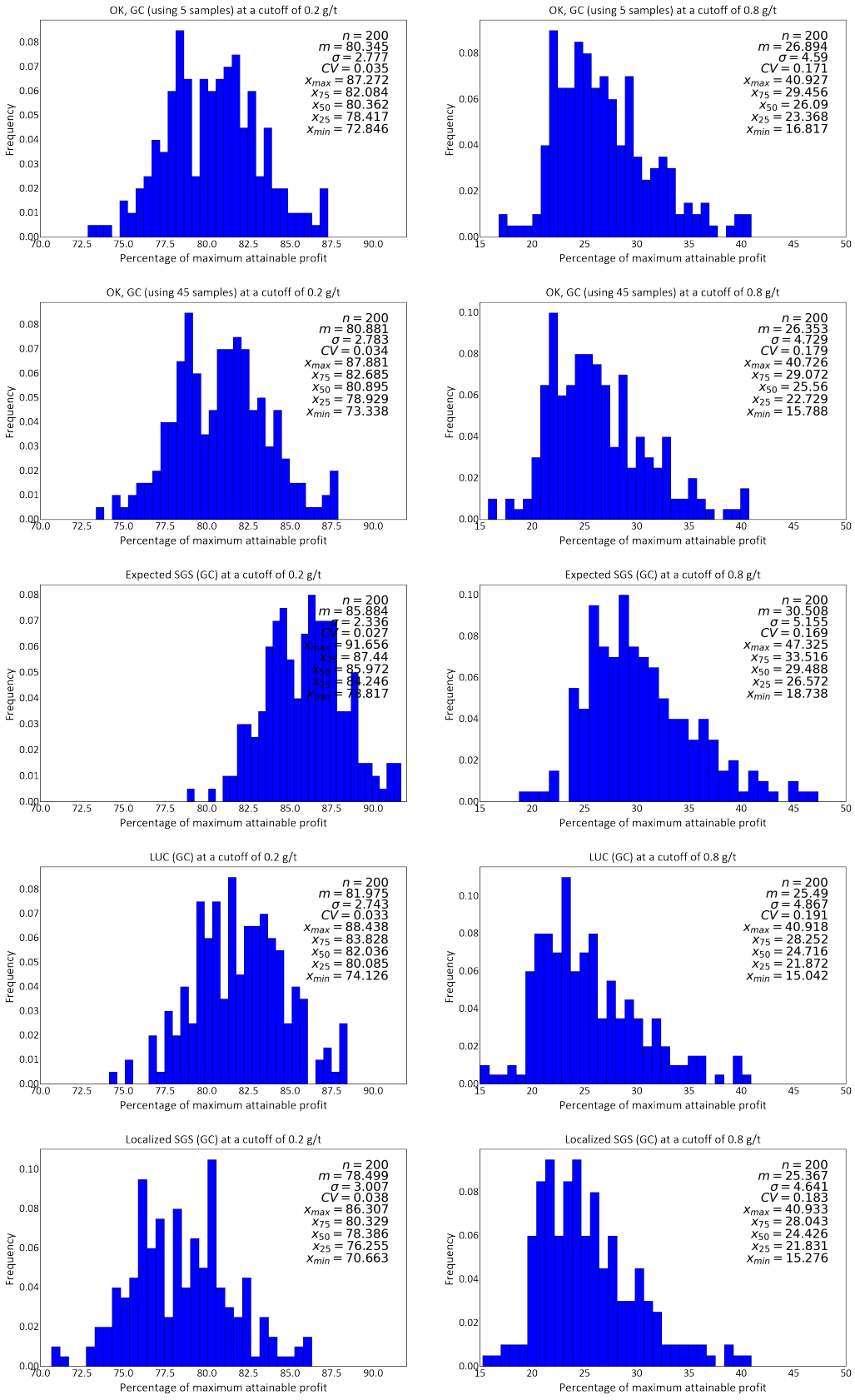

Figure 3.42: Summary statistics of percentage of maximum attainable profit for OK, ExpSGS, LUC and LocSGS models at a cutoff grade of 0.2 g/t and 0.8 g/t.

Chapter 4

Long Term Model

Mining operations require a long-term perspective for planning expansion in prospective zones, and the Long-term model (LTM) provides an estimate of the underlying mineralization using widely spaced drill holes. Long-term resource models are essential for understanding trends and patterns in data and making informed decisions about resource management. These models capture spatial and temporal relationships between variables and provide acceptable tonnage and grade estimates for each period until the end of the mine's life. The LTM uses selective mining units (SMUs) as block size, resulting in a low-resolution model. Although the long-term models provide accurate global predictions, it is not sufficient for daily mining operations, so other resource models with higher resolution and accuracy are necessary.

Long-term models are designed to provide an overall estimate of a mining operation's mineral resources and reserves, typically for several years or more. They are not intended to provide precise estimates of individual blocks or small volumes of ore. This is because the accuracy of the estimates decreases as the block size increases due to the inherent variability and uncertainty in the geological and mineralogical characteristics of the deposit. In contrast, short-term models, such as the SMU used in grade control, are designed to provide more accurate estimates for smaller volumes of ore, typically for weeks to months. Overall, the LTM and STM are complementary models used for different purposes in a mining operation. The LTM provides an approximate resource perspective over a long time frame, while the short-term model is used for short-term planning and production control. The accuracy and resolution of these models depend on various factors, including the drilling data used, the estimation parameters chosen, and the block size selected. Careful consideration of these factors is critical to ensuring that the resource and reserve estimates are accurate and reliable. Also, each model uses different data types, estimation parameters, block sizes, etc., as shown in Figure 4.1.

4.1 Sampling for Long Term Modeling

The mining industry relies on drilling data as the primary source of information for various purposes, such as estimation, design, and sterilization. Surface sampling is another method that collects samples from the top layer of soil or rock but may not provide sufficient information on deeper subsurface layers. There are several drilling methods in the industry, each with different technical features and sampling protocols, resulting in samples with varying geostatistical features, sample type, quality, and confidence. Drilling data can be classified as primary or secondary based on the

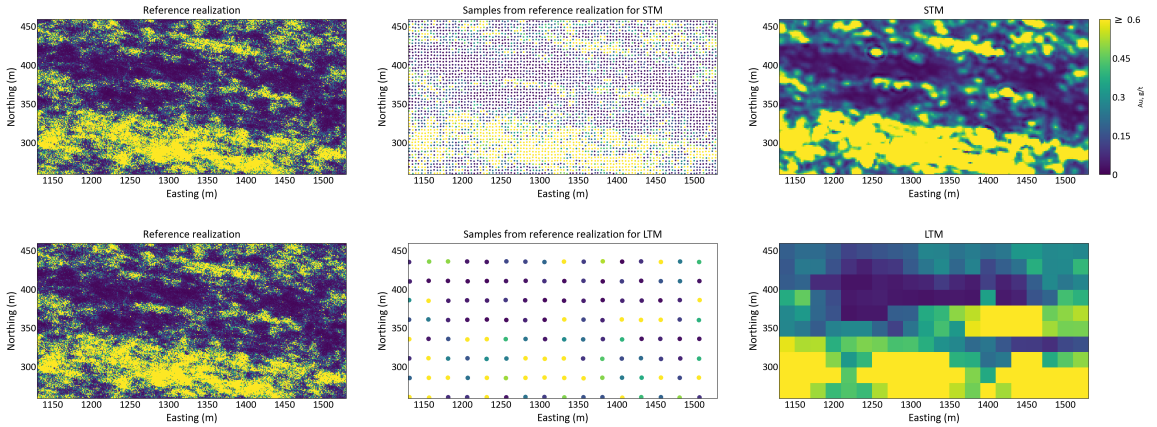

Figure 4.1: (a) Reference realization, 1m block size (b) Samples, 4m x 4m spacing, (c) STM , 2m block size, (d) True model, 1m block size (e) Samples, 25m x 25m spacing, (f) LTM, 20m block size.

quality of the information provided. Primary data is of the highest quality and reliability and is extensively used for resource estimation and research. In contrast, secondary data is less reliable due to lax quality controls in the drilling and sampling processes. The optimal drill spacing for obtaining data for long-term modeling depends on several factors, including the size and shape of the target mineral deposit, the type of mineral being sought, and the surrounding rock and soil characteristics.

4.2 Volume Variance Relations for SMU Variability

When dealing with widely spaced data, using more than enough samples for estimation can badly affect the accuracy of the estimates. To determine the optimal number of data to use in Kriging when dealing with widely spaced data, the study aimed to identify the point at which the variance of the estimates reaches a balance given a desired variance determined from the SMU block scale. The variance of a distribution with respect to its support is characterized by the dispersion variance notation $D^2(v, V)$ where v represents a small support of the values, and V represents a larger support of the mean. This is the variability of the data of smaller support within the larger volume. As shown above, the total variance in a domain A is equal to the sum of the average variance of points within blocks of some volume V and the variance of those blocks within the domain A (Isaaks & Srivastava, 1989):

$$D^2(v, A) = D^2(v, V) + D^2(V, A)$$

This relationship is known as Krige's Relation. As we are interested in the dispersion variance of blocks V within some domain A, we re-arrange the above equation to:

$$D^2(V, A) = D^2(v, A) - D^2(v, V)$$

The dispersion variance of the data within the domain is equal to the sample variance, $D^2(v, A) = \sigma^2$, and the dispersion variance of point data within the block, $D^2(v, V)$, can be calculated from the

variogram model.

By plotting the variance of the estimates against the number of data points, this investigation aimed to provide insights into the ideal number of data required for accurate kriging predictions. The widely spaced data consisted of samples taken at $25m \times 25m$ intervals, covering a $400m \times 200m \times 10m$ area. The samples were collected to represent realistic scenarios encountered in the field. Figure 4.2 (left) shows the location plot of the samples. Variograms were calculated and modeled in original

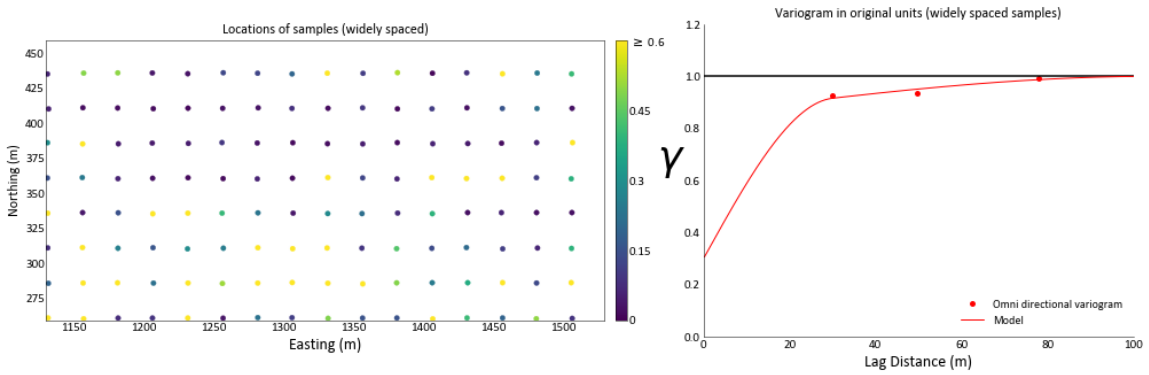

Figure 4.2: Configuration of samples for LTM.

units for the sample configuration, Figure 4.2 (right). Using the variogram model, kriged models were generated using different maximum number of samples. The maximum number of samples used are 1, 2, 3, 4, 5, 6, 7, 8, 9, 10, 11, 12, 13, 14, 15, 16, 17, 18, 19, 20, 21, 22, 23, 24, and 25. The standardized average variogram ($\bar{\gamma}$) for the block size of $20m \times 20m \times 10m$ is 0.7758. The sample variance is 2.1576. This equates to an actual average variogram ($\bar{\gamma}$) of $0.7758 \times 2.1576 = 1.6739$. The block variance is $2.1576 - 1.6739 = 0.4837$. From Figure 4.3, the block variance of 0.4837 intersects the curve of the estimate variance at a point where the number of data is equal to 7. This indicates the approximate optimal number of data needed to achieve the anticipated block variance.

4.3 Case Study

To obtain data for the long-term modeling, the same 200 reference realizations used for the examples demonstrated in Chapter 3 are sampled at regular $25m \times 25m$ spacing. A 1% sampling error was added to the coordinates to mimic potential errors in the field. Figure 4.4 shows the sampling configuration used to generate samples for long-term modeling. Four different geostatistical modeling techniques, including ordinary kriging, ExpSGS, LUC, and LocSGS, are applied to each of the sampled datasets from the 200 reference realizations. This leads to the creation of 200 ordinary kriging models for each search plan, 200 ExpSGS models, 200 LUC models, and 200 LocSGS models. The expected values obtained from the distribution of these models are then graphed for analysis. For all final models generated to evaluate the performance of estimators used to generate long-term modeling, an SMU size of $20m \times 20m \times 10m$ is considered. The goal or purpose is to tune the

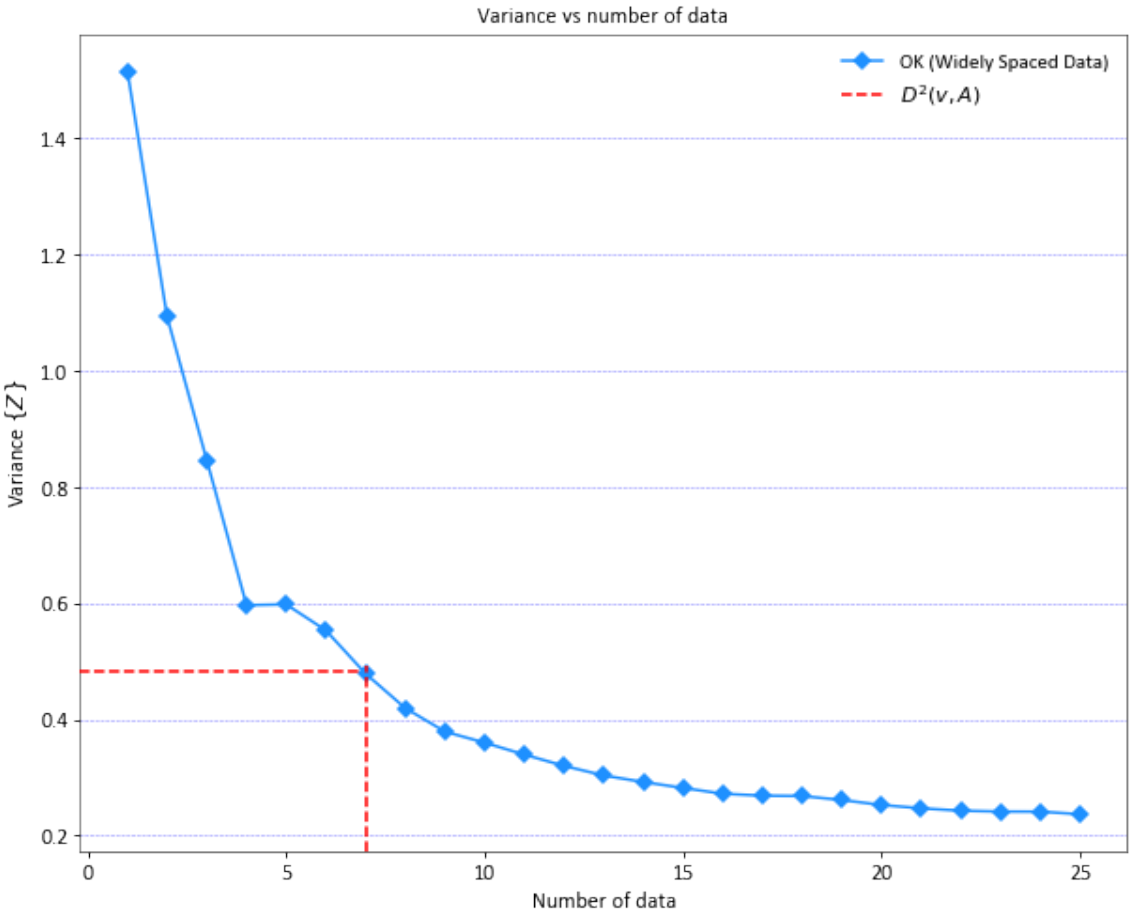

Figure 4.3: Variance of estimates against number of data.

prediction to get the correct resource in the future. The global predictions will match the tonnage and grade above the cutoff from the grade control model. The SMU size is also chosen to mimic selectivity in the future.

4.3.1 Variography

Variograms are calculated in both original and Gaussian units. The original units variogram is required for ordinary kriging in original units. The variogram in Gaussian units is required for SGS. For both cases, the variograms are modeled in two directions in the horizontal plane following Equation 3.11. The variograms are constructed with a major direction of continuity at 100 degrees from the north and a minor direction at 190 degrees from the north. For all the 200 sampled datasets derived from the 200 reference realizations, the variograms are calculated with consistent directions of continuity and modeled using two nested spherical variogram structures. The range of parameters for the two hundred variograms is described in Equation 4.1.

$$\gamma(\mathbf{h}) = (0.1:0.3) + (0.1:0.7)\cdot \mathrm{Sph}_{\substack{a^1_{hmax}=30:100 \\ a^1_{hmin}=0:20}} + (0.1:1)\cdot \mathrm{Sph}_{\substack{a^2_{hmax}=85:400 \\ a^2_{hmin}=0:80}} \tag{4.1}$$

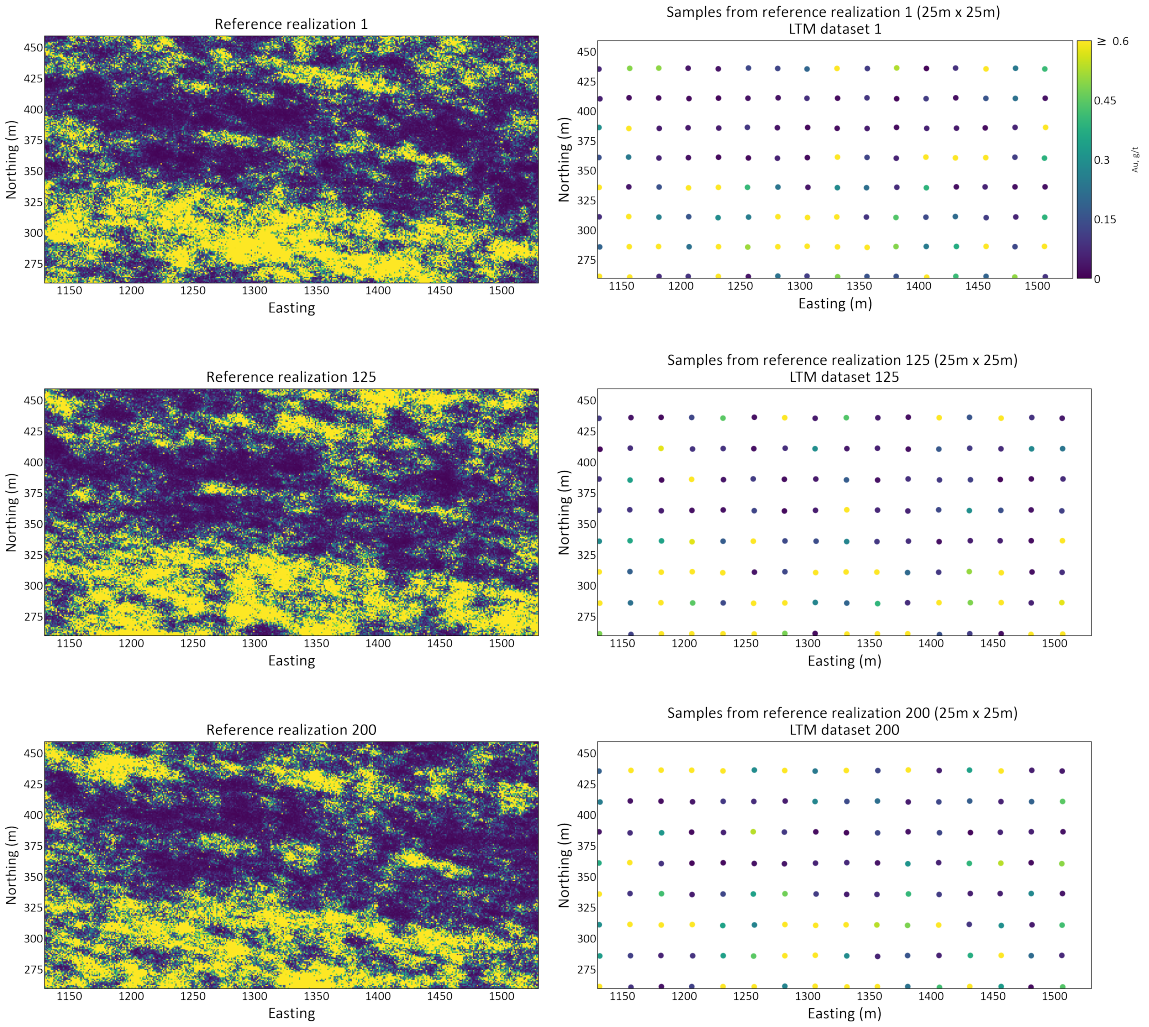

Figure 4.4: Reference data map against samples from reference data.

The nugget effect for all the variograms falls within the range of 0.1 to 0.3. The first spherical structure has a variance contribution ranging from 0.1 to 0.7, a minimum range from 0 to 20, and a maximum range from 30 to 100. The second spherical structure has a variance contribution ranging from 0.1 to 1, a minimum range between 0 and 80, and a maximum range between 85 and 400. More detailed parameters for some selected datasets derived from the two hundred realizations are provided in Table 4.1. Figure 4.5 illustrates six of the 200 variograms computed and modeled in original units.

Modelling in Gaussian space requires an additional set of variograms calculated using the normal scores of the sampled data. The range of parameters for the two hundred normal score variograms is described in Equation 4.2.

$$\gamma(\mathbf{h}) = (0.1:0.3) + (0.1:0.7)\cdot \mathrm{Sph}_{\substack{\mathrm{a}^1_{hmax}=30:100 \\ \mathrm{a}^1_{hmin}=0:20}} + (0.1:1)\cdot \mathrm{Sph}_{\substack{\mathrm{a}^2_{hmax}=85:400 \\ \mathrm{a}^2_{hmin}=0:80}} \tag{4.2}$$

The nugget effect for all the variograms falls within the range of 0.1 to 0.3. The first spherical

LTM dataset	Nugget effect	Structure types	Variance contribution (cc)	Range		
				a_{hmax}	a_{hmin}	a_{vert}
1	0.3	spherical	0.555	30	20	10
		spherical	0.145	104.52	80	10
30	0.3	spherical	0.672	36.93	20	10
		spherical	0.028	85	80	10
65	0.3	spherical	0.575	36.88	20	10
		spherical	0.125	85	80	10
100	0.3	spherical	0.453	47.33	20	10
		spherical	0.247	85	80	10
150	0.251	spherical	0.739	43.14	20	10
		spherical	0.01	85	80	10
200	0.268	spherical	0.579	30	20	10
		spherical	0.153	85	80	10

Table 4.1: Parameters of variogram model in original units for some selected LTM datasets.

structure has a variance contribution ranging from 0.1 to 0.7, a minimum range from 0 to 20, and a maximum range from 30 to 100. The second spherical structure has a variance contribution ranging from 0.1 to 1, a minimum range between 0 and 80, and a maximum range between 85 and 400. More detailed parameters for selected datasets are provided in Table 4.2. Figure 4.6 illustrates six of the 200 normal score variograms for the sampled data in Gaussian units.

LTM dataset	Nugget effect	Structure types	Variance contribution (cc)	Range		
				a_{hmax}	a_{hmin}	a_{vert}
1	0.279	spherical	0.386	30	20	10
		spherical	0.335	109.21	80	10
30	0.3	spherical	0.507	39.87	20	10
		spherical	0.193	85	80	10
65	0.3	spherical	0.479	47.24	20	10
		spherical	0.221	102.23	80	10
100	0.22	spherical	0.406	53.20	20	10
		spherical	0.374	85	80	10
150	0.234	spherical	0.726	50.39	20	10
		spherical	0.040	85	80	10
200	0.267	spherical	0.361	30	20	10
		spherical	0.372	86.21	80	10

Table 4.2: Parameters of variogram model in Gaussian units.

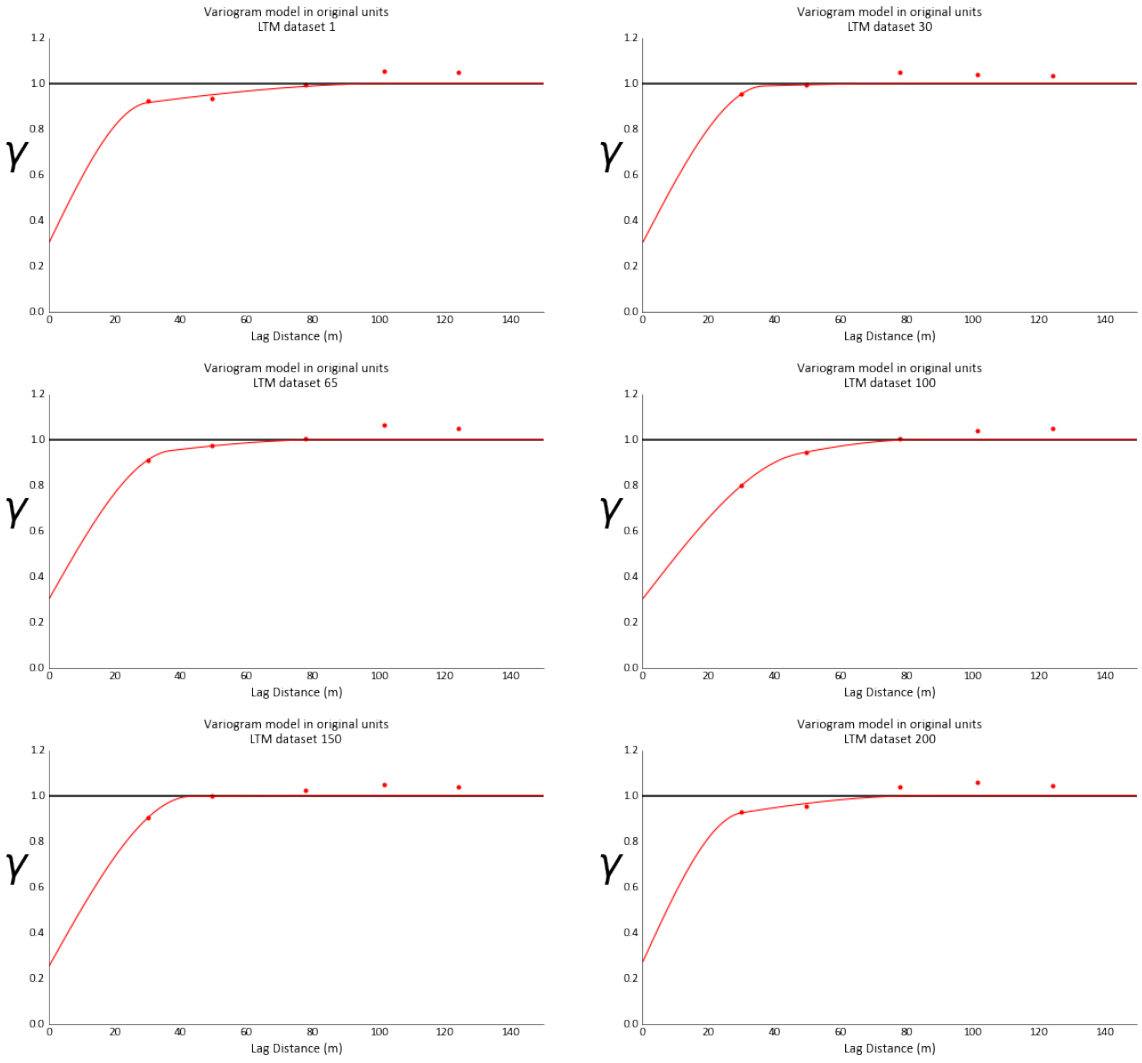

Figure 4.5: Standardized variograms calculated and fitted with two spherical structures for LTM datasets.

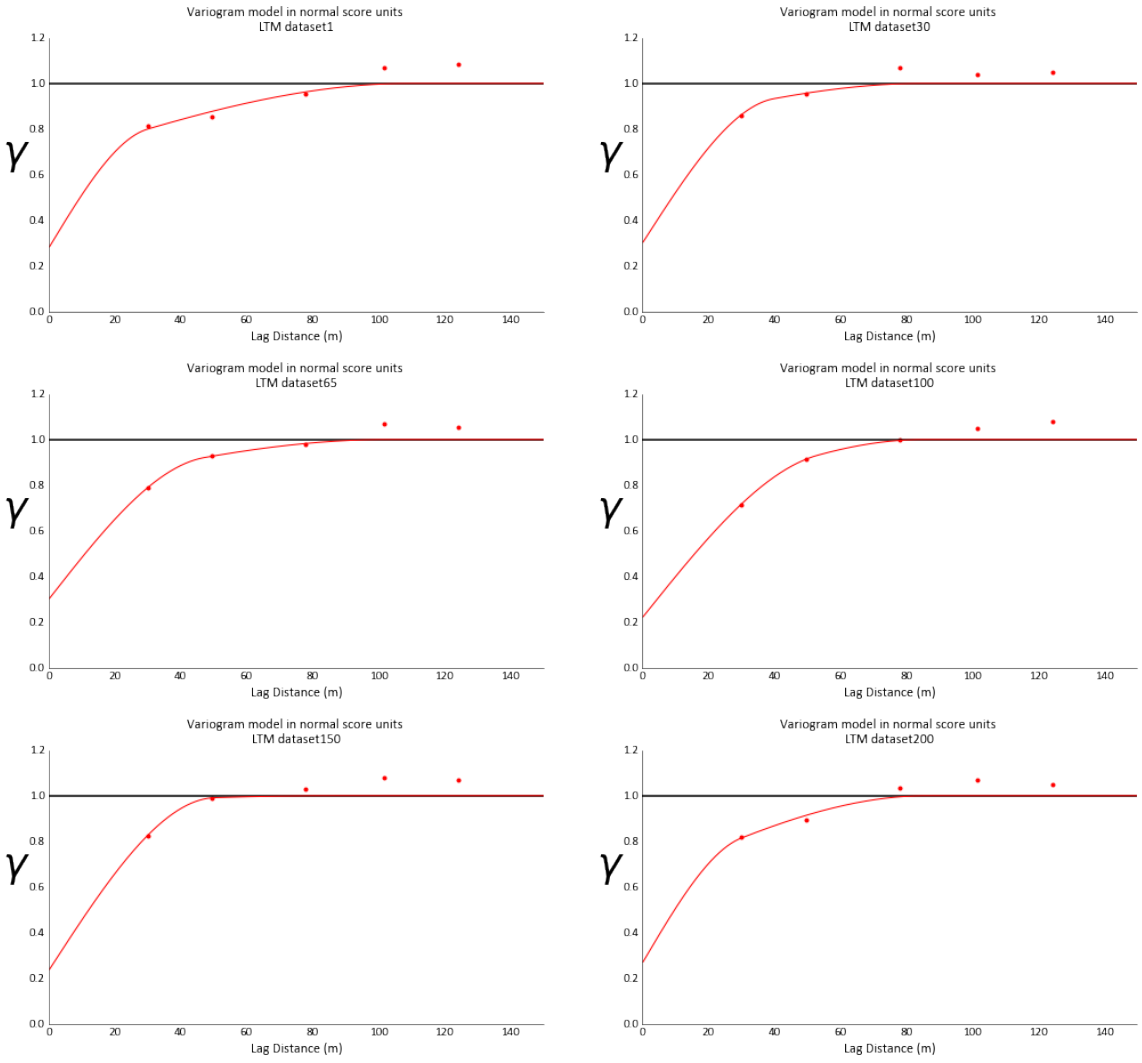

Figure 4.6: Normal score variograms calculated and fitted with two spherical structures for LTM datasets.

4.3.2 Ordinary Kriging

The sample data are obtained by sampling from each of the 200 reference maps at a regular $25m \times 25m$ spacing, as shown in Figure 4.4. A small random sampling error is added to the coordinates of the sampled data to mimic potential errors in the field. Subsequently, the sampled data are used to perform grade estimation at an SMU scale defined at a $20m \times 20m \times 10m$ grid using ordinary kriging. Various maximum data sizes, ranging from 1 to 20 data points, are considered for the estimation. Specifically, the sample sizes of 1, 3, 7, and 20 are elaborated upon in this chapter due to their significance in demonstrating the key outcomes. Experimental variograms are calculated and then modeled in the original units for ordinary kriging by using Equation 4.1. A maximum search radius of $400m$ and $200m$ is used for both the major and minor direction of continuity, respectively, and $10m$ is used for the vertical direction. This ensures that the required number of data is met. Figure 4.7 shows a map of the kriged estimates using different sample numbers.

To convert the ordinary kriging estimates to profit values, arbitrary values that are reasonable and consistent with the case of real costs are used. $C_T = -10\$/t$, $C_w = -1.5\$/t$. Where C_T is the total cost of processing, administration, mining, etc. C_w is waste mining cost. z_c is the cutoff grade. As before, the cutoff grade considered are 0.2, 0.4, 0.6, 0.8, 1.0, 1.2, 1.4, 1.6, 1.8, and 2.0 g/t

From the profit functions defined in Equation 3.1, there are only two destinations for mined material: waste dump (waste) and processing plant (ore). Equation 3.7-3.8 calculates the profits for the kriged estimates and corresponding optimal destinations. In this instance, the L for ordinary Kriging will be one since we only have one realization or model from Kriging. However, this procedure for the profit calculation will be repeated 200 times for the 200 models generated from each borehole data. Figure 4.6 shows a numerical model in profits for some selected ordinary Kriging, long-term models.

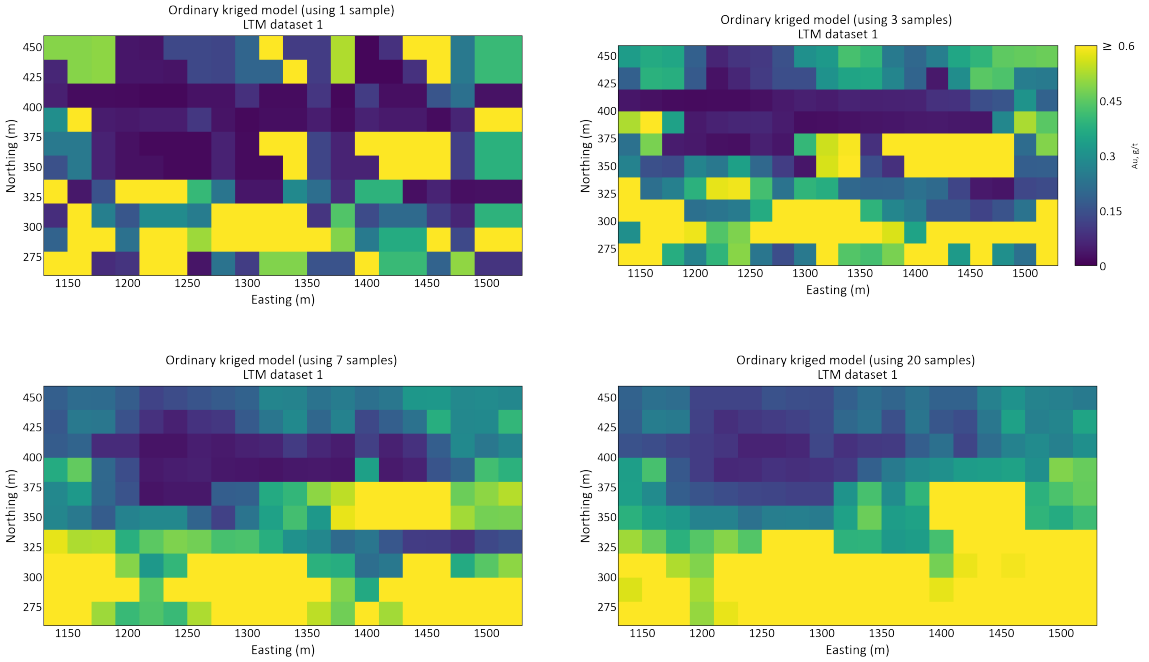

(a) Ordinary kriging models from LTM dataset 1 using different maximum number of samples.

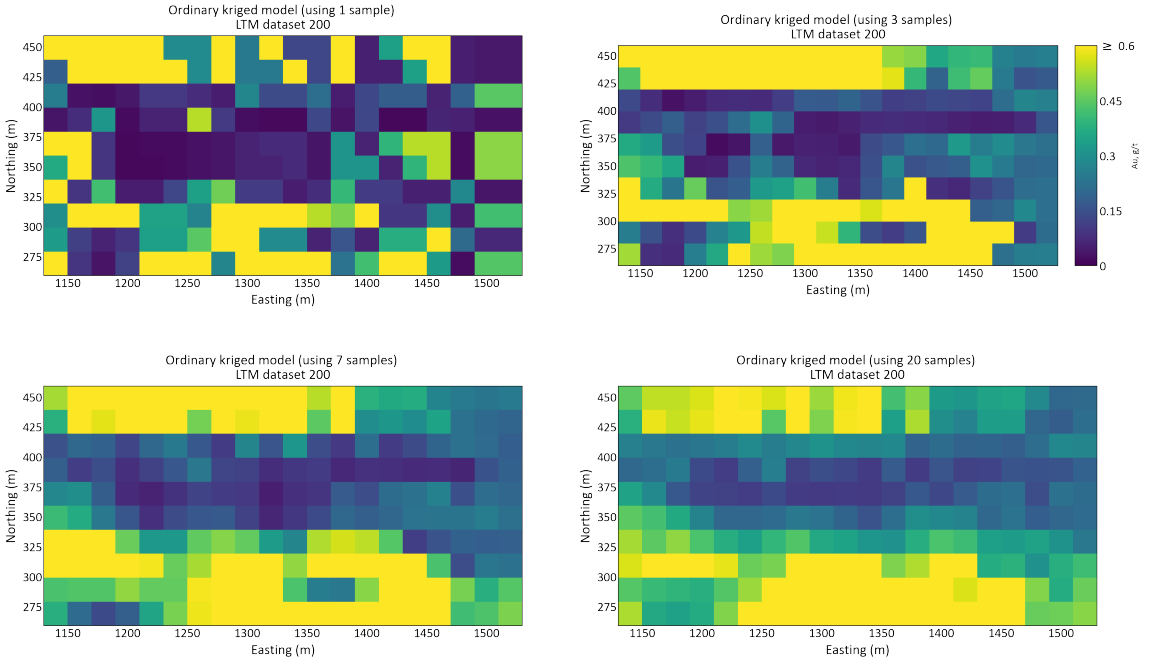

(b) Ordinary kriging models from LTM dataset 200 using different maximum number of samples.

Figure 4.7: Some selected ordinary kriging models for long term modelling using different search plans.

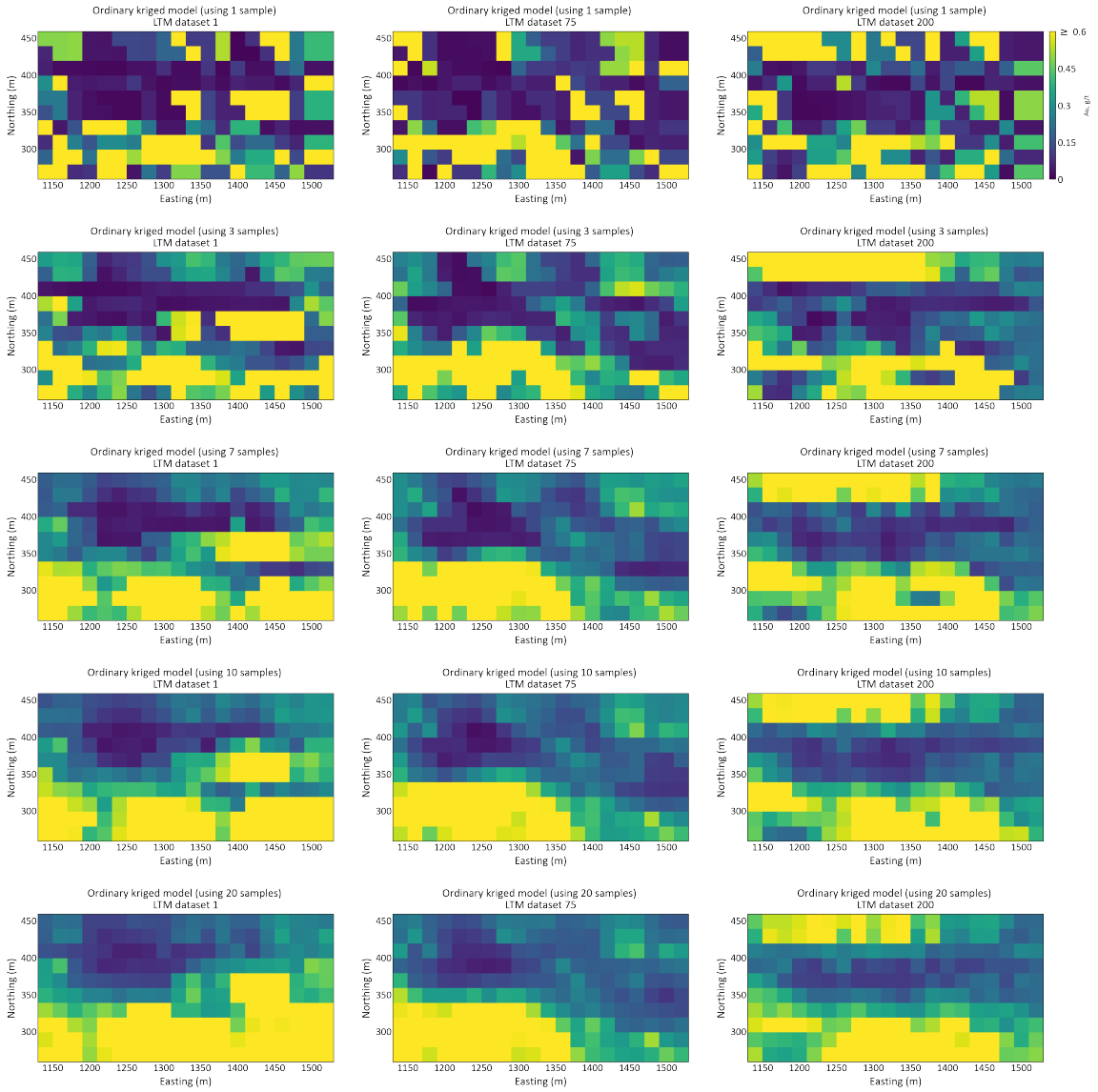

Figure 4.8: Ordinary kriging models from LTM dataset 1, 75 and 200 using a different search plans.

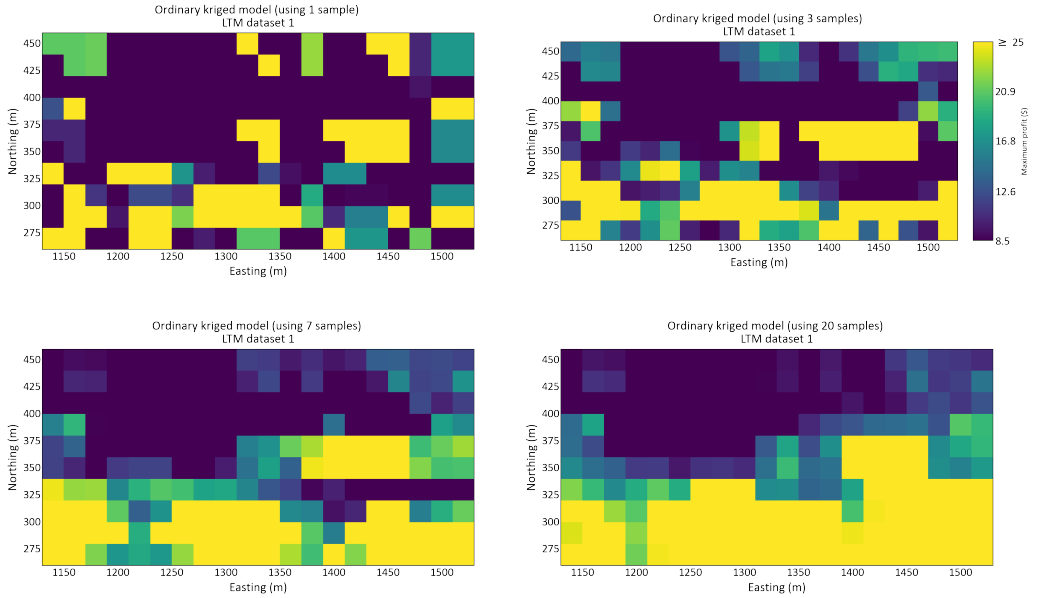

(a) Ordinary kriging models in profits from LTM dataset 1 using different maximum number of samples.

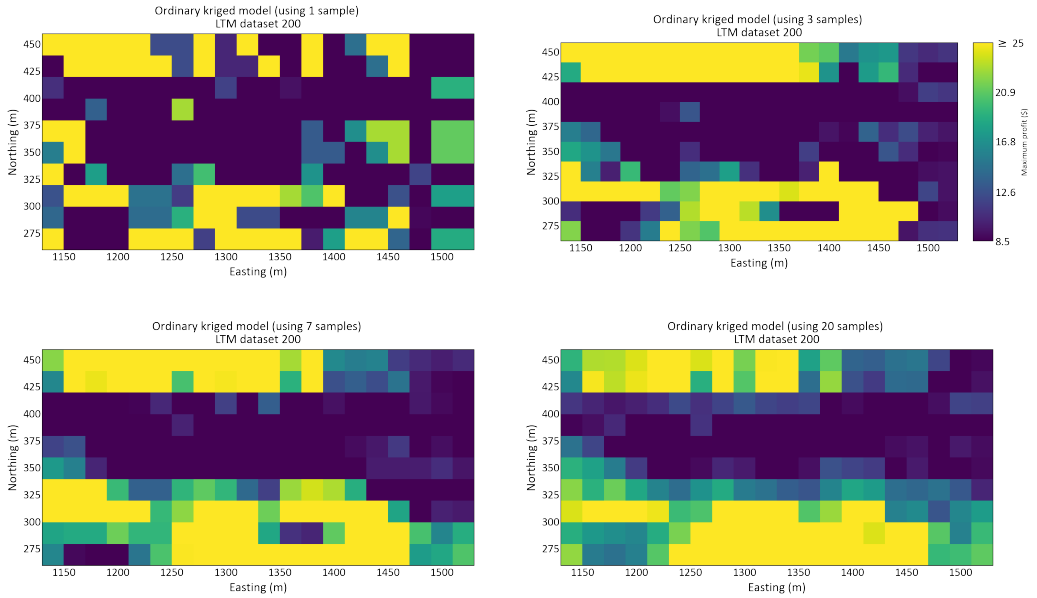

(b) Ordinary kriging models in profits from LTM dataset 200 using different maximum number of samples.

Figure 4.9: Some selected ordinary kriging models in profit for long term modelling using different search plans.

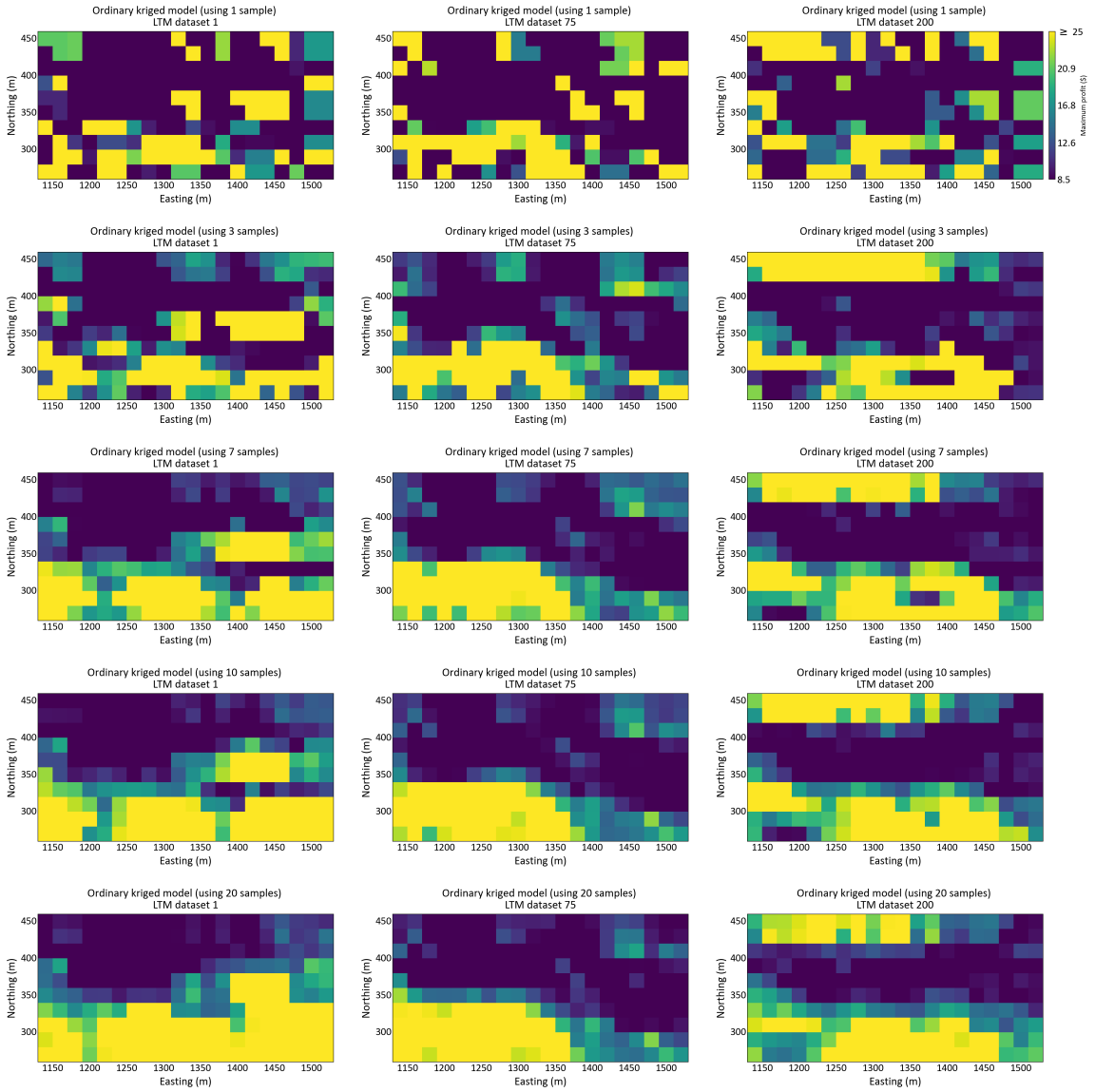

Figure 4.10: Ordinary kriging models in profits from LTM dataset 1, 75 and 200 using a different search plans.

4.3.3 Expected Sequential Gaussian Simulation

In this section, the same set of normal-scored sampled data values modeled by Gaussian variograms described by Equation 4.2 and described in Table 4.2 are used. These normal scored data values are obtained by transforming the original LTM datasets for generating the ordinary kriging, long-term models. Each of the 200 sampled datasets is transformed to have a mean of zero and a standard deviation of one using the *nscore* program. The number of conditioning data used for simulation varies between 0 and 20. A large search radius ensures sufficient data is used to simulate each location. Realizations are generated at a $10m \times 10m \times 10m$ grid resolution. This provided adequate discretization to average results to the larger $20m \times 20m \times 10m$ SMU size. This SMU size is necessary to accurately predict the correct resources at the time of grade control in the future. In each unsampled location, 20 previously simulated values are incorporated into the dataset for conditioning future distributions. This means that 20 simulated values are included as part of the dataset at each location where data was not initially sampled. The *SGSIM* program is used for the conditional simulation. Finally, 100 realizations were generated for each of the 200 normal-score transformed sampled datasets and then back-transformed to original units. Figure 4.11 shows a histogram reproduction of the conditioning data against the 100 realizations generated. The plot in Figure 4.12 (a) shows a more realistic variability of grades for realization one at the point scale compared to the same realization but this time averaged to the SMU scale, Figure 4.12 (b). Figure 4.12 (c) shows the expected SGS model from the 100 realizations for LTM dataset 1. The calculated mean values for all locations $\mathbf{u}$ from the 100 realizations generated for each sampled dataset is the expected SGS (ExpSGS) model for that dataset. Some of the ExpSGS models from selected datasets are shown in Figure 4.13.

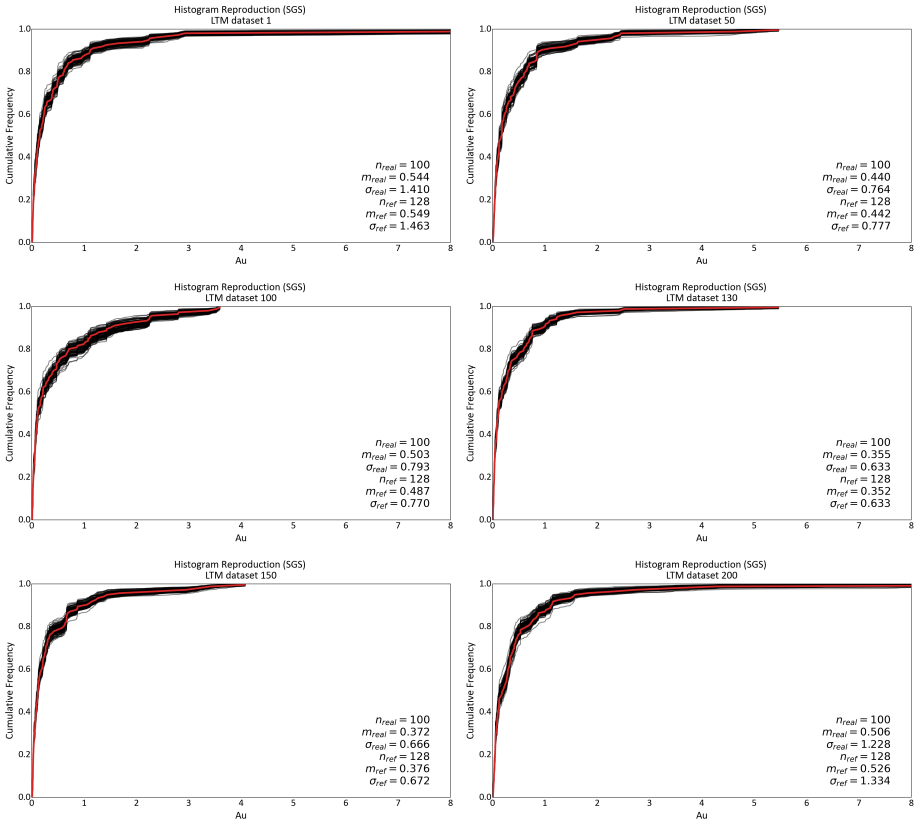

Figure 4.11: Histogram reproduction of the realizations generated for expected SGS. The overlaid red CDF represents the original distribution of the samples used for the conditioning.

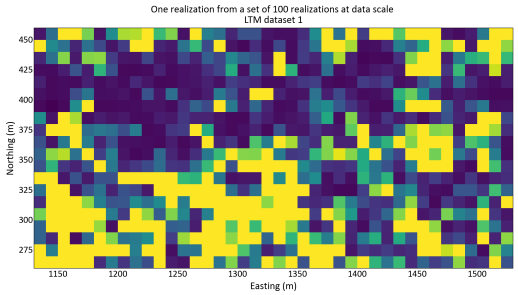

(a) A single realization at the point scale out of the 100 generated from LTM dataset 1

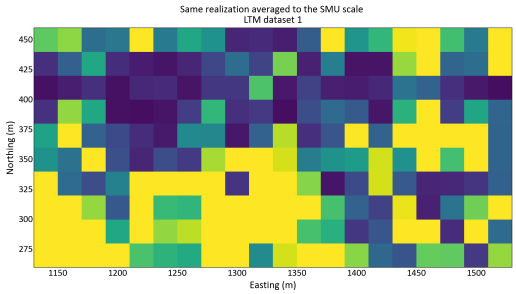

(b) A single realization averaged to the SMU volume.

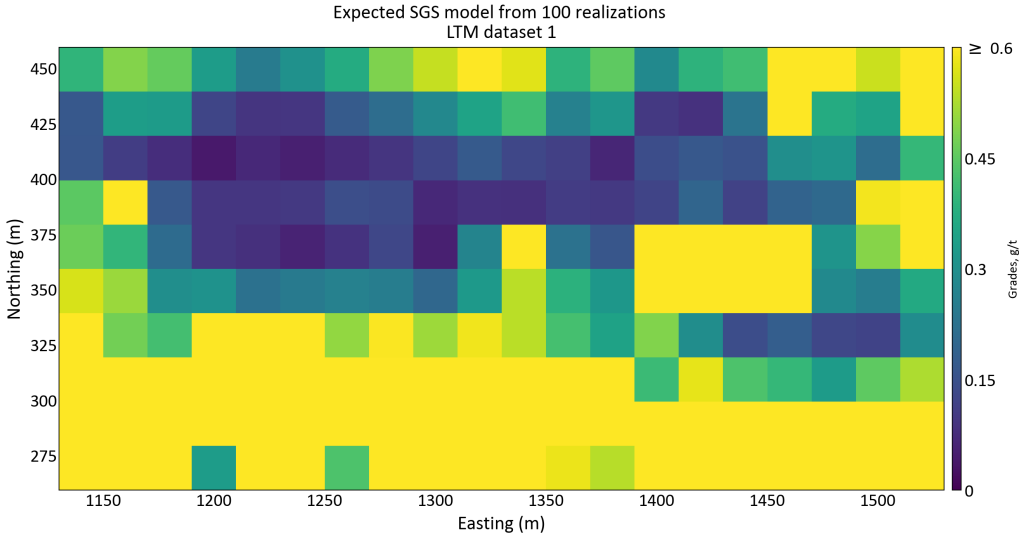

(c) Expected SGS model from the average of the 100 realizations for LTM dataset 1.

Figure 4.12: Comparison of grade variability: Point Scale vs. SMU Scale.

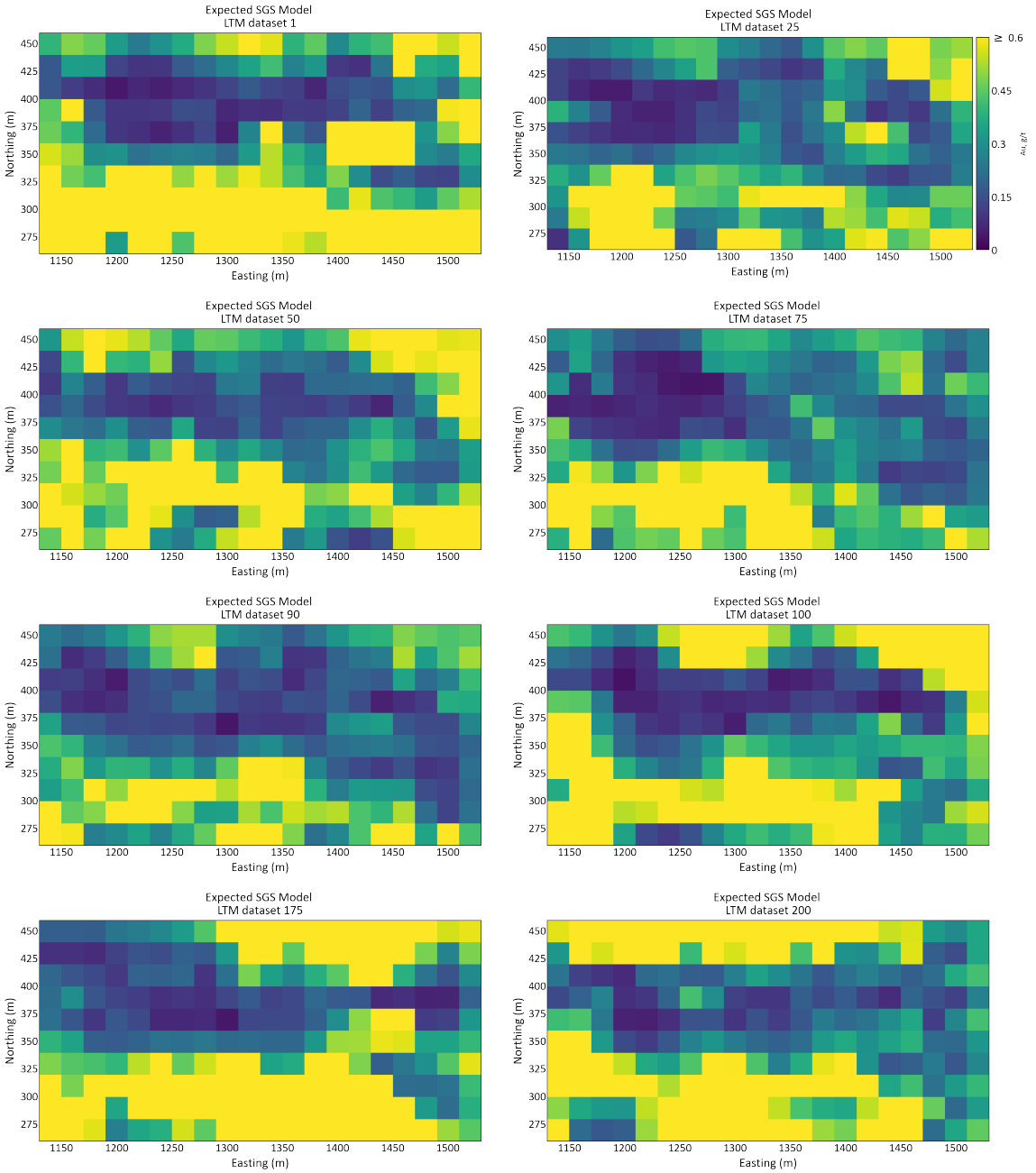

Figure 4.13: Some selected expected SGS map. Each expected SGS map displayed here is an average of one hundred realizations.

4.3.4 Expected Profits

The same arbitrary values used to convert the ordinary kriging estimates are also used here. This ensures consistency for a better evaluation of performance. From the profit functions defined in Equation 3.1, there are only two destinations for the mined material: the waste dump (waste) and the processing plant (ore). Equations 3.7 and 3.8 are used to calculate the profits for the Expected SGS models. In this case, the value of L for expected SGS is 100 since there are only 100 realizations from conditional simulation of each reference sampled dataset. However, this procedure for profit calculation will be repeated 200 times for the 200 LTM datasets used to generate the conditional SGS models shown in Figure 4.11. Figure 4.14 presents a numerical model illustrating the expected profits for some selected ExpSGS models.

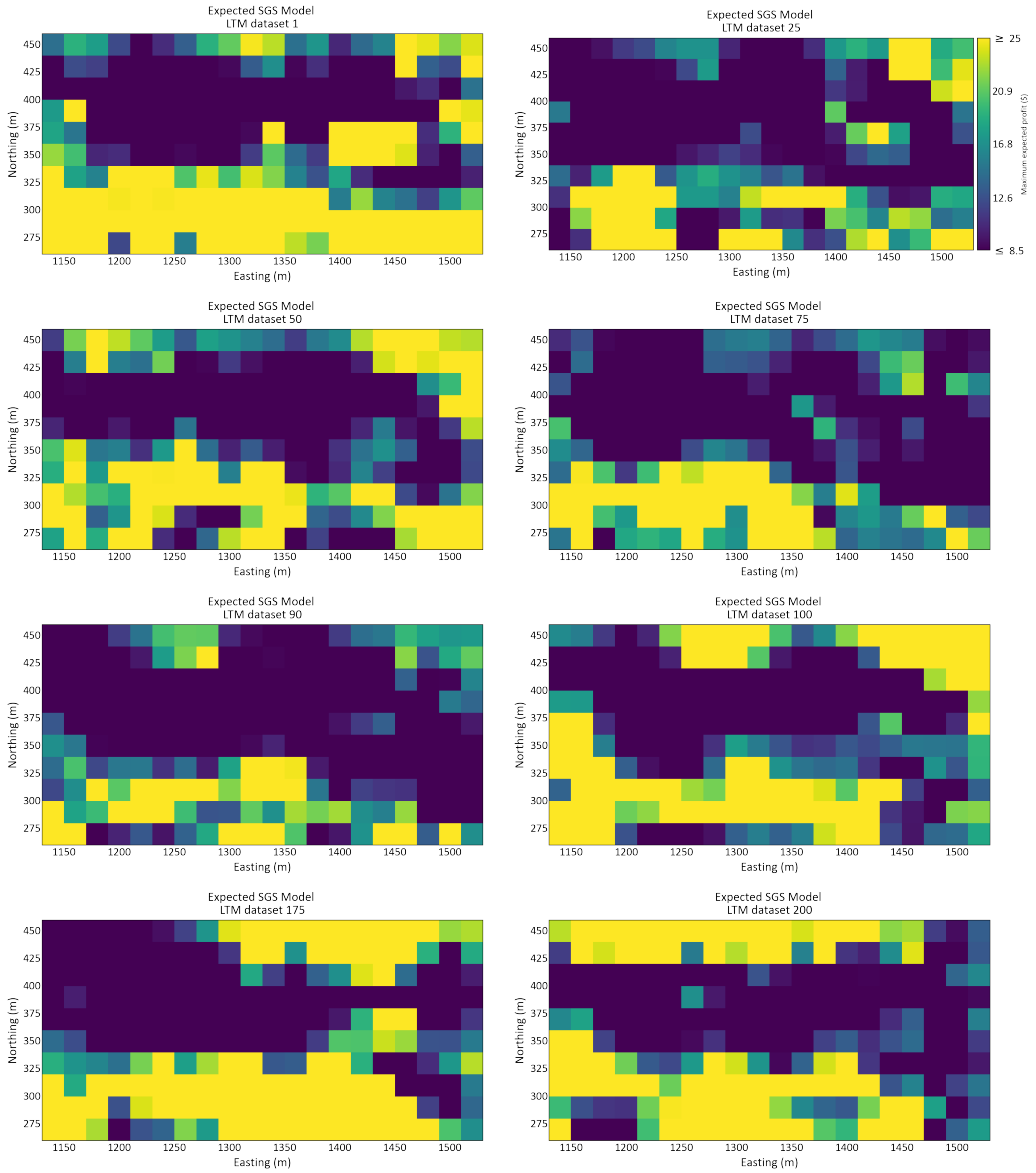

Figure 4.14: Some selected numerical models in expected profits from expected SGS.

4.3.5 Localized Uniform Conditioning

The LUC program C. V. Deutsch and Journel (1997) is used for this purpose following the workflow from (Neufeld, 2005). The panel scale is $40m \times 40m \times 10m$, and the SMU scale is $20m \times 20m \times 10m$. The panel grades are estimated using ordinary Kriging on a $40m \times 40m \times 10m$ grid. The variogram models from equation 4.1 are used as the basis for the Kriging. A maximum of 20 data is used in the search neighborhood of $400m$ by $200m$ in the major and minor direction of continuity, respectively. A maximum search radius of $10m$ is used for the vertical direction. The order of Hermite polynomials to be fitted to blasthole data was 200. The SMU estimates from the OK, LTM (using 20 samples) are used as the localizing variable to rank the SMU blocks within a panel. After the result for each panel was localized following the localization workflow discussed in Chapter 2. The distribution of panel scale estimates used for uniform conditioning is shown in Figure 4.16. The panel estimates reveal a decrease in variability, with a value of 0.202, in contrast to the 0.25 variance observed for the localizing variable at the SMU scale. The LUC estimate is shown in Figure 4.17.

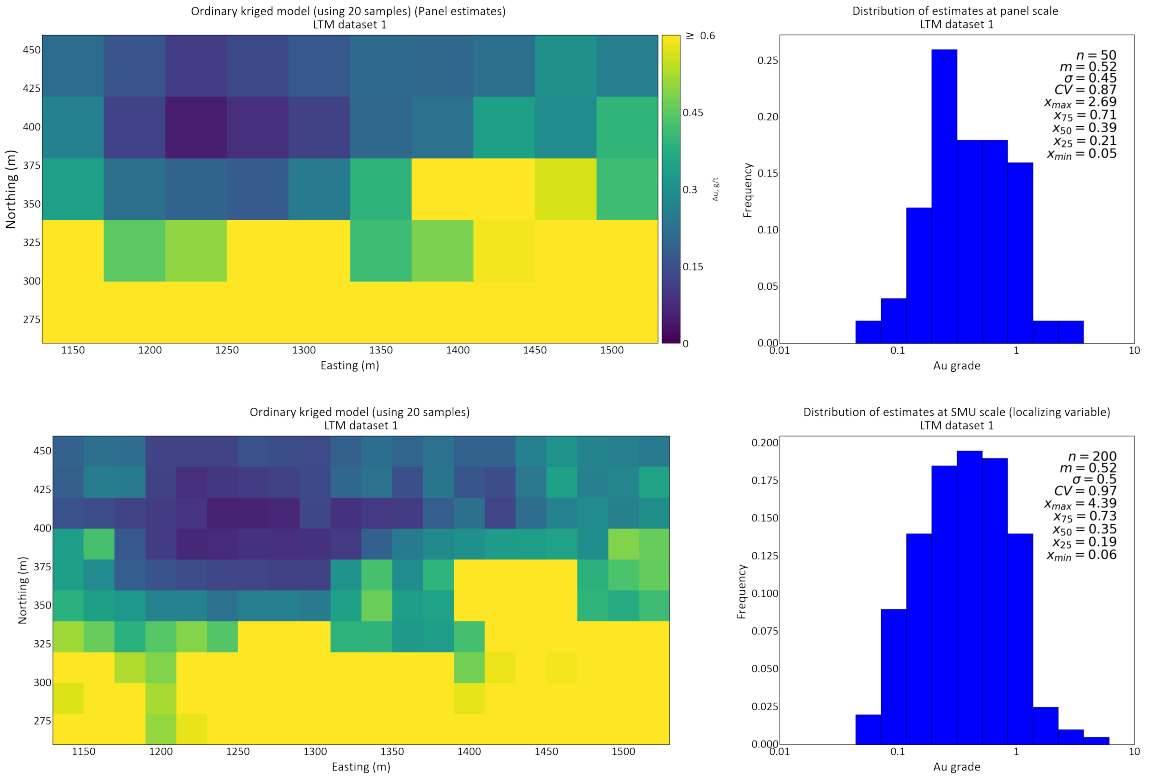

Figure 4.15: Distribution of panel scale and SMU scale estimates used for localized uniform conditioning (LTM dataset 1).

To convert the grades to profit values, consistent parameters as used for the profit conversion of ordinary kriged estimates are used here, including $C_T = -10\$/t$, $C_w = -1.5\$/t$. Where C_T is the total cost related to processing, administration, mining , etc. C_w is waste mining cost. z_c is the cutoff grade. The cutoff grades are 0.2, 0.4, 0.8, 1.0, 1.2, 1.4, 1.6, 1.8 and 2.0 g/t.

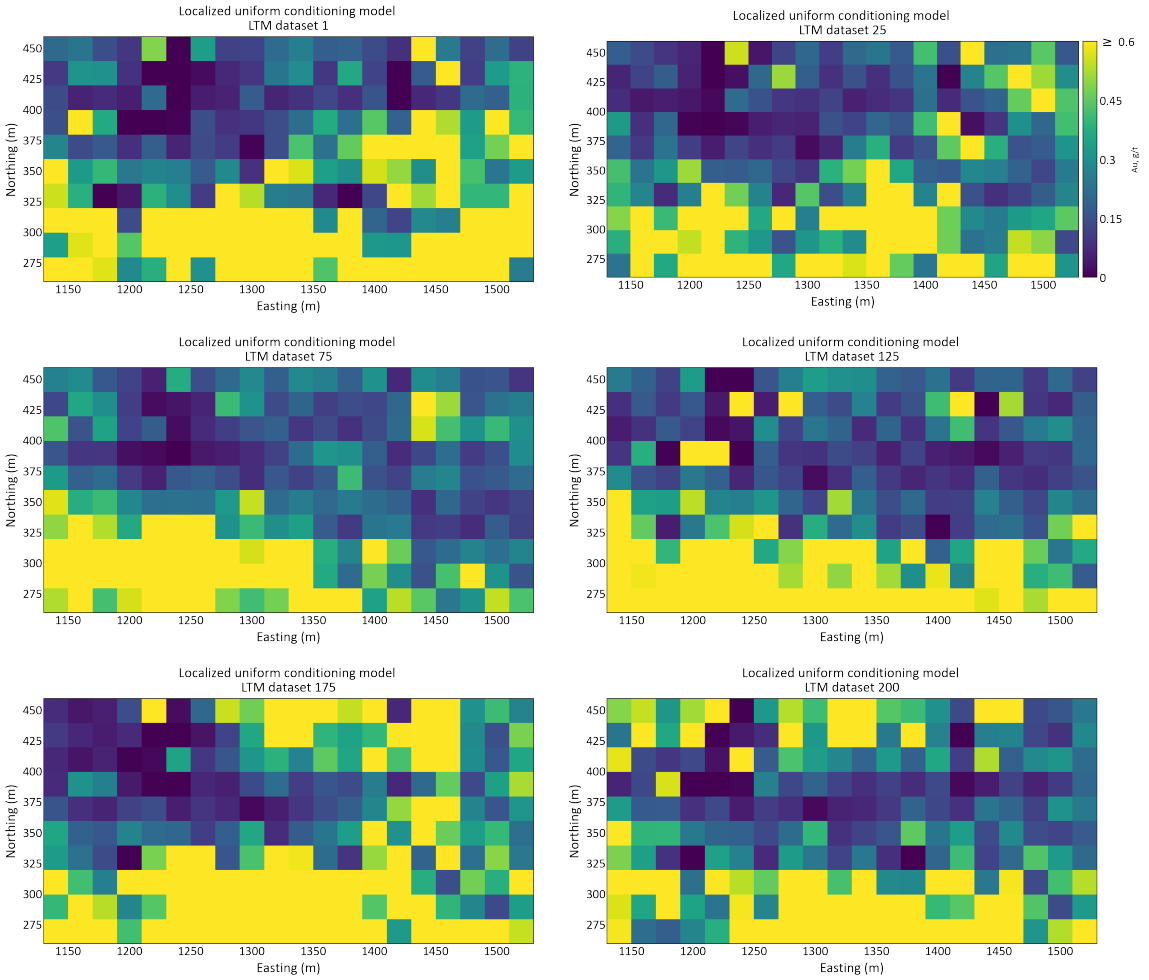

Figure 4.16: Localized uniform conditioning map, LTM

From the profit functions defined in Equation 3.1, there are only two destinations for mined material: waste dump (waste) and processing plant (ore). Equation 3.3-3.8 calculates the profits for the LUC models. In this instance, the L for LUC will be one since we only have one realization or model from localized uniform conditioning. However, this procedure for the profit calculation will be repeated 200 times for the 200 models generated from each LTM dataset. Figure 4.18 shows a numerical model of profits for some selected LUC models.

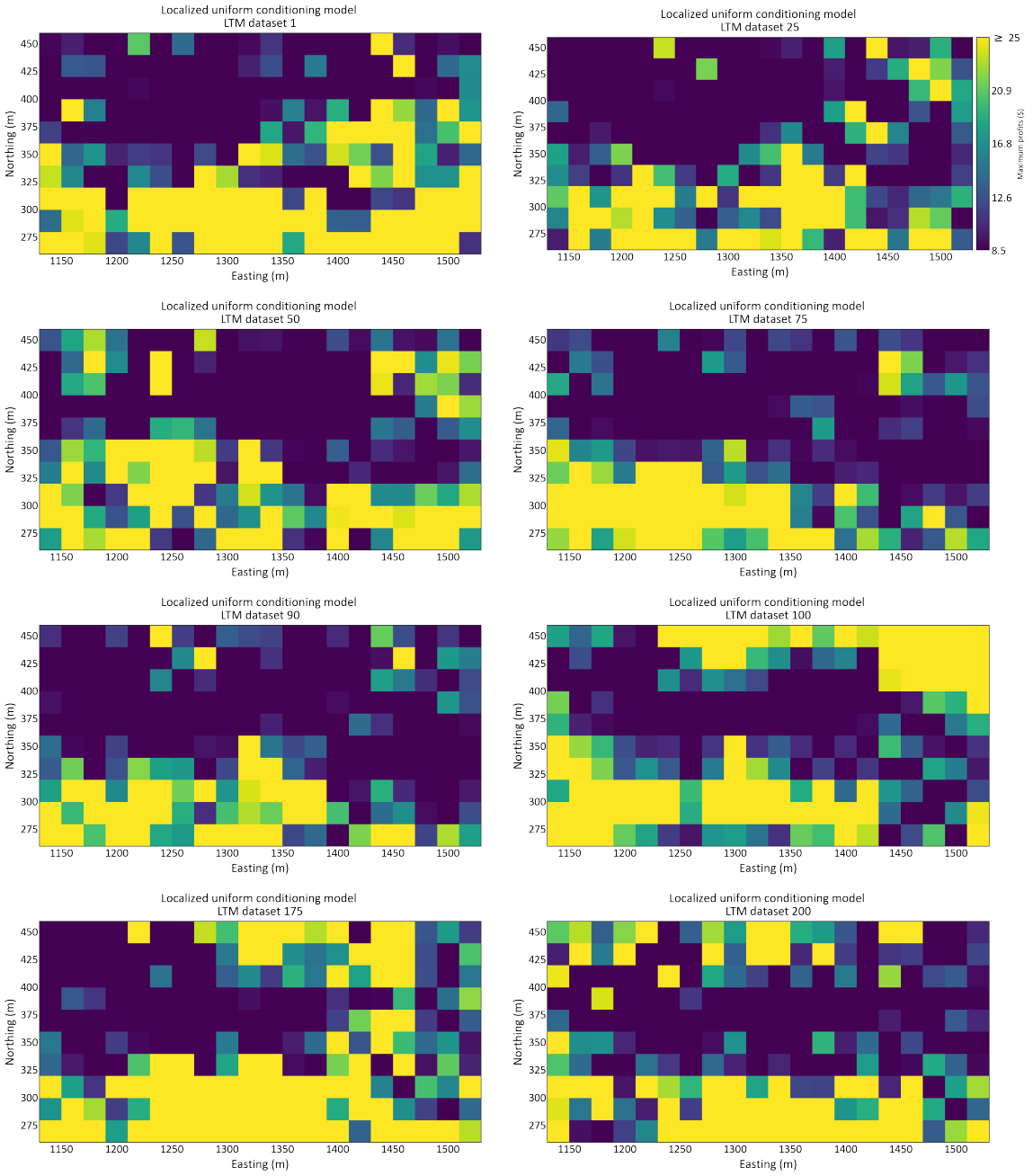

Figure 4.17: Numerical model in profits for some selected LUC models.

4.3.6 Localized Sequential Gaussian Simulation

After generating and checking 100 simulated realizations for each LTM dataset, the data was back-transformed to the original units for localization. For proper assignment of grades at the SMU scale, a localizing variable is required to rank each SMU within a panel. The localizing variable is the SMU estimates from the ordinary kriging, LTM using 20 samples. Figure 4.19 shows a map of kriged estimates at the SMU volume, which is used as the localizing variable to localize the 100 realizations generated via conditional simulation of LTM dataset 1. The panel scale is defined at $40m \times 40m \times 10m$, which nests properly with the smaller scale SMU grid. The simulated SMU grades falling within each panel (for all 100 realizations) are compiled to form a single distribution for each panel. This process is repeated for each panel in the model and is performed 200 times for the 200 different LTM datasets. The *localization* program by Daniels (2015) is utilized for this purpose. The localized SGS models are shown in Figure 4.20.

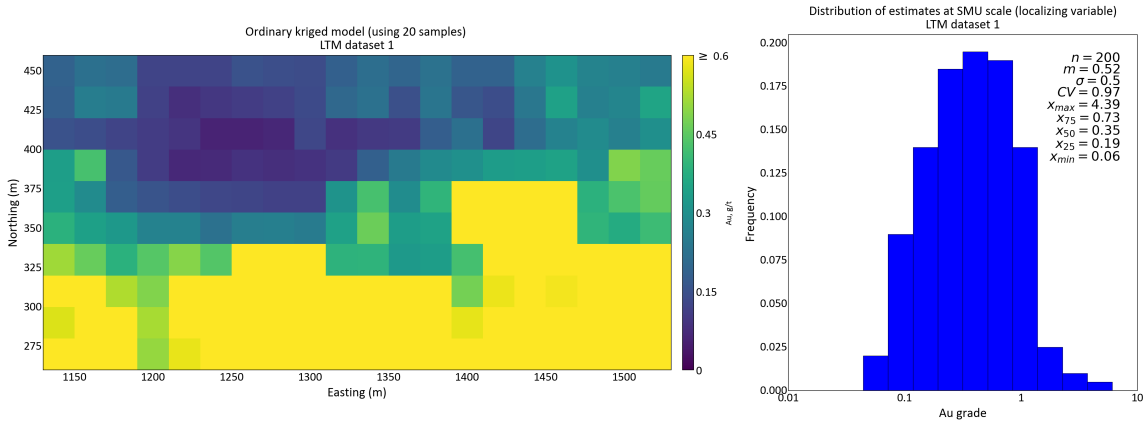

Figure 4.18: Distribution of localizing variable at the SMU scale

As before, $C_T = -10\$/t$, $C_w = -1.5\$/t$. Where C_T is the total cost of processing, administration, mining, etc. C_w is waste mining cost. z_c is the cutoff grade. From the profit functions defined in Equation 3.1, there are only two destinations for mined material: waste dump (waste) and processing plant (ore). Equation 3.7-3.8 calculates the profits for the LocSGS models. In this instance, the L for LocSGS will be one since we only have one realization or model from localized SGS. However, this procedure for the profit calculation will be repeated 200 times for the 200 models generated from each LTM dataset. Figure 4.21 shows a numerical model in profits for some selected localized SGS models.

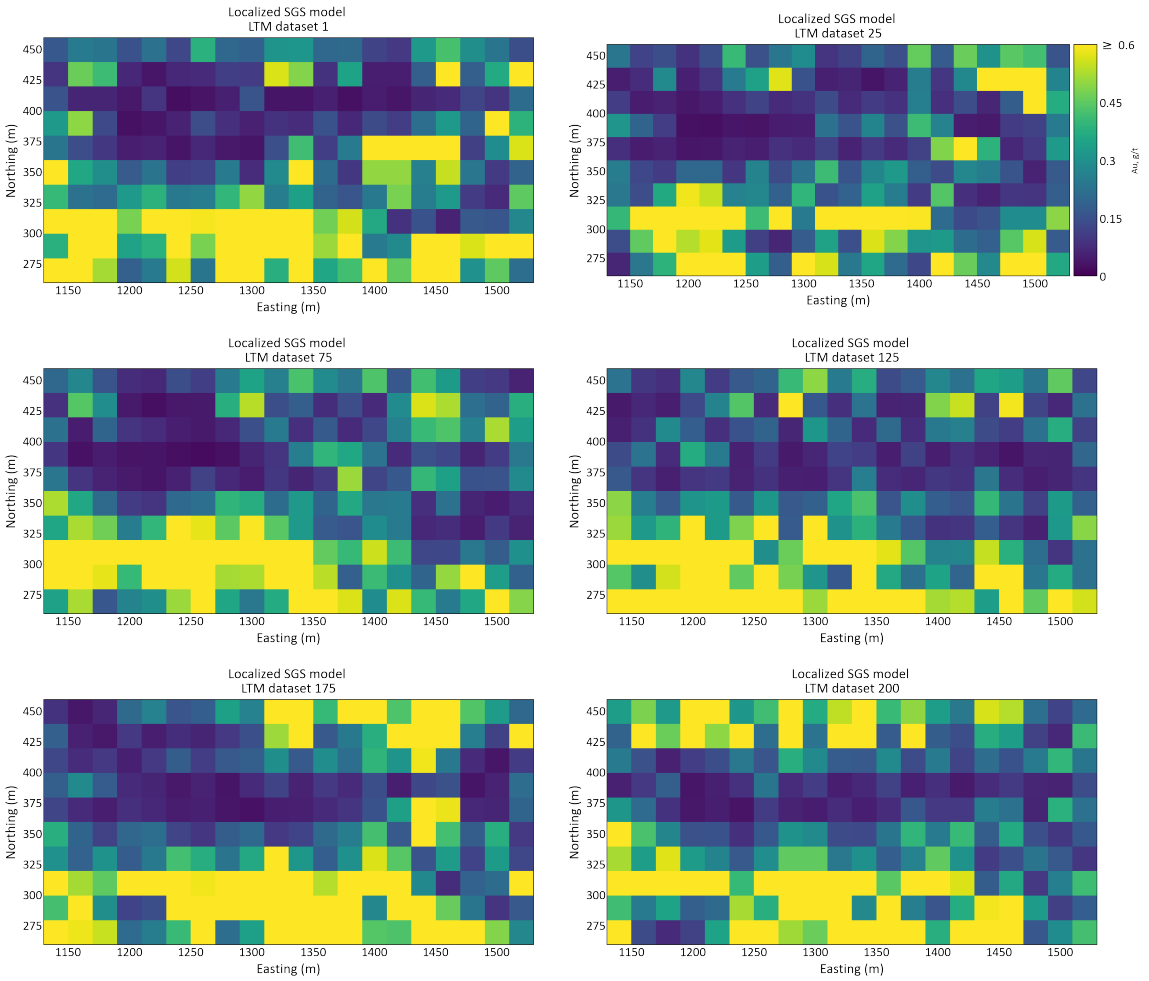

Figure 4.19: Some selected Localized SGS models. Each localized SGS model is generated from localizing 100 realizations.

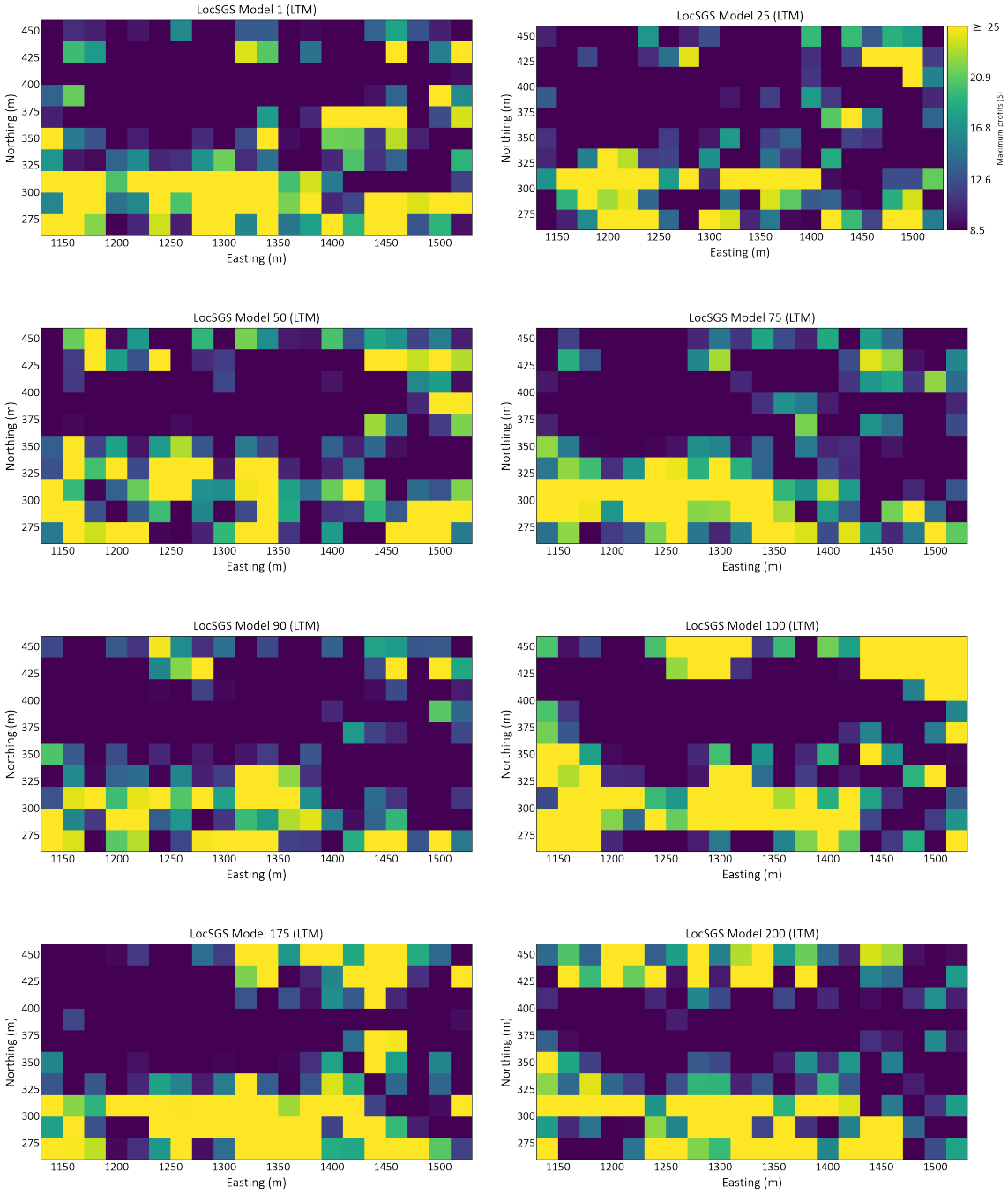

Figure 4.20: Numerical model in profits for some selected localized SGS models.

4.3.7 Grade-Tonnage Analysis

Quantifying the grade and total tons of material present is crucial in long-term planning for a deposit. A cutoff grade determined based on overhead cost and the market value of the ore is used to classify which SMUs are ore and waste based on the estimated grade at each location. In order to identify the optimal technique for long-term modeling, the efficacy of predicting tonnage and grades that closely match those during mining is assessed. First we need to calculate the resources at the time of mining. This involves evaluating the dig limit of the ExpSGS method at various cutoff grades: 0.2, 0.4, 0.6, 0.8, 1.0, 1.2, 1.4, 1.6, 1.8, and 2.0 g/t against the reference or "true" models. This process entails superimposing the dig limit at each cutoff onto the corresponding reference realization, as illustrated in Figure 4.21(a). Within the outlined red boundary, 11,609 grade values fall within the defined dig limit. The average of these grade values constitutes the grade above the cutoff of 0.2 for reference realization 1.

Calculating the tonnage above the 0.2 cutoff involves multiplying the volume of each block ($2m \times 2m \times 10m$) by the specific gravity (2.7), yielding 108 tonnes per block. Figure 4.21(a) equates to a tonnage above the 0.2 cutoff of 108 tonnes $\times 11,609 = 1,253,772$ tonnes. Similarly, for Figure 4.21(b), where 3,380 grade values from the reference realization align within the dig limit of ExpSGS model 1 at the 0.8g/t cutoff, the average of these grades yields the grade above the 0.8g/t cutoff for reference realization 1. Consequently, the tonnage above the 0.8 g/t cutoff is 108 tonnes $\times 3,380 = 365,040$ tonnes.

This procedure is iterated for each of the 200 reference realizations and across all the cutoff grades using the corresponding dig limit for the ExpSGS models. This outcome, showing the expected tonnage and grade above each cutoff grade, is summarized in Tables 4.3, 4.4, and 4.5. This table presents the average grade, tonnage, and percentage of tonnage above the cutoff for all 200 models of each technique implemented. The graphical representation of these expected grades and tonnage corresponding to the evaluated cutoff grades is depicted in Figure 4.22. The calculations undertaken for these assessments are outlined in the appendix.

While the primary focus of long-term models is not on accurately predicting local estimates, their main objective is to accurately predict global resources that align with the grade and tonnages above the cutoff during grade control. Table 4.6 contains all long-term methods' expected total misclassification, maximum attainable profit, and mean squared error (MSE) at some specified cutoff grades. To obtain the mean squared errors and the reference models at the fine $1m \times 1m \times 10m$ grid in Figure 4.4 was block averaged to the SMU block scale used for the long-term modeling, thus, $20m \times 20m \times 10m$. The results shows that localization produces resource models with poor local accuracy. Figure 4.24 shows the relations between the cutoff grades, maximum attainable profit, and MSE for ordinary kriging, ExpSGS, LUC, and LocSGS.

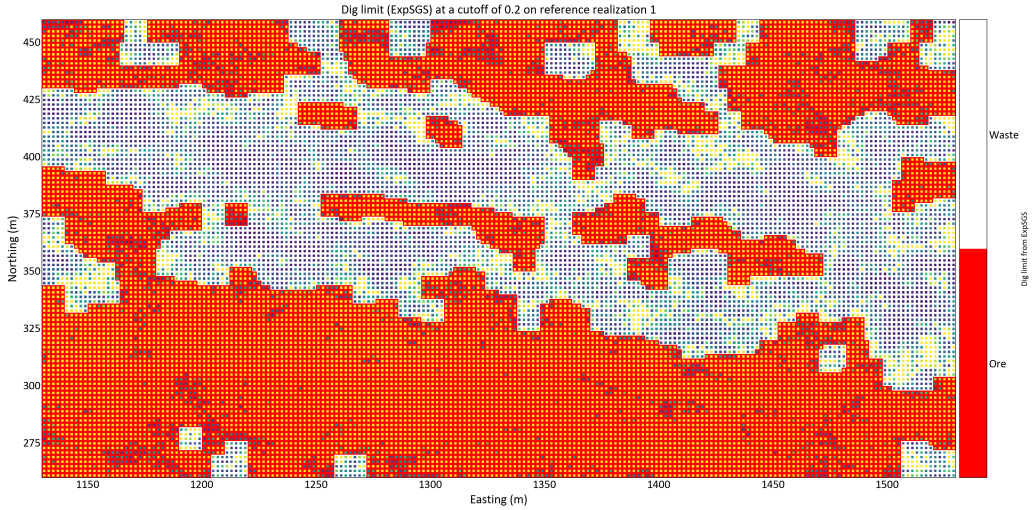

(a) Dig limits from ExpSGS at a cutoff of 0.2 g/t on reference realization 1.

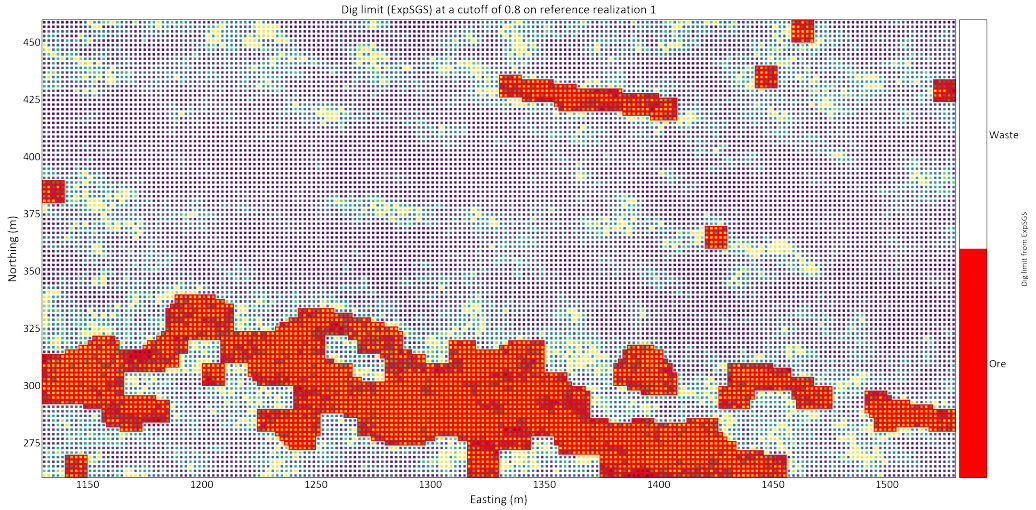

(b) Dig limits from ExpSGS at a cutoff of 0.8 g/t on reference realization 1.

Figure 4.21: Dig limit from ExpSGS model 1 on reference realization 1.

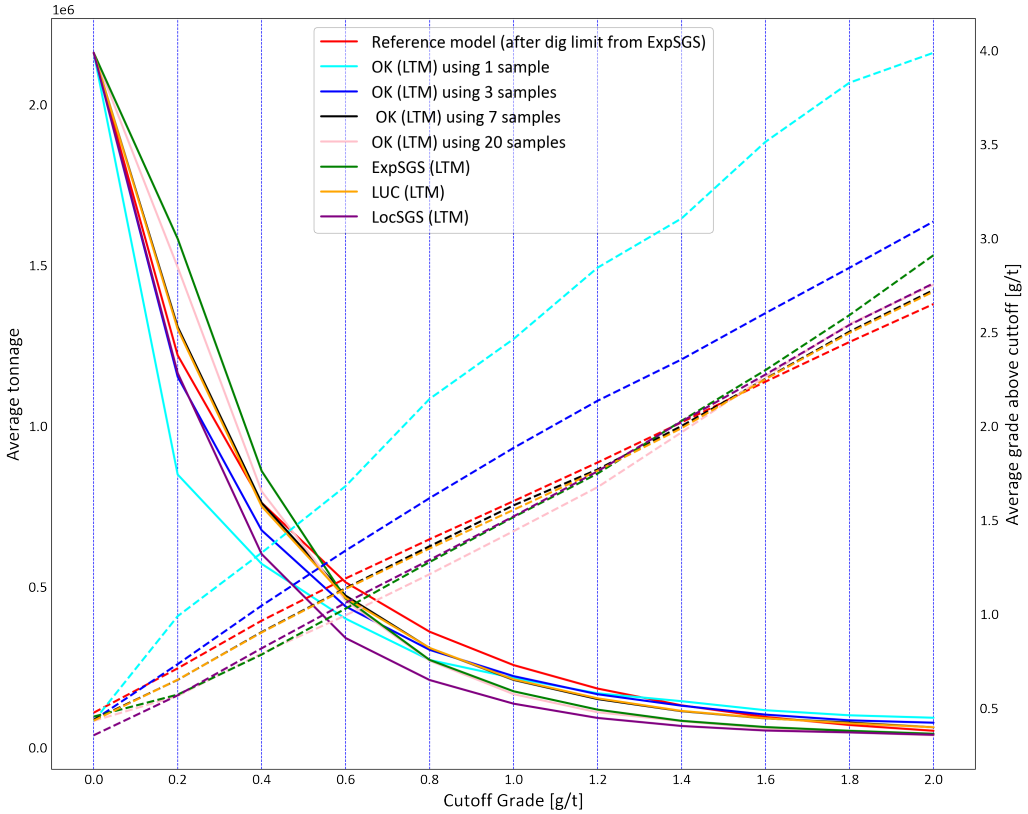

Figure 4.22: Average grade tonnage curve for long term models.

Cutoff	Reference model	OK (using 1 sample)	OK (using 3 samples)	OK (using 7 samples)	OK (using 20 samples)	ExpSGS	LUC	LocSGS
0	2160000	2160000	2160000	2160000	2160000	2160000	2160000	2160000
0.2	1219409	848610	1152630	1307772	1493478	1581822	1300914	1164024
0.4	760713	570942	675216	760374	796284	859518	749682	601236
0.6	513431	400356	438372	471906	456840	463158	465480	340200
0.8	359882	271998	303588	309184	269783	272214	309510	209682
1	256110	216108	221753	210079	165802	174655	211658	136124
1.2	183124	168426	165473	150480	109486	117588	152806	91800
1.4	130999	143910	129874	112813	81659	82800	113690	66802
1.6	94951	115815	102124	90474	59832	63434	90900	52683
1.8	69845	100022	84357	77328	47007	51868	75112	46800
2	51938	92424	77006	62746	37926	42592	62761	39378

Table 4.3: Expected tonnage above cutoffs for long term models.

Cutoff	Reference model	OK (using 1 sample)	OK (using 3 samples)	OK (using 7 samples)	OK (using 20 samples)	ExpSGS	LUC	LocSGS
0	0.474	0.429	0.435	0.437	0.430	0.453	0.432	0.354
0.2	0.710	0.988	0.732	0.649	0.564	0.570	0.650	0.566
0.4	0.964	1.325	1.044	0.903	0.790	0.783	0.901	0.817
0.6	1.189	1.680	1.337	1.137	0.992	1.028	1.133	1.059
0.8	1.397	2.144	1.616	1.360	1.211	1.276	1.348	1.287
1	1.600	2.463	1.883	1.578	1.440	1.515	1.554	1.519
1.2	1.806	2.843	2.134	1.769	1.674	1.747	1.762	1.759
1.4	2.019	3.105	2.354	2.000	1.966	2.027	1.989	2.024
1.6	2.236	3.513	2.601	2.252	2.265	2.298	2.250	2.274
1.8	2.447	3.827	2.842	2.502	2.542	2.590	2.495	2.538
2	2.649	3.987	3.088	2.724	2.752	2.909	2.715	2.759

Table 4.4: Expected grade above cutoffs for long term models.

Cutoff	Reference model	OK (using 1 sample)	OK (using 3 samples)	OK (using 7 samples)	OK (using 20 samples)	ExpSGS	LUC	LocSGS
0	100.00	100.00	100.00	100.00	100.00	100.00	100.00	100.00
0.2	56.45	39.29	53.36	60.55	69.14	73.23	60.23	53.89
0.4	35.22	26.43	31.26	35.20	36.87	39.79	34.71	27.84
0.6	23.77	18.54	20.30	21.85	21.15	21.44	21.55	15.75
0.8	16.66	12.59	14.06	14.31	12.49	12.60	14.33	9.71
1	11.86	10.01	10.27	9.73	7.68	8.09	9.80	6.30
1.2	8.48	7.80	7.66	6.97	5.07	5.44	7.07	4.25
1.4	6.06	6.66	6.01	5.22	3.78	3.83	5.26	3.09
1.6	4.40	5.36	4.73	4.19	2.77	2.94	4.21	2.44
1.8	3.23	4.63	3.91	3.58	2.18	2.40	3.48	2.17
2	2.40	4.28	3.57	2.90	1.76	1.97	2.91	1.82

Table 4.5: Expected percentage of tonnage above cutoffs for long term models.

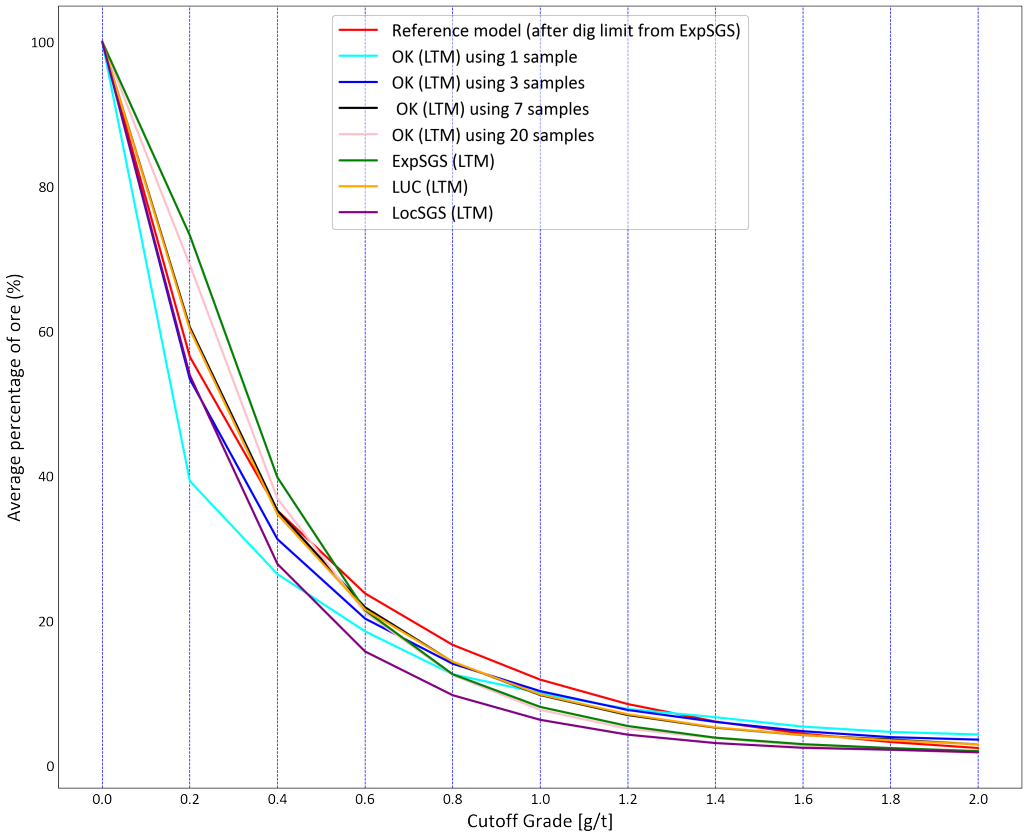

Figure 4.23: Average percentage of tonnage above cutoffs for long term models.

Model	Misclassified errors (%)	Maximum attainable profit(%)	Mean squared error ($)
Cutoff grade of 0.2			
OK (using 1 sample)	35.25	75.32	1477
OK (using 3 samples)	28.60	79.97	615
OK (using 7 samples)	25.94	82.52	398
OK (using 20 samples)	28.43	85.57	322
Expected SGS	25.44	93.749	323
Localized UC	31.48	82.33	450
Localized SGS	50.28	76.06	1907
Cutoff grade of 0.8			
OK (using 1 sample)	16.17	27.33	101
OK (using 3 samples)	15.57	24.46	48
OK (using 7 samples)	15.25	21.98	35
OK (using 20 samples)	14.53	17.87	28
Expected SGS	13.67	31.98	26
Localized UC	15.69	22.06	36
Localized SGS	24.84	14.95	125

Table 4.6: Expected percentage of misclassified errors, maximum attainable profit and mean squared error of long term models.

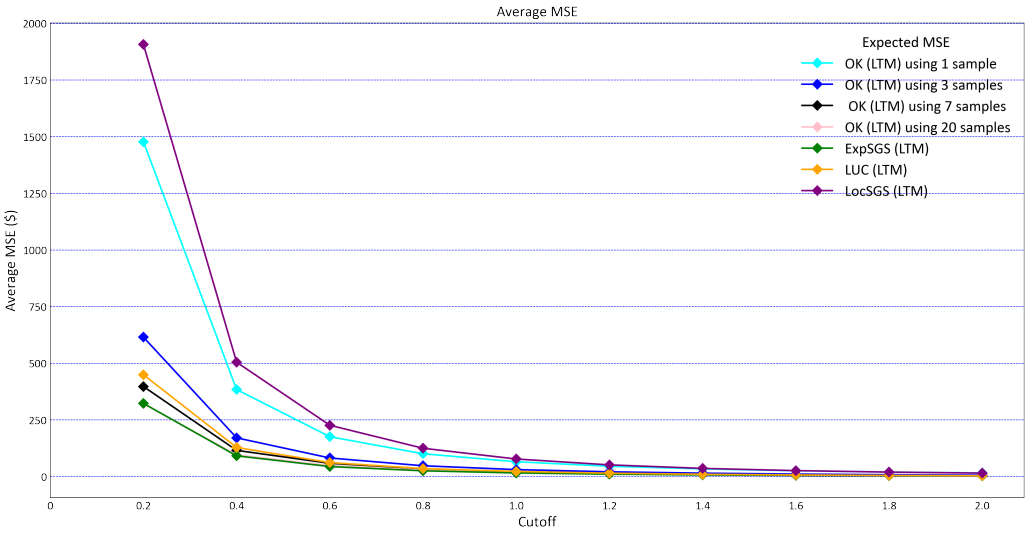

(a) Expected mean square error for OK, ExpSGS, LUC and LocSGS at different cutoff grades.

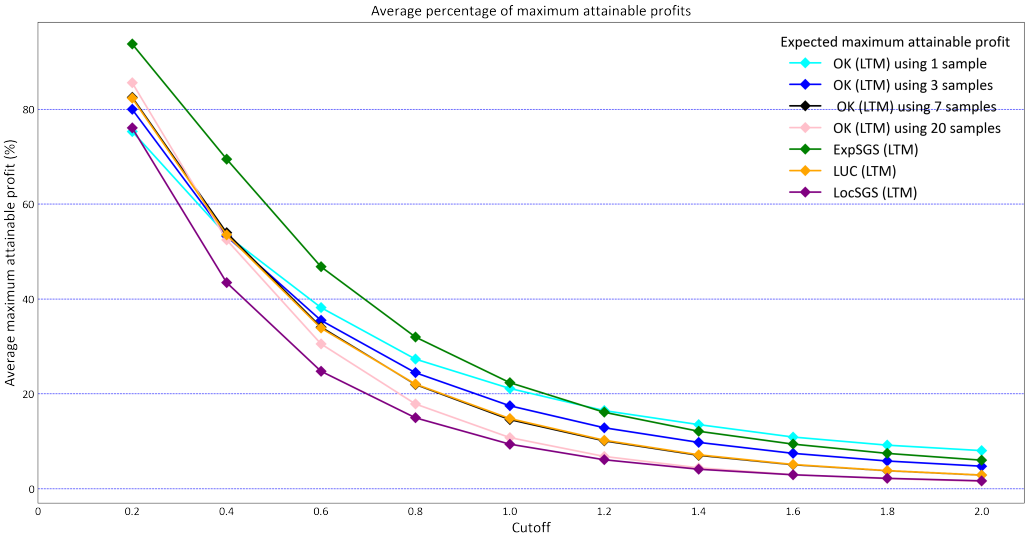

(b) Expected percentage of maximum attainable profit for OK, ExpSGS, LUC and LocSGS at different cutoff grades.

Figure 4.24: Expected percentage of maximum attainable profit and mean squared error of long term models at different cutoff grades.

Chapter 5

Conclusion

Geostatistical modeling typically relies on limited data, which constitutes a small portion compared to the mining-relevant volume. Evaluating uncertainty within a geostatistical model is a crucial task. The importance of prerequisites for estimation outweighs the importance of the estimation plan. These foundational requirements include validating data quality, compositing, addressing outliers, partitioning data into logical domains, establishing a fitting coordinate system for estimation, selecting the appropriate block size, and addressing substantial large-scale trends and contacts between estimation domains. Once these prerequisites are appropriately dealt with, the estimation details become noteworthy. In long-term resource modeling, the focus shifts to the scale of the selective mining unit, which encompasses a larger volume than the scale of available data and is more relevant for resource evaluation. This concluding chapter encapsulates the core aspects of this research, highlighting key findings, contributions, and avenues for future exploration.

5.1 Summary of Contributions

The issues of conditional bias and histogram smoothing that result from estimation techniques have been discussed and demonstrated. These downfalls of estimation demonstrate the need for a measure of uncertainty in a geostatistical model. An overview of four common techniques for estimation at the SMU scale is presented in Chapter 2. These modeling techniques are ordinary Kriging, sequential Gaussian simulation, localized uniform conditioning, and localized sequential Gaussian simulation. Examples demonstrating these modeling techniques are presented in Chapter 3 and Chapter 4. The benefits and challenges of each technique are summarized, considering complexity and computational expense. Despite the time and computational requirements, the findings of this research suggest that the benefits of multiple realizations outweigh the computational cost of this technique. The review of change of support techniques, including numerical block averaging, is given in Chapter 2. The ratio of the block and point scale variances is found to be dependent on the proximity and value of conditioning data. The expected sequential Gaussian simulation results suggest that the robust numerical approach of block averaging simulated realizations is a very effective and reliable method. The expected sequential Gaussian simulation for grade control modeling produces the best results in the expected percentage of maximum attainable profit, mean square, and misclassified errors. Expected SGS also produced the closest grade and tonnage above the cutoff at very low and high cutoff grades. For long-term modeling, ordinary Kriging using as low as seven samples and as high as fifteen samples is ideal for yielding grades and tonnage close to the anticipated grade and tonnage

during mining. Localized uniform conditioning is the second closest.

Grade control models constructed using reasonable grid sizes show better results in grade control. The grid size for grade control models should be considered with respect to the sample spacing. Theoretical experiments in Chapter 3 allow concluding that a reasonable grid size for grade control models should not be be more than 45% sample data spacing. In most cases, the amount of misclassified material increases after this limit. Traditionally, estimation has been a conventional method employed in mines for the purpose of grade control. Among these methods, Kriging techniques hold significant popularity. These techniques exhibit a strong capability to generate reliable estimates of grades at locations where no samples have been taken. Unfortunately, the predictions yielded by methods like ordinary Kriging, demonstrated in this research, as well as other deterministic interpolation methodologies, possess a smoothness that fails to capture the entirety of uncertainty inherent in the input grades.

In the context of grade control, estimation models are frequently constructed individually for each variable. Subsequently, these models are utilized in the development of dig limits. However, this approach overlooks the intricate multivariate connections between variables, which play a pivotal role in the recovery of metals. This is a limitation as it disregards the complex interdependencies among these important variables. To address this limitation, simulation emerges as a viable alternative. Simulation enables the consideration of all pertinent variables crucial for effective grade control simultaneously. This involves creating numerous realizations of simulated grades to calculate the expected profit associated with each grade control decision.The final decision brings the largest expected profit. Also, although there are no issues of histogram smoothing, localization generates a resource model with poor local precision. This issue makes localization questionable for long term planning. The practical demonstration of four geostatistical modeling techniques using data collected from two hundred reference realizations established through conditional simulation using gold deposit. Chapter 3 and Chapter 4 showcases ordinary kriging, sequential Gaussian simulation, localized uniform conditioning and localized sequential Gaussian simulation. This provides summary and overview of implementation details for each method in a realistic setting to quantify the resource. Through modeling and validation processes, the four geostatistical techniques generate consistent results at both the global and local scale. The objectives outlined in Chapter 1 have been successfully achieved throughout the discussion of these various topics. The conventional approach of relying on a single model has been questioned by critically examining techniques that effectively model uncertainty. These methods avoids the dilemma of choosing between excessive smoothing and introducing conditional bias into estimates. Furthermore, localization has been thoroughly tackled. This involved explaining the methodology and presenting a synthetic example that effectively illustrates the advantages and challenges associated with this new approach to constructing a single model that captures uncertainty. In conclusion, a comprehensive case study has been conducted, which explains the modeling process for four distinct methods. This case study underscores the

merits of utilizing Sequential Gaussian Simulation in conjunction with robust change of support via block averaging for grade control.

5.2 Limitations

The major limitation of this thesis lies in the exclusive reliance on 2D models for the case studies and examples. While these 2D models provide valuable insights, it is important to acknowledge that mining operations often occur in three-dimensional spaces. The methodologies, techniques, and challenges in 3D modeling can differ significantly from their 2D counterparts. For instance, in 3D scenarios, there may be a necessity to compute downhole variograms, which can substantially impact the grade control strategies. Downhole samples could enhance variogram calculations and subsequently improve modeling accuracy, but this thesis does not delve into the intricacies of 3D modeling. Another notable limitation is the use of a dataset containing only a single variable. In practical mining scenarios, datasets often encompass multiple collocated variables, geochemical, and geophysical data. These additional variables can introduce complexities and correlations that may lead to different modeling outcomes. The thesis does not explore the potential variations and challenges associated with handling larger, multi-variable datasets. The results presented in this thesis are sensitive to the parameters chosen for the cost of mining waste, total mining cost, and cutoff grades. Varying these parameters can yield different outcomes, which is a common challenge in mining optimization. However, the thesis does not provide an in-depth exploration of the impacts of parameter choices or offer guidance on selecting appropriate parameter values. It is important to note that understanding the rationale behind parameter choices and their effects on results is crucial for practical implementation. The thesis lacks detailed explanations regarding why certain results are superior or preferable over others. Mining operations require decisions that have financial and operational consequences. Providing insights into the factors that drive specific results or strategies would have been beneficial for stakeholders seeking to apply the research findings in real-world scenarios. Inverse Distance Weighting (IDW) is a widely used estimation technique in the mining industry for interpolating grade values. However, this thesis does not explore the application of IDW. The thesis also didn't explore the use of hand drawings to establish mining dig limits. Hand drawings can be a valuable tool in the mining industry for visualizing and communicating mining plans.

In summary, while this thesis provides valuable insights into grade control and long-term models based on 2D models and single-variable datasets, it is important to acknowledge the limitations associated with these choices. The thesis does not address the challenges and nuances of 3D modeling, multi-variable datasets, parameter sensitivity, explanatory insights, alternative estimation techniques like IDW, or the use of hand drawings for establishing mining limits. These limitations should be considered when applying the research findings to practical mining scenarios.

5.3 Future Work

Several areas may be considered to improve the methods for accurately predicting close estimates of ore tonnage, ore grade and waste tonnage within reasonably large production volumes during long term modeling. Also, despite the contributions made to establish the best techniques for grade control modeling, future work remains. Specifically, topics including artifact reduction in localization and tools for mine planning over multiple realizations require further attention. A more comprehensive research may be conducted to obtain the reasonable range for grid sizes relative to sample data. Theoretical results should be checked with real data from different types of deposits. Practical recommendations for different geological types of deposits could be developed. Simulation is a more effective tool for grade control provided it is used properly. A number of different factors may influence its performance. More information should be gathered on the performance of simulation in different conditions. More practical recommendations for using simulation for short-term grade control should be developed. Prospectively, simulation should become a primary tool for grade control. Some new software may be developed to implement simulation for any number of variables. The goals of presentation, discussion and implementation of methods for quantifying SMU uncertainty have been accomplished here. Additionally, change of support techniques have been analyzed and implemented with respect to local variation and conditioning data. The improved flexibility of localization paired with artifact reduction provides a framework for generating a single model when required. Despite the improvements in local change of support, and flexible localization, the findings of this thesis support conditional simulation, paired with block averaging for change of support, as best practice in resource modeling to quantify uncertainty for improved resource evaluation.

References

Abzalov, M. (2006). Localised uniform conditioning (luc): A new approach for direct modelling of small blocks. *Journal of the Southern African Institute of Mining and Metallurgy.*

Amihere, N., & Deutsch, C. V. (2022). Localization of Probabilistic Resource Models. *In J. L. Deutsch (Ed.), Geostatistics Lessons.*. Retrieved from `http://www.geostatisticslessons.com/lessons/localization`

Boisvert, J. B., & Deutsch, C. V. (2012). A short note on a general framework and software for localization of mining reserves. *paper 313, CCG Annual Report(14).*

Chambers, R. L., & Yarus, J. M. (2007). *PEH:Geologically Based, Geostatistical Reservoir Modeling.* Society of Petroleum Engineers.

Chilès, J. T., & Delfiner, P. (1999). *Geostatistics: Modeling Spatial Uncertainty.* Wiley, New York.

Collet, D., & Corley, D. (2000). Transparent grade control: Improvements from the application of sequential indicator simulation and optimisation at Ravenswood gold mines. *International Symposium on Geostatistical Simulation in Mining, Perth, Australia.*

Daniels, E. B. (2015). *Prediction of Local Uncertainty for Resource Evaluation* (Master of Science). University of Alberta.

Daniels, E. B., & Deutsch, C. V. (2014). Case study on localisation. *Paper 306, CCG Annual Report(16).*

Daniels, E. B., Deutsch, C. V., & Boisvert, J. B. (2014). Developments towards artifact free localiza on. *Paper 306,CCG Annual Report(16).*

Deutsch, C. V., & Journel, A. G. (1997). *GSLIB Geostatistical Software Library and User's Guide.* Oxford University Press, New York.

Deutsch, J. L., & Deutsch, C. V. (2015). Introduction to Choosing a Kriging Plan. *In J. L. Deutsch (Ed.), Geostatistics Lessons.*. Retrieved from `https://geostatisticslessons.com/lessons/introkrigingplan`

Dominy, S. C. (2010). Grade control sampling methods in undergroundgold mine grade control. *Proc. Sampling Conf., 7–20, Melbourne,The Australasian Institute of Mining and Metallurgy.*

Gelfand, I. (1955). Generalized random processes. *Dokl. Acad. Nauk.,USSR*, *100*, p 853–856.

Glacken, I. M. (1996). *Change of support by direct conditional block simulation.* Master of Science,Stanford University, Stanford, CA, USA.

Harding, B., & Deutsch, C. V. (2019). Change of support and the Volume Variance Relation. *In J. L. Deutsch (Ed.), Geostatistics Lessons.*. Retrieved from `https://geostatisticslessons.com/lessons/changeofsupport`

Hardtke, W., Allen, L., & Douglas, I. (2011). Localised indicator kriging. *In 35th apcom symposium (p. 141-147).*

Hengl, T. (2009). A practical guide to geostatistical mapping. *University of Amsterdam, Amsterdam.*

Isaaks, E. H. (1991). *The application of Monte Carlo methods to the analysis ofspatially correlated data* (Doctoral Thesis). Stanford University.

Isaaks, E. H., & Srivastava, R. M. (1989). An introduction to applied geostatistics. *Oxford University Press,New York*, p 561.

Journel, A., & Huijbregts, C. J. (1978). Mining Geostatistics. *Academic Press, New York.*

Journel, A. G. (1984). MAD and conditional quantile estimators. *In Geostatistics for natural resources characterization (pp. 261–270). Springer.*

Journel, A. G. (1989). Fundamentals of geostatistics in five lessons. *Washington, DC: American Geophysical Union..*

Markowitz, H. (1952). Portfolio selection. *7(1), 77-91, The Journal of Finance.*

Millard, A. R. (1987). *Cartography in the ancient Near East." The History of Cartography. Volume 1: Cartography in Prehistoric, Ancient, and Medieval Europe and the Mediterranean.* Ed. J. B. Harley and D. Woodward. Chicago: University of Chicago Press,.

Montgomery, D. C., Peck, E. A., & Vining, G. (2012). *Introduction to linear regression analysis.* 5th ed., John Wiley & Sons.

Neufeld, C. T. (2005). *Guide to recoverable reserves with uniform conditioning.* Guidebook series, vol 4. Centre for Computational Geostatistics, Edmonton.

Neufeld, C. T., Norrena, K., & Deutsch, C. (2005). *Guide to geostatistical grade control and dig limit determination.* Guidebook series, vol 1. Centre for Computational Geostatistics, Edmonton.

Norrena, K. P. (2007). *Decision making using geostatistical models of uncertainty* (Doctoral Thesis). University of Alberta.

Pitard, F. F. (1993). *Pierre Gy's sampling theory and sampling practice. Heterogeneity, sampling correctness, and statistical process control.* CRC Press, Inc.

Rivoirard, J. (1987). Two key parameters when choosing the kriging neighborhood. *Mathematical geology, 851-856..*

Rossi, M. E., & Deutsch, C. V. (2014). *Mineral Resource Estimation.* Springer Dordrecht.

Salomons, W. (1999). *Environmental impact of metals derived from mining activities: processes, predictions, prevention.* Journal of Geochemical Exploration.

Srivastava, R. M. (1987). Minimum variance or maximum profitability. *CIM Bulletin,80(901), 63–68..*

Verly, G. (2005). Grade Control Classification of Ore and Waste: A Critical Review of Estimation and Simulation Based Procedures1. *Mathematical Geology*, *37*(5), 451–475.

Wiener, N. (1966). Extrapolation, Interpolation, and Smoothing of Stationary Time Series. *MIT Press,Cambridge, 7th edition.*

Appendix A

Appendices

A.1 Variogram Calculations

Consider a regionalized variable $Z(\mathbf{u}), \mathbf{u} \in A$, where $\mathbf{u}$ is a coordinate vector that specifies a location within the domain A. Consider the bivariate nature of comparing $Z(\mathbf{u})$ and $Z(\mathbf{u+h})$ where h is a spatial lag vector. The variogram calculated for lag vector h, corresponds to the expected value of squared difference.

$$2\gamma(\mathbf{h}) = E\left\{(Z(\mathbf{u}) - Z(\mathbf{u}+\mathbf{h}))^2\right\} \tag{A.1}$$

The variogram is considered as a function $\gamma(\mathbf{h})$ for all $\mathbf{h}$:

- h is a vector of distance and direction
- $\gamma(\mathbf{h})$ is squared variability for $\mathbf{h}$

The variogram, covariance and correlation coefficient are equivalent tools for characterizing two-point correlation (assuming stationarity):

$$\begin{aligned}\gamma(\mathbf{h}) &= C(0) - C(h) \\ &= C(0)[1 - \rho(\mathbf{h})]\end{aligned}$$

where $C(\mathbf{h}) = E\{Z(\mathbf{u}) \cdot Z(\mathbf{u}+\mathbf{h})\} - E\{Z(\mathbf{u})\} \cdot E\{Z(\mathbf{u}+\mathbf{h})\} \quad C(0) = \sigma^2$
Stationarity entails that:

$$m(\mathbf{u}) = m(\mathbf{u}+\mathbf{h}) = m = E\{Z\}, \forall \mathbf{u} \in A$$

$$\mathrm{Var}(\mathbf{u}) = \mathrm{Var}(\mathbf{u}+\mathbf{h}) = \sigma^2 = \mathrm{Var}\{Z\}, \forall \mathbf{u} \in A$$

A.2 Kriging Equations

We require a measure of the goodness of an estimate to get the best. Minimizing the squared error is reasonable

$$\sigma_E^2 = E\left\{\left[Y^* - Y\right]^2\right\}$$

Like maximizing R^2. The true value is not precisely known, but we can still calculate the error variance in expected value. The mean or expected value (the local conditional one) is always the estimate that minimizes the squared error criterion. The estimate that minimizes this error variance by construction will be called kriging in geostatistics.

Consider a linear estimator:

$$y^*(\mathbf{u}) = \sum_{i=1}^{n} \lambda_i y(\mathbf{u}_i)$$

Expand the squared expected error, or error variance:

$$E\left\{[y*(\mathbf{u}) - y(\mathbf{u})]^2\right\} = E\left\{[y*(\mathbf{u})]^2\right\} - 2E\{y*(\mathbf{u})y(\mathbf{u})\} + E\left\{[y(\mathbf{u})]^2\right\}$$

Substitute the estimate equation, moving the expected value inside the summation since it is a linear operator

$$= \sum_{i=1}^{n}\sum_{j=1}^{n} E\left\{\lambda_i y(\mathbf{u}_i)\,\lambda_j y\left(\mathbf{u}_j\right)\right\} - 2\cdot\sum_{i=1}^{n} E\left\{\lambda_i y(\mathbf{u}_i)\, y(\mathbf{u})\right\} + C(0)$$

Substitute the estimate equation, moving the expected value inside the summation since it is a linear operator

$$= \sum_{i=1}^{n}\sum_{j=1}^{n} \lambda_i\lambda_j C\left(\mathbf{u}_i, \mathbf{u}_j\right) - 2\sum_{i=1}^{n} \lambda_i C\left(\mathbf{u}, \mathbf{u}_i\right) + C(0)$$

Given the function of squared estimate error:

$$\sigma_e^2 = E\left\{[y*(\mathbf{u}) - y(\mathbf{u})]^2\right\} = \sum_{i=1}^{n}\sum_{j=1}^{n} \lambda_i\lambda_j C\left(\mathbf{u}_i, \mathbf{u}_j\right) - 2\sum_{i=1}^{n} \lambda_i C\left(\mathbf{u}, \mathbf{u}_i\right) + C(0)$$

Take the partial derivatives:

$$\frac{d\sigma_e^2}{d\lambda_i} = 2\sum_{j=1}^{n} \lambda_j C\left(\mathbf{u}_i, \mathbf{u}_j\right) - 2C\left(\mathbf{u}, \mathbf{u}_i\right) \text{ for } i = 1, \ldots, n$$

Set to zero and solve for the weights:

$$\sum_{j=1}^{n} \lambda_j C\left(\mathbf{u}_i, \mathbf{u}_j\right) = C\left(\mathbf{u}, \mathbf{u}_i\right) \text{ for } i = 1, \ldots, n$$

This is referred to as simple kriging. There are other variant of this fundamental kriging estimator. For ordinary kriging, the sum of the weights is constrained to be one.

A.3 Grade - Tonnage Calculations

The total tonnage (T_{total}) is calculated based on the dimensions of the domain and the specific gravity (ρ) of the material:

$$T_{\text{total}} = length \times width \times height \times \rho$$

Where: Length = 400 m, Width = 200 m, Height = 10 m, $\rho = 2.7$

The cutoff grade (C_{cutoff}) is calculated using linear interpolation between the minimum cutoff grade $\left(C_{\min}\right)$ and the maximum cutoff grade $\left(C_{\max}\right)$:

$$C_{\text{cutoff}} = C_{\min} + \frac{(i-1)}{(\mathrm{u}-1)} \times \left(C_{\max} - C_{\min}\right)$$

Where:

- i is the current iteration (from 1 to n)

- n is the total number of iterations (cutoff levels)

For each grade value (v_r) above the cutoff grade $\left(C_{\text{cut off}}\right)$, the tonnage $\left(T_{\text{tons}}\right)$ and grade (G_{grade}) are updated:

$$T_{\text{tons}} = T_{\text{tons}} + (xsize \times ysize \times zsize) \times \rho$$

$$G_{\text{grade}} = G_{\text{grade}} + v_r$$

Where, $xsize$,$ysize$,$zsize$ is the size/spacing of the blocks/nodes.

The average grade (G_{avg}) is calculated by dividing the accumulated grade by the number of values above the cutoff:

$$G_{\text{avg}} = \frac{1}{\mathbf{N}} G_{\text{grade}}$$

Where: **N** is the total number of values above the cutoff.

The percentage tonnage above cutoff $\left(P_{\text{TAC}}\right)$ is calculated as a ratio of the accumulated tonnage above cutoff to the total tonnage:

$$P_{\text{TAC}} = \frac{T_{\text{tons}}}{T_{\text{total}}} \times 100$$